AMRITA BHARAT - FUNCTION AND ACTIVITY OF ENGA

INVESTIGATION OF THE RIBOSOMAL FUNCTION AND GTPASE ACTIVITY OF *ESCHERICHIA COLI* ENGA

By

AMRITA BHARAT, B.Sc.

A Thesis

Submitted to the School of Graduate Studies

in Partial Fulfilment of the Requirements

for the Degree

Doctor of Philosophy

McMaster University

DOCTOR OF PHILOSOPHY (2012)   McMaster University

(Biochemistry and Biomedical Sciences)   Hamilton, Ontario

TITLE: Investigation of the Ribosomal Function and GTPase Activity of *Escherichia coli* EngA

AUTHOR: Amrita Bharat, B.Sc. (McMaster University)

SUPERVISOR: Professor and Chair Dr. Eric D. Brown

NUMBER OF PAGES: x, 113

Abstract

Ribosome biogenesis is a major metabolic expense of bacteria and a promising target for antibacterial drug discovery. *Trans*-acting proteins, called ribosome biogenesis factors, aid this complex and cooperative process. EngA (YfgK, Der) is a widely distributed bacterial GTPase that is shown here to be important for normal ribosome biogenesis. EngA is an attractive antibacterial target because it is essential for viability in bacteria but is absent in humans.

The GTPase activity and cellular function of EngA was investigated in *Escherichia coli*. Depletion of EngA caused accumulation of 30S and 50S ribosomal subunits at the expense of 70S ribosomes, showing for the first time that EngA is important for normal ribosome biogenesis. Mutation of either of the tandem GTPase domains of EngA led to abnormal ribosome profiles, cell death and loss of GTPase activity, revealing that the two GTPase domains act cooperatively to carry out an essential function. EngA bound the 50S subunit of the ribosome in cells and *in vitro*. Depletion of EngA resulted in sensitization to aminoglycoside antibiotics, which bind at the aminoacyl-tRNA binding site of ribosomes. To search for an inhibitor of ribosome biogenesis, a high-throughput screen of the GTPase activity of EngA was developed. A specific inhibitor was not identified, however, this robust screen can be extended to other compound libraries. Thus, we showed that the GTPase domains of EngA have a cooperative function in ribosome biogenesis, probably in maturation of the 50S subunit, and that EngA is an amenable target for further inhibitor screens.

Table of Contents

List of Figures

List of Tables

List of Abbreviations

A-site	amino acyl-tRNA binding site
Amp	ampicillin
BODIPY	4,4-difluoro-4-bora-3a-4a-diaza-*s*-indacene
BSA	bovine serum albumin
Cm	chloramphenicol
DAPI	4`, 6-diamino-2-phenyl indole
DTT	dithiothreitol
E-site	exit-tRNA binding site
G-domain	GTP-binding domain
GAP	GTPase activating protein
GDP	guanosine-5`-diphosphate
GEF	guanine nucleotide exchange factor
GMP	guanosine-5`-monophosphate
GMPCP	guanosine-5`-phosphate-methylene-phosphate
GMPPNP	guanosine-5`-diphosphate-imino-phosphate
GTP	guanosine-5`triphosphate
GTPase	guanosine triphosphatase
HPLC	high performance liquid chromatography
IPTG	isopropyl β-D-1-thiogalactopyranoside
Kan	kanamycin
LB	Luria-Bertani
MANT	2′/3′-O-N-methylanthraniloyl
P-loop	phosphate-binding loop
P-site	peptidyltransferase-tRNA binding site
ppGpp	guanosine-5`-diphosphate-3`-diphosphate
r-protein	ribosomal protein
RBF	ribosome biogenesis factor

rRNA	ribosomal RNA
SD	Shine-Dalgarno
SIMIBI	Signal recognition particle, MinD and BioD
Spec	spectinomycin
Tet	tetracycline
TRAFAC	translation factor associated class

1   CHAPTER 1 – INTRODUCTION

1.1   The Antibiotic Gap

The introduction of antibiotics during the Second World War represented a major breakthrough in medicine. Infectious diseases, such as tuberculosis and bacterial pneumonia, were a leading cause of death in the pre-antibiotic era (Cohen, 1998). Improvements in sanitation and housing helped to reduce the frequency of infections, while antibiotics dramatically improved the prognosis of an infection. After the introduction of penicillin to the clinic in 1943, several new classes of antibiotics were isolated over the next two decades. Most of the chemical scaffolds of current antibiotics were discovered during this so called "golden age", including the beta-lactams, aminoglycosides, tetracyclines, glycopeptides and fluoroquinolones (Wright, 2010). Resistance to an antibiotic was often observed a few years after it was introduced into the clinic but this was countered by a steady influx of new antibiotics.

Over the last four decades, the frequency of antibiotic resistance has continued to climb while the number of new antibiotics has continued to fall, creating a gap in treatment options. The World Health Organization has named antibiotic resistance as the top concern to human health for which there is an urgent need for pharmaceuticals (Kaplan *et al.*, 2004). Antibiotic resistance also causes longer, more expensive hospital stays (Roberts, Chicago, 2009). The pathogens that cause most of the hospital acquired infections in both the developed and developing world have been dubbed "the ESKAPE bugs" (for *Enterococcus faecalis*, *Staphylococcus aureus*, *Klebsiella pneumonia*, *Acinetobacter baumannii*, *Pseudomonas aeruginosa* and *Enterobacter sp*) because they escape the lethality of antibiotics (Rice, 2008). Some strains are resistant to several antibiotics, such as the multidrug resistant *Acinetobacter*, and some are resistant to our antibiotics of last resort, such as the vancomycin-resistant *Enterococci* (Boucher *et al.*, 2009).

Antibiotic stewardship is a crucial measure for slowing resistance. (Stamm *et al.*, 2001). In the United States, 29 million pounds of antibiotics were given to livestock in 2009 (Food and Drug Administration, 2009). The use of antibiotics as growth promoters has been banned in the European Union but this practice, as well as the prophylactic use

of antibiotics in animals, continues worldwide (Marshall *et al.*, 2011). In medicine, continued education of patients and physicians about the inappropriate use of antibiotics to treat non-bacterial illness is being encouraged (Bush *et al.*, 2011).

As our arsenal of antibiotics dwindle, there is an urgent need for the discovery and development of new antibiotics. The Infectious Diseases Society of America has set a goal of 10 new antibiotics by the year 2020 (Infectious Diseases Society of America, 2010). This will be a challenge because most of the large pharmaceutical companies have discontinued their antibacterial research programs due of the high cost of development, regulatory barriers to approval and low returns on antibiotics (Bush *, et al.*, 2011). Not only is the number of drugs approved by the Food and Drug Administration each year declining, but most new drugs are structural derivatives of existing drugs (Silver, 2011). In the last 40 years, there have been 3 new chemical classes of antibiotics: the oxazolidinone linezolid, the cyclic lipopeptide daptomycin and the macrocyclic fidaxomicin (Difficid) – a narrow-spectrum nonabsorbed antibiotic that was approved in 2011 for the treatment of gastrointestinal infections by *Clostridium difficile* (Duggan, 2011). Current antibiotics target a small number of processes in bacteria, namely (i) cell wall synthesis (ii) protein synthesis (iii) DNA replication and repair (iv) a metabolic enzyme dihydrofolate reductase and (v) RNA polymerase (Figure 1-1). A wealth of genome sequencing data has revealed that about a third of the bacterial genome encodes proteins of unknown function (Tatusov *et al.*, 2003). Many of these proteins are essential and may represent attractive antibacterial targets. Academic laboratories can contribute to the earliest stages of antibacterial drug discovery by characterizing novel potential targets in bacteria such as ribosome biogenesis.
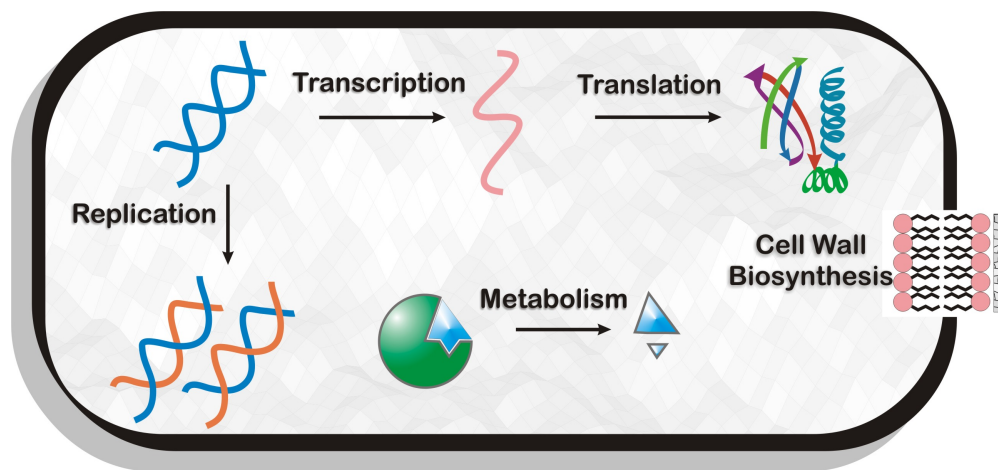
Figure 1-1. Cellular pathways that are targets of antibiotics.
The processes in bacteria that are inhibited by current antibiotics include cell wall biosynthesis, protein translation, DNA replication, RNA transcription and the enzyme dihydrofolate reductase, which produces a metabolic coenzyme.

1.2   Structure and function of the bacterial ribosome

Ribosomes are massive ribonucleoprotein complexes that function as the protein synthesis machinery of the cell. Many details of the translation process were clarified by high-resolution structures of the 2500 kDa 70S ribosome and its subunits from the laboratories of Ramakrishnan, Steitz and Yonath who were awarded the Nobel Prize in Chemistry in 2009. The prokaryotic 70S ribosome is composed of a 30S small subunit and a 50S large subunit that are named after their sedimentation coefficients (Figure 1-2). The 30S subunit decodes messenger RNA while the 50S subunit carries out the peptidyltransferase reaction (Ramakrishnan, 2002). A set of translation factors help to regulate initiation, elongation and release of the new polypeptide chain. The active site or peptidyltransferase centre (PTC) of the ribosome contains three tRNA-binding sites: (i) the A-site (for amino-acyl), where the tRNA carrying the next amino acid binds, (ii) the P-site (for peptidyltransferase), where the new amino acid is added to the growing polypeptide chain, and E-site (for exit), where the de-acylated tRNA leaves

(Ramakrishnan, 2002) (Figure 1-2). The polypeptide is threaded through an exit tunnel as it grows. The ribosome is a ribozyme, meaning that RNA, not protein, carries out catalysis. Indeed, the ribosome is two-thirds rRNA by mass and the catalytic site is almost devoid of proteins (Wilson *et al.*, 2005) (Figure 1-2). Many classes of antibiotics that bind near the active site of the ribosome and inhibit translation have been discovered. Aminoglycosides and tetracyclines bind different RNA residues near the A-site while macrolides bind near the P-site.

Legend:
- ■ A-site tRNA
- ■ P-site tRNA
- ■ E-site tRNA
- ■ 23S rRNA
- ■ 5S rRNA
- ■ 50S proteins
- ■ 16S rRNA
- ■ 30S proteins
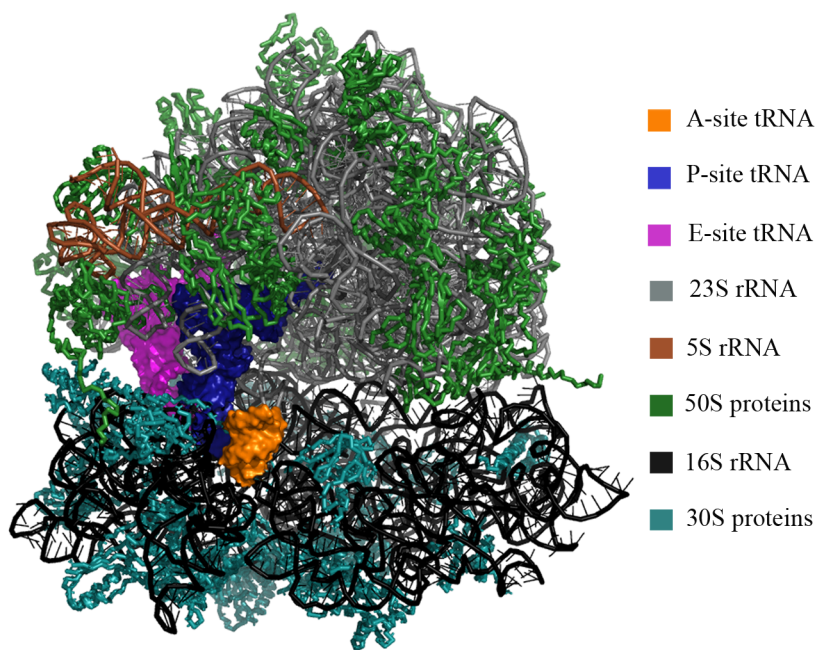
Figure 1-2. Structure of the prokaryotic ribosome.
The 2.8 Å resolution structure of *Thermus thermophilus* 70S ribosome bound to A, P and E-site t-RNAs (PDB ID: 2J01) (Selmer *et al.*, 2006). The 70S ribosome is composed of a large 50S subunit (top) and small 30S subunit (bottom). The active site of the ribosome, where polypeptide synthesis is catalyzed, contains the aminoacyl-tRNA site (A-site), the polypeptide-tRNA site (P-site) and the exit site (E-site). Two-thirds of the ribosome is made of rRNA, which includes 16S, 23S and 5S rRNA. Some regions of the ribosome are devoid of proteins, especially around the subunit interface. The structure was rendered with MacPyMOL v. 1.5 software.

1.3   Prokaryotic Ribosome Biogenesis

In fast growing bacteria, ribosomes constitute up to 30% of the dry mass of the cell and ribosome synthesis is a large energy expenditure (Wilson *et al.*, 2007). The ribosome is synthesized from 54 proteins and 3 rRNA species through a complex and cooperative process that is aided by dozens of *trans*-acting factors (Wilson*, et al.*, 2007). Some of these factors, such as the GTPase EngA, are essential for bacterial survival and do not have a homolog in humans. Perturbation of ribosome assembly by inhibition of a ribosome biogenesis factor may be an attractive target for development of a new antibacterial agent.

In bacteria, the basic steps of ribosome biogenesis are (i) transcription, processing and folding of rRNA, (ii) translation and folding of r-proteins (iii) binding of r-proteins and rRNA and (iv) modification of rRNA and r-proteins (Figure 1-3). The 30S subunit consists of 16S rRNA and 21 ribosomal proteins, called S1 - 21, while the 50S subunit consists of 5S and 23S rRNA and 33 ribosomal proteins, called L1-36. The r-proteins were named according to the order of migration on a 2D electrophoretic gel. Three spots named, L7, L8 and L26, were later discovered to be incorrectly assigned as unique proteins (Wilson*, et al.*, 2005).
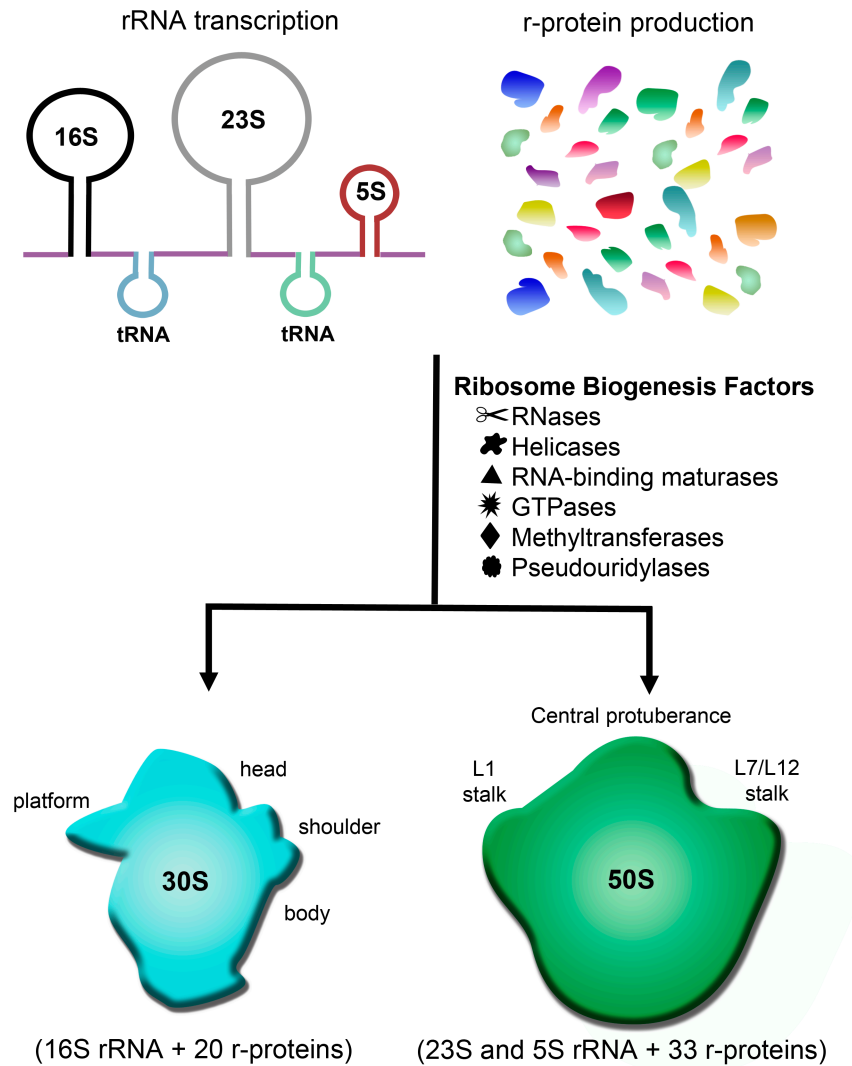
Figure 1-3. Ribosomal subunit biogenesis is bacteria.
Ribosome biogenesis starts with the transcription of three rRNA species and at least one intervening tRNA as a single cotranscript. This transcript is later processed by a set of RNases (endonucleases and exonucleases) to produce mature 16S, 5S and 23S rRNA. As rRNA emerges from the polymerase, folding and nucleation of r-proteins begin. RNA-binding maturases may help the r-proteins to bind while helicases unwind rRNA to enable structural rearrangements along the way. In later stages of assembly, specific residues in the rRNA are modified by methyltransferases and pseudouridylases. Other classes of proteins, such as GTPases and the so-called maturases, are important for ribosome biogenesis but they have an undefined role in the process. The landmark features of the 30S and 50S subunits are shown.

1.3.1 *In vitro* Reconstitution of Ribosome Biogenesis

It was shown four decades ago that ribosomes could be assembled *in vitro* from purified rRNA and r-proteins (Mizushima *et al.*, 1970; Nierhaus *et al.*, 1974; Nomura *et al.*, 1970; Nomura *et al.*, 1968). By varying the order of protein addition, reconstitution experiments revealed that protein binding to rRNA is hierarchical and that there is interdependency of binding.   Primary binding r-proteins bind directly to the rRNA and facilitate the binding of secondary r-proteins, which in turn facilitate the binding of tertiary r-proteins. The assembly map of the 50S subunit is more complex than that of 30S because there are more r-proteins (33 *versus* 21 proteins) and there seems to be more interdependency in protein binding (Rohl *et al.*, 1982). Reconstituted ribosomes were capable of translation but at a much slower rate than native ribosomes (Culver *et al.*, 1999b). The reconstitution experiments helped to provide valuable information about biogenesis but may not paint an entirely accurate picture of how biogenesis occurs in the cell. During this process, subunit intermediates are formed which require long incubations, high ionic concentrations and elevated temperature in order to mature (Nierhaus*, et al.*, 1974; Traub *et al.*, 1969). In the cell, ribosome biogenesis is coupled to transcription so proteins start to bind as soon as the 5` end emerges from the RNA polymerase, however, reconstitution experiments use mature rRNA so proteins are presented with the full length rRNA from the outset.

1.3.2 Ribosome biogenesis precursors

Ribosomal precursors have been isolated from *E. coli* by pulse-chase labeling of newly formed ribosomes. These precursors only account for 2% − 5% of total ribosomes (Lindahl, 1975). There were two precursors to 30S, called $p_1 30$ and $p_2 30$, which sediment at 21S - 27S and 30S, respectively, and three precursors to the 50S, called $p_1 50$, $p_2 50$ and $p_3 50$, which sediment at 30S - 36S, 40S - 43S and 50S, respectively (Lindahl, 1975). It is interesting that the majority of the precursor particles sediment at the same rate as the mature particle. This suggests that ribosomes assemble very quickly to an almost mature form and then there is a rate-limiting late or final step. There was some similarity between the protein compositions of the *in vivo* precursors and the

intermediates produced in the *in vitro* reconstitution experiments, however, almost half of the proteins were different (Shajani *et al.*, 2011). Small subunit 21S precursors were generated by treatment of cells with the antibiotic neomycin and these precursors were compared to the *in vitro* 21S intermediates generated by reconstitution (Sykes *et al.*, 2010). Again, the composition was similar but the central domain proteins were present at higher levels in the *in vivo* precursors. This suggests that the *in vitro* reconstitution is not totally representative of ribosome biogenesis in cells.

1.3.3   Transcription of rRNA

In *E. coli*, ribosome biogenesis begins with transcription of rRNA by RNA polymerase. There are seven rRNA operons in *E. coli* (*rrnA, rrnB, rrnC, rrnD, rrnE, rrnG* and *rrnH*) that are expressed to similar levels (Dennis *et al.*, 2004). Each operon encodes 16S, 23S and 5S rRNA and at least one tRNA (Figure 1-3). Ribosome synthesis is regulated mainly at the level of initiation of transcription or rRNA (Paul *et al.*, 2004b). Many mechanisms of regulation exist to ensure that rRNA transcription is finely tuned to nutrient availability and growth rate of the cell. This ensures that cells make enough ribosomes to take advantage of the available nutrients without wasting resources since ribosome synthesis is a major metabolic expense. The synthesis of rRNA is regulated at two levels: firstly, the promoters are controlled by transcription factors and effectors (corepressors, inducers and small molecules such as ppGpp and initiator nucleoside triphosphates) and secondly, the activity of the transcription factors and effectors is modulated by the availability of amino acids and the use of those amino acids in translation (Dennis*, et al.*, 2004). Each operon is transcribed from two tandem promoters: P1, which is very active during exponential phase, and P2, which provides a low level of activity during all stages of growth. The rRNA promoters can be transcribed to an exceptionally high level during exponential growth due to upstream activating sequences, which include $3 - 5$ sites for binding of the transcriptional activator Fis and UP elements for binding of the α-subunits of RNA polymerase (Dennis*, et al.*, 2004). Mechanisms also exist for efficient elongation by RNA polymerase and a Nus anti-termination system that allows read-through of potential termination sites.

1.3.4   Ribosomal proteins

Ribosomal proteins start to bind to rRNA as it is being transcribed. Ribosomal proteins facilitate the folding of rRNA by shielding negative charges and stabilizing certain conformations. The ribosomal proteins, S1 - S21 on the small subunit and L1-L36 on the large subunit, were named according to their arrangement on a 2D gel (Kaltschmidt *et al.*, 1970). All of the S proteins and more than half of the L proteins have one globular domain and a long basic extension which snakes deep into the core of the ribosome (Wilson*, et al.*, 2005). Proteins L2 and L3 bind at the surface of the 50S but they have extensions that come within 20Å of the peptidyltransferase centre (Wilson*, et al.*, 2005). Ribosomal proteins tend to be positively charged, with an average pI of 10.1, which helps them to stabilize the negative charges of the phosphates of rRNA. There is an uneven distribution of proteins on the ribosome e.g on the 30S subunit, only protein S12 is at the interface while all other proteins are on the cytoplasmic side.

R-proteins appear to have a mostly structural role but some are found in functionally important sites such as the entrance pore for mRNA, the translation factor binding site and the exit tunnel where they appear to be important for binding of translation factors and the signal recognition particle (Wilson*, et al.*, 2007). Some r-proteins (S16, L15, L16, L20 and L24) are important for ribosome assembly but are dispensable after assembly (Nierhaus, 1991). At least 14 r-proteins are dispensable in *E. coli* but mutation of some of these dispensable genes cause slow growth or cold sensitivity (Wilson*, et al.*, 2005). Ribosomal protein production is subject to post-transcriptional regulation. For some r-proteins, the mRNA contains a binding site that mimics the rRNA binding site so excess protein will bind its own mRNA, which inhibits further translation of that r-protein and others in the same operon (Guillier *et al.*, 2005). The level of free rRNA that is available for binding thus controls the production of r-proteins.

1.4   Ribosome Biogenesis Factors

It only takes about 2 minutes to make a ribosome in fast-growing *E. coli*, whereas, it takes about 90 minutes during *in vitro* reconstitution (Lindahl, 1975). This is likely because the process is aided by many *trans*-acting factors in the cell. In yeast, more than 200 *trans*-acting factors have been identified but there are far fewer factors in bacteria (Kressler *et al.*, 2010). Part of the added complexity in yeast is due to the fact that the ribosomal components are made in the nucleus and then exported into the cytoplasm but bacteria do not have this compartmentalization. In bacteria, ribosome biogenesis is aided by helicases, RNases, modification enzymes, RNA-binding maturases and GTPases.

1.4.1   Helicases

Helicases assist in the proper formation of the ribonucleoprotein complex. Time resolved footprinting studies have suggested that within the first 100 msec of transcription, many protein-RNA intermediates form from different nucleation points (Linder *et al.*, 2011; Woodson, 2008). Over the next few seconds, rearrangements and refolding occur. DEAD-box helicases, and the related DExD/H family, may have multiple roles in ribosome biogenesis, including unwinding rRNA, folding and rearrangement of RNA-protein complexes. Helicases have RNA-dependent ATPase activity and contain at least 9 conserved motifs, including the DEAD motif (Linder*, et al.*, 2011). In *E. coli*, five members of the DEAD-box helicase family are believed to be involved in ribosome biogenesis (SrmB, CsdA, DbpA, RhlE and RhlB). The five-gene mutation of *srmB*, *csdA*, *rhlE*, *rhlB* and *dbpA* only grew 30% slower than the *deaD* deletion alone (Jagessar *et al.*, 2010). Depletion of either SrmB or CsdA led to accumulation of 40S intermediates but the compositions of the two 40S intermediates were different (Charollais *et al.*, 2003). Both SrmB and CsdA are more important for growth at lower temperature. As the temperature decreases the thermal energy available for changes in rRNA structure also decreases and the rRNA is more likely to be trapped in a misfolded state (Shajani*, et al.*, 2011). It is thought that SrmB and CsdA help to release the rRNA from misfolded states by an unknown mechanism.

1.4.2   RNases

A set of RNases processes the rRNA cotranscript to yield mature 16S, 23S and 5S rRNA. First, the rRNA is cleaved by RNase III to give the precursors 17S, p23S and 9S rRNA, which are further trimmed at the 5` and 3` termini to yield 16S, 23S and 5S, respectively (Srivastava *et al.*, 1990). For 17S rRNA, 115 nucleotides (nts) are trimmed at the 5` end by RNase E and RNase G and 33 nts are trimmed at the 3` end by an unknown enzyme(s) (Li *et al.*, 1999b). For p23S rRNA, 7 nts are trimmed at the 5`end by RNase III and an unknown enzyme and 7-9 nts are trimmed at the 3` end by RNase T (Li *et al.*, 1999a). For 9S rRNA, 84 nts are trimmed at the 5` end by RNase E and an unknown enzyme and 42 nts are trimmed at the 3` end by RNase E and RNase T (Li *et al.*, 1995; Misra *et al.*, 1979). The final cleavages in both subunits do not occur until the 30S and 50S subunits are incorporated into 70S ribosomes (Srivastava*, et al.*, 1990). A defect in biogenesis of one subunit usually leads to accumulation of precursors to both 16S and 23S since the defective subunit cannot form 70S ribosomes and complete the final steps of rRNA processing.

1.4.3   Modification Enzymes

Modifications of rRNA cluster near the catalytic centre of the ribosome and are thought to be important for fine-tuning ribosome biogenesis or translation (Chow *et al.*, 2007). On the *E. coli* ribosome, the rRNA is subject to 21 methylations by enzymatic transfer of a methyl group from S-adenosyl methionine and 11 pseudouridylations by conversion of uridine residues to pseudouridines (Siibak *et al.*, 2010). Most modifications are not essential but some mutants display slow growth, inefficient translation or ribosome biogenesis defects. For example, the pseudouridylation of three positions in 23S rRNA by RluD are important for the binding of ribosome release factor 2 and for correct reading of stop codons (Kipper *et al.*, 2011). There has been a large divergence in the modification systems of eukaryotes and prokaryotes but the KsgA / Dim1p family, which methylates residues A1518 and A1519, is conserved in all three kingdoms of life (Connolly *et al.*, 2008). KsgA appears to interact with the same region of the 30S subunit as initiation factor 3, suggesting that KsgA may act as a checkpoint

protein to ensure that only mature 30S ribosomes initiate protein translation (Xu *et al.*, 2008). The methyltransferase activity of KsgA is important for its dissociation from the 30S subunit (Connolly*, et al.*, 2008).

1.4.4 RNA-binding Maturases

There are a group of small RNA-binding proteins that have important but undefined roles in ribosome assembly that are referred to as maturases. Apart from the RNA-binding domain, maturases do not usually have other functional domains (Wilson*, et al.*, 2007). The better-studied ones in *E. coli* are RbfA, RimM and RimP. Deletion of *rbfA* caused cold sensitivity and accumulation of precursor 16S rRNA, which was suppressed by Era (Inoue *et al.*, 2003). RbfA suppressed the cold sensitivity of a C23U mutation in 16S rRNA. A cryo-electron structure of RbfA bound to 30S indicated that subunit association could not occur when RbfA is bound, thus RbfA may prevent immature subunits from entering translation (Datta *et al.*, 2007). When RimM was added to the 30S *in vitro* reconstitution, the binding rates of 4 r-proteins (S9, S19, S10 and S3) were increased while the rate of addition of S13 was decreased (Bunner *et al.*, 2010). In a similar experiment, RimP increased the binding rates of 8 r-proteins (Sykes*, et al.*, 2010). These results suggest that RimM and RimP may be chaperones of 30S r-protein incorporation.

1.5 GTPases

The GTP-binding superfamily of proteins regulates a diverse range of cellular processes such as ribosome biogenesis, signaling, translation and cell cycle control (Caldon *et al.*, 2003). GTPases hydrolyze GTP to GDP through nucleophilic attack of the γ-phosphate by a water molecule (Verstraeten *et al.*, 2011). Bacterial P-loop (phosphate-binding loop) GTPases contain a central β-sheet of at least 6 β-strands surrounded by α-helices. P-loop GTPases are characterized by conserved sequence motifs and can be divided into two large classes based on sequence and structural similarities (Leipe *et al.*, 2002). The TRAFAC (translation factor associated) class includes GTPases involved in translation and other ribosome functions, signal transduction, cell motility and transport.

The SIMIBI (signal recognition particle, MinD and BioD) class includes proteins that are involved in signal recognition (FtsY and Ffh), MinD-like ATPases and a group of kinases. The TRAFAC class is further divided into seven families: TrmE, Era, EngA, YihA, Obg, HflX and the classic translation factors (Verstraeten*, et al.*, 2011). The translation factors and the signal recognition factors have well-defined roles, however, the exact functions of the other small bacterial GTPases have not been established.

1.5.1 The GTPase cycle

GTPases normally act as regulators of the processes that they are involved in. They take advantage of conformational changes associated with the GTP / GDP cycle of the protein to interact with, or dissociate from, a downstream effector (Bourne *et al.*, 1990, 1991). Binding of GTP produces an "on" state where the GTPase has increased affinity for its downstream effector (Figure 1-4). Subsequent hydrolysis of GTP to GDP produces an "off" state where the affinity for its effector molecule is reduced. GTPases use this mechanism to function as molecular switches where the timing of the switch is unique to each GTPase.
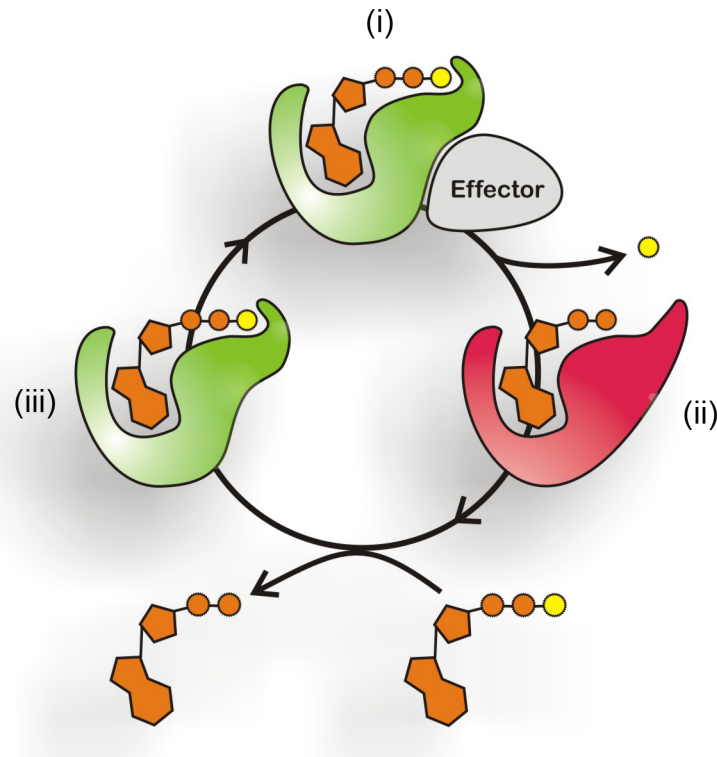
Figure 1-4. The canonical GTPase cycle.
(i) When the GTPase is bound to GTP, this is called the "on" state and its affinity for an effector molecule is increased. Binding of the GTPase to the effector activates the effector. (ii) Hydrolysis of GTP to GDP produces the "off" state where the affinity for the effector is reduced and the effector dissociates. (iii) Exchange of GDP for GTP regenerates the "on" state to continue the cycle.

1.5.2   Signature Motifs of P-loop GTPases

GTPases share a common architecture in the GTP-binding domain that is characterized by the prototype Ras. There are four conserved amino acid motifs (G1 through G4) that coordinate the binding of GTP and a catalytic Mg^{2+} in the active site (Bourne*, et al.*, 1991). The G1 motif (also known as switch 1) binds the α and β phosphates of GTP and is usually found between a β-strand and α-helix on a loop containing the signature sequence GxxxxK[ST]. The G2 motif has a common sequence of xxTxx but the exact sequence is unique to each subfamily and is thought to provide the

15

specificity for the effector molecule of that subfamily (Caldon *et al.*, 2001). G3 (also known as switch II) contains the signature sequence DxxG and coordinates a catalytic Mg^{2+} ion. G4 contains the sequence NKx[DE] and binds the guanine ring, which provides specificity of GTPases for guanine nucleotides. The TRAFAC GTPases usually function as timed switches rather than as sources of energy, except for elongation factor EF-G, where the energy of hydrolysis is proposed to drive translocation of the ribosome along the nascent polypeptide chain (Nguyen *et al.*, 2010).

1.5.3   GTPases in Ribosome Biogenesis

All of the bacterial GTPases that are thought to be important for ribosome biogenesis belong to the TRAFAC class. For many of these GTPases, some studies suggest a role in ribosome biogenesis, whereas other studies suggest roles in diverse processes such as chromosome segregation, sporulation or cellular differentiation (Britton, 2009). These differing observations may be reconciled by the hypothesis that a defect in ribosome formation will result in reduced synthesis of proteins that are involved in many cellular processes. Alternatively, the role of GTPases may be to coordinate ribosome assembly with cell cycle progression or other cellular processes. Some GTPases of unknown function have been found to bind specifically to ribosomal RNA and ribosomal proteins (Table 1-1). Ribosome profiles carried out in mutants of GTPases usually show a decrease in the levels of 70S ribosome and an accumulation of the 30S and 50S subunits (Verstraeten*, et al.*, 2011). The putative ribosome biogenesis GTPases in bacteria tend to have very low intrinsic activity (1 h^{-1} to 10 h^{-1}) and low affinity for GTP (μM affinity *versus* the nM affinity of Ras GTPases) (Britton, 2009). In eukaryotes, the activity of many GTPases is increased by extrinsic factors known as GTPase activating proteins (GAPs) and guanine nucleotide exchange factors (GEFs), which promote hydrolysis of GTP and release of GDP, respectively. The activity of some bacterial GTPases is stimulated by interaction with the ribosome, indicating that the ribosome may function as a GAP or GEF for these proteins (Daigle *et al.*, 2004; Tu *et al.*, 2009). Thus it is likely that many of the conserved bacterial GTPases may have roles in ribosome assembly.

Table 1-1. Bacterial TRAFAC GTPases that are implicated in ribosome biogenesis.

GTPase (*B. subtilis* orthologue)	Essen-tial?	Distribution	Ribosomal Phenotypes	Additional Domains
Era (Bex)	Yes	Bacteria, Eukaryotes	30S costructure, accumulation of subunits and precursor rRNA, ribosome binding is mutually exclusive with r-protein S1	KH
YjeQ / RsgA (YloQ)	No	Bacteria	30S costructure, accumulation of subunits and precursor rRNA, GTPase stimulation by 30S	OB-fold, Zn-finger
ObgE / CgtA (Obg)	Yes	Bacteria, Eukaryotes	50S binding, accumulation of subunits and precursor rRNA	N-term obg domain, C-term domain
YihA / EngB (YsxC)	Yes	Bacteria, Eukaryotes, Archaea	50S binding, accumulation of subunits	-
HflX (YnbA)	No	Bacteria, Eukaryotes, Archaea	50S binding, 16S and 23S rRNA binding	N-term domain
EngA / Der (YphC)	Yes	Bacteria, Chloroplast	50S factor, subject of this thesis	KH-like

1.5.4   Era

Era (*E. coli* Ras-like protein) is an enigmatic GTPase that may be important for 30S ribosome assembly but is also implicated in other cellular processes such as cell division, cell cycle progression, carbon utilization and nitrogen utilization. Era is an essential bacterial protein that also has homologs in eukaryotes. It has an N-terminal GTPase domain followed by a K homology domain that contains the RNA-binding motif, VIGxxGxxIK. A cold sensitive mutant of Era was suppressed by overexpression of the 16S rRNA methyltransferase, KsgA (Lu *et al.*, 1998). Era bound the 30S subunit between the head and cleft on the inter-subunit face of 30S, suggesting that Era may be a checkpoint protein to prevent premature subunit association (Sharma *et al.*, 2005). During initiation of translation, the Shine-Dalgarno (SD) sequence at the 5` end of mRNA binds the complementary anti-SD sequence near the 3` end of 16S rRNA. A crystal structure of Era showed its KH domain bound to a 16S rRNA fragment containing the anti-SD sequence in an interaction that modestly stimulated the GTPase activity of Era by 6-fold (Tu*, et al.*, 2009). This observation further supports a checkpoint role for Era in preventing premature 30S from recruiting mRNA.

1.5.5   YjeQ / RsgA

The *E. coli* protein YjeQ (RsgA) is a dispensable but conserved GTPase in bacteria. YjeQ is a 30S ribosome biogenesis factor. In addition to the GTPase domain, YjeQ contains an N-terminal S1-like OB-fold, which is normally found in RNA-binding proteins, and a C-terminal zinc-finger motif (Daigle*, et al.*, 2004). YjeQ interacted preferentially with the 30S subunit *in vitro* and its activity was stimulated 160-fold upon interaction with the 30S subunit (Daigle*, et al.*, 2004). This is the strongest stimulation by ribosomes seen for any of the putative ribosome biogenesis factors. Depletion of YjeQ led to accumulation of 17S precursor rRNA containing immature 5` and 3` termini (Jomaa *et al.*, 2011a). The cryo-electron structure of the immature 30S subunit from YjeQ-depleted cells showed severe distortion of the 3` minor domain (Jomaa*, et al.*, 2011a).  This distorted region includes helix 44, which would form part of the decoding centre in mature 30S.  The unprocessed 3` terminus of 17S rRNA was displaced,

suggesting that YjeQ may be an important chaperone for processing of the 3` terminus of rRNA. The cryo-electron costructure of YjeQ and 30S showed that YjeQ was bound simultaneously to helix 44 and to the head and shoulder of 30S (Jomaa *et al.*, 2011b). The binding site of YjeQ partially overlapped with the binding sites of initiation factors 1 and 2 and covered an area of 30S that would form three intersubunit bridges upon association with 50S. This suggested that YjeQ might prevent premature formation of the initiation complex or premature subunit association. It was recently found that the YjeQ deletion could be suppressed by mutations in the maturase, RbfA (Goto *et al.*, 2011). Two observations supported the hypothesis that the function of YjeQ is to remove RbfA from the mature 30S subunit: firstly, the suppressor mutations in YjeQ promoted spontaneous release of RbfA from 30S and secondly, YjeQ promoted release of RbfA from mature (but not precursor) 30S in a GTP-dependent manner *in vitro*.

1.5.6 CgtA/ObgE

CgtA / ObgE is perhaps the most enigmatic of the GTPases because it has been implicated in many cellular processes, such as assembly of the 50S ribosomal subunit, general stress response, DNA replication, DNA segregation, sporulation and morphological development (Britton, 2009). CgtA is an essential protein that is conserved in prokaryotes and also present in eukaryotes (Datta *et al.*, 2004). The yeast protein, Nog1, whose N-terminal half is homologous to CgtA, is required for production of the large ribosomal subunit (Jensen *et al.*, 2003). A temperature sensitive mutation of *Caulobacter crescentus cgtA$_C$* caused rapid cell death at the non-permissive temperature, even before ribosomal defects were observed, suggesting that the ribosomal phenotypes associated with CgtA may be due to secondary effects (Datta*, et al.*, 2004). Other evidence is consistent with an important function for CgtA in ribosome assembly. In *E. coli*, overexpression of either *cgtA$_E$* or *engA* rescued the slow growth defect and altered ribosome profile of a deletion of the 23S rRNA methyltransferase, *rrmJ* (Tan *et al.*, 2002b). Depletion of CgtA$_E$ led to accumulation of ribosomal subunits and rRNA precursors (Jiang, 2006; Sato *et al.*, 2005) and the protein cosedimented exclusively with the mature 50S subunit (Wout *et al.*, 2004). The 50S subunit from CgtA$_E$-depleted cells

had reduced levels of r-proteins L16, L33 and L34 (Jiang *et al.*, 2007b). These results all point to a possible role for CgtA in maturation of the 50S subunit. CgtA$_E$ also interacted with SpoT, a bifunctional enzyme that synthesizes and degrades the alarmone (p)ppGpp, which modulates rRNA transcription (Wout*, et al.*, 2004). Thus, CgtA$_E$ may help to regulate ribosome biogenesis by modulating the production of new rRNA.

1.5.7 Other GTPases

The GTPase YihA has not been linked to ribosome biogenesis in *E. coli* but a mutant of the *B. subtilis* homologue, *ysxC*, led to a defective ribosome profile (Schaefer *et al.*, 2006). YsxC cofractionated with the 50S subunit in *B. subtilis* and *S. aureus* (Cooper *et al.*, 2009; Wicker-Planquart *et al.*, 2008). Another GTPase, HflX, was found to interact with the 50S subunit in *E. coli* and *Chlamidophila pneumoniae* but less is known about this protein (Jain *et al.*, 2009; Polkinghorne *et al.*, 2008). There are also a few GTPases, such as YlqF and YqeH, that are linked to ribosome biogenesis in the model Gram-positive *B. subtilis* but do not have homologues in *E. coli*. These two GTPases are both important for normal ribosome distribution and both associate with the 50S subunit (Uicker *et al.*, 2006; Uicker *et al.*, 2007).

1.6 EngA

Here, we studied the bacterial GTPase EngA (Essential *Neisseria gonorrhea* GTPase A). EngA is broadly conserved in bacteria but absent in humans. In *E. coli*, EngA is also known as YfgK or Der (for Double Era) while the *B. subtilis* orthologue is YphC. The *engA* gene was shown to be indispensable in a variety of Gram-positive and Gram-negative organisms (Forsyth *et al.*, 2002; Hwang *et al.*, 2001; Mehr *et al.*, 2000; Morimoto *et al.*, 2002). EngA is unusual in that it contains tandem GTP-binding domains, referred to as G-domain 1 (GD1) and G-domain 2 (GD2). The two G-domains are followed by a C-terminal (KH)-like domain, which stands for K-homology, and was named after the RNA-binding human protein K (Robinson *et al.*, 2002). EngA does not contain the RNA-binding sequence that is normally found in KH domains but the arrangement of α-helices and β-sheets resembles a KH domain (Robinson*, et al.*, 2002).

In the x-ray crystallographic structure of *Thermotoga maritima* EngA, the two G-domains fold on either side of the KH-like domain (Figure 1-5).

G-domain 1   KH-like domain   G-domain 2
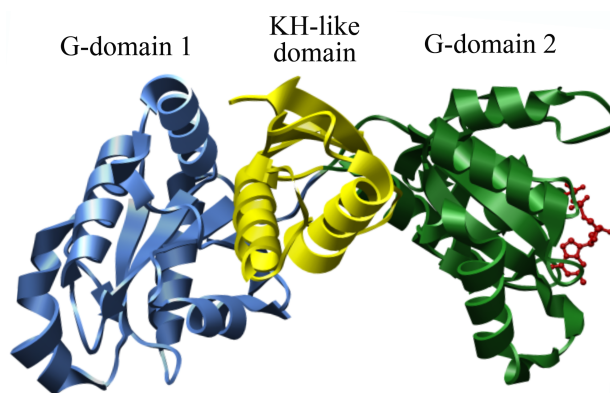
Figure 1-5. The structure of *T. maritima* EngA.
The crystal structure was resolved to 1.9 Å (PDB ID: 1MKY). The tandem GTPase domains of EngA, G-domain 1 and G-domain 2, folded on either side of the C-terminal domain that resembles an RNA-binding KH domain. In this structure, G-domain 2 is bound to GDP. Compared to G-domain 1, G-domain 2 forms a smaller interface with the KH-like domain and its orientation relative to the KH-like domain is different. The structure was rendered with MacPyMOL v1.5 software.

In *E. coli* EngA, there is 52% sequence similarity between the two G-domains. Each G-domain contains the four conserved P-loop sequence motifs, G1 – G4 as highlighted in the primary sequence alignment (Figure 1-6). A highly acidic sequence of about 20 – 40 amino acids links the two G-domains.

```
                        G1                      G2                         G3
Consensus   MXKPXVAIVGRPNVGKSTJFNRJVGERXXIVEDTPGVTRDRIYSSAEWLGXDFNLIDTGGI-DIGDDPFXTQXREQAXIA
E. coli       MVALVGRPNVGKSTLFNRLTRTRDALVADFPGLTRDRKYGRAEIEGREFICIDTGGI-DGTEDGVETRMAEQSLLA   80
S. aureus   MTKPIVAIVGRPNVGKSTIFNRIVGERVSIVEDTPGVTRDRIYSSGEWLTHDFNIIDTGGI-EIGDAPFQTQIRAQAEIA
B. subtilis MGKPVVAIVGRPNVGKSTIFNRIAGERISIVEDTPGVTRDRIYSSAEWLNYDFNLIDTGGI-DIGDEPFLAQIRQQAEIA
T. maritima   MATVLIVGRPNVGKSTLFNKLVKKKKAIVEDEEGVTRDPVQDTVEWYGKTFKLVDTCGVFDNPQDIISQKMKEVTLNM

                                                  G4
Consensus   IDEADVXJFMVBGREGLTXADEXVAKILXKSKKPXVLXXNKXDNL-EMRAXVY-DFYSLGFGEPYPISXSHGLGLGDLLX.
E. coli     IEEADVVLFMVDARAGLMPADEAIAKHLRSREKPTFLVANKTDGLDPDQAVV--DFYSLGLGEIYPIAASHGRGVLSLLE  160
S. aureus   IDEADVIIFMVNVREGLTQSDEMVAQILYKSKKPVVLAVNKVDNM-EMRTDVY-DFYSLGFGEPYPISGSHGLGLGDLLD
B. subtilis MDEADVIIFMVNGREGVTAADEEVAKILYRTKKPVVLAVNKLDNT-EMRANIY-DFYSLGFGEPYPISGTHGLGLGDLLD
T. maritima IREADLVLFVVDGKRGITKEDESLADFLRKSTVDTILVANKAENLREFEREVKPELYSLGFGEPIPVSAEHNINLDTLLE

                                                        G1                          G2
Consensus   AVX-----------------------XEHXXEEEEDPYDEDX--IKLAIXGRPNVGKSXLVNAIIGEERVIVSNVXGT
E. coli     HVLLPWMEDLAPQEEVDEDAEYWAQFEAEENGEEEEEDDFDPQSLPIKLAIVGRPNVGKSTLTNRIIGEERVVVYDMPGT  240
S. aureus   AVV-----------------------SHFGEEEEDPYDEDT--IRLSIIGRPNVGKSSLVNAIIGEDRVIVSNVAGT
B. subtilis AVA-----------------------EHFKNIPETKYNEEV--IQFCLIGRPNVGKSSLVNAMIGEERVIVSNVAGT
T. maritima TIIK-------K--------------LEEKGLDLESKPEITDA--IKVAIVGRPNVGKSTLFNAIINKERALVSPIPGT

                G2                    G3
Consensus   TRDAXDTEXXYDGXEYVLXDTAGMRKKGKVY-ETXEKYSVLRALKAIERXNVVXVVJDAEZGIIEQDKRIAGYAHEXGXA
E. coli     TRDSIYIPMERDGREYVLIDTAGVRKRGKIT-DAVEKFSVIKTLQAIEDANVVMLVIDAREGISDQDLSLLGFILNSGRS  320
S. aureus   TRDAIDTEYSYDGQDYVLIDTAGMRKKGKVY-ESTEKYSVLRALKAIERSNVVLVVIDAEQGIIEQDKRVAGYAHEQGKA
B. subtilis TRDAVDTSFTYNQQEFVIVDTAGMRKKGKVY-ETTEKYSVLRALKAIDRSEVVAVVLDGEEGIIEQDKRIAGYAHEAGKA
T. maritima TRDPVDDEVFIDGRKYVFVDTAGLRRKSRVEPRTVEKYSNYRVVDSIEKADVVVIVLDATQGITRQDQRIAGLVERRGRA

                G4
Consensus   VVIVVNKWDXVEKDEKTMKEFEEXXRXXXQFJDYAPIXFXSALXGXRIXTLFPAINEAXEXHTXRVQXSXLNXVXTDAVA
E. coli     LVIVVNKWDGLSQEVK--EQVKETLDFRLGFIDFARVHFISALHGSGVGNLFESVREAYDSSTRRVGTSMLTRIMTMAVE  400
S. aureus   VVIVVNKWDTVEKDSKTMKKFEDEVRKEFQFLDYAQIAFVSAKERTRLRTLFPYINEASENHKKRVQSSTLNEVVTDAIS
B. subtilis VVIVVNKWDAVDKDESTMKEFEENIRDHFQFLDYAPILFMSALTKKRIHTLMPAIIKASENHSLRVQTNVLNDVIMDAVA
T. maritima SVVVFNKWDLVEHREKRYDEFTKLFREKLYFIDYSPLIFTSADKGWNIDRVIDAINLAYASYTTKVPSSAINSALQKVLA

Consensus   MNPTPTXXGRRLKIFYATQVXIKPPTFVVFVNDVELMHFSYKRXLENXIRD-AFGFEGXPIXIXXXXXRXNPYANKRNTLT  480
E. coli     DHQPPLVRGRRVKLKYAHAGGYNPPIVVIHGNQVKDLPDSYKRYLMNYFRK-SLDVMGSPIRIQFKEGENPYANKRNTLT
S. aureus   MNPTPTDKGRRLNVFYATQVAIEPPTFVVFVNDVELMHFSYKRYLENQIRA-AFGFEGTPIHIIARKRN
B. subtilis MNPTPTHNGSRLKIYYATQVSVKPPSFVVFVNDPELMHFSYERFLENRIRD-AFGFEGTPIKIFARARK
T. maritima FTNLP----RGLKIFFGLQVDIKPPTFLFFVNSIEKVKNPQKIFLRKLIRDYVFPFEGSPIFLKFKRSR

Consensus   PTQMRKRKRLMKHIKKNK
E. coli     PTQMRKRKRLMKHIKKNK 498
```

Figure 1-6. Protein sequence alignment of EngA.

The primary sequences of the EngA orthologues of two Gram negative strains, *E. coli* and *T. maritima*, and two Gram positive strains, *B. subtilis* and *S. aureus*. Black shading indicates 100% identity while gray shading indicates at least 75% similarity. The sequence motifs G1 – G4, which coordinate binding and hydrolysis of GTP in G-domain 1 and G-domain 2, are indicated. The consensus for these motifs are G1 ($GX_4GK[S/T]$), G2 (XXTXX), G3 (DXXG) and G4 (NKXD). The alignment was performed with the Geneious program using the Blossum62 scoring matrix (Drummond *et al.*, 2006).

The physiological role of EngA is unknown. Two early studies suggested that EngA might be important for cell cycle regulation. The first study was conducted in *E. coli*, where a deletion of was complemented in *trans* by a plasmid with a temperature sensitive origin of replication (Hwang*, et al.*, 2001). Light microscopy of cells that were grown at the nonpermissive temperature ($42^{o}C$) showed cell filamentation, abnormal chromosome segregation and unidentified vacuole-like structures. In *B. subtilis*, deletion of *yphC* (the *engA* homologue) was complemented by a copy of the gene at the *amyE* locus under the control of the IPTG-inducible *spac* promoter (Morimoto*, et al.*, 2002). Fluorescence microscopy of cells depleted of YphC revealed cell filamentation, cell curvature and apparent nucleoid condensation.

There was some indirect evidence for a role for EngA in ribosome function. The first evidence came from a large-scale study of protein interactions in *E. coli* (Butland *et al.*, 2005)*.* Affinity-tagged proteins, called baits, were expressed at native levels and gently purified from log phase cultures to homogeneity. The interaction partners of 650 proteins, including EngA, were examined by mass spectrometry. EngA copurified with two 30S subunit proteins, RpsB and RpsC, three 50S proteins, RplB, RplD and RplN, and a putative SAM-dependent 16S rRNA methyltransferase, YnbC. A nonspecific nuclease that is known to degrade rRNA was added to the lysate so it is likely that the observed interactions occurred between EngA and free ribosomal proteins, rather than proteins that were a part of the ribosome. The putative interacting r-proteins bind different positions on the ribosome so they are not expected to be part of the same complex.

Other evidence that EngA may be involved in ribosome function came from a genome-wide search for genes that could suppress the slow growth phenotype of a deletion of *rrmJ / ftsJ*, an *E. coli* heat-shock 23S rRNA methyltransferase (Tan*, et al.*, 2002b). Overexpression of either EngA or ObgE / CgtA$_E$ could complement both the slow growth and the defective polysome profile of a mutant of *rrmJ*. RrmJ transfers a methyl group from S-adenosyl methionine to uridine 2552 on helix 44 of 23S rRNA (Caldas *et al.*, 2000). The mechanism of suppression is not known but the methylation at

U2552 was still missing. This means that although EngA was able to restore wildtype levels of 70S, it was not acting as a methyltransferase.

1.7   Research objectives and organization of thesis

The central hypothesis of this work is that the essential function of the bacterial GTPase EngA is in the assembly of ribosomes. My research has focused on exploiting a range of biochemical and phenotypic methods to uncover the function of EngA. Chapter 2 explores the importance of EngA to ribosome biogenesis and the importance of the two GTPase domains for activity and function. A strain containing a deletion of *engA* and an inducible copy of the gene was created to confirm that *engA* is essential in *E. coli* and to look for phenotypes associated with depletion of the protein. The distribution of 30S, 50S and 70S species in EngA-depleted cells was examined. To investigate the importance of each G-domain, a single residue mutation was created in each active site and the effect of the mutation on viability, ribosome function and GTPase activity was examined. Chapter 3 explores phenotypes associated with depletion of EngA and provides further evidence that it is important for ribosome biogenesis. Sensitivity to growth at low temperature and the transcriptional activity of an rRNA reporter in EngA-depleted cells was tested. The binding of EngA to guanine nucleotides and 30S, 50S and 70S ribosomes were examined. We also looked for chemical-genetic interactions between various classes of ribosomal antibiotics and depletion of EngA. Chapter 4 describes a high-throughput screen for a small molecule inhibitor of the GTPase activity of EngA. Such an inhibitor could serve as an *in vitro* probe of ribosome assembly or a lead for the development of a new antibacterial agent. In Chapter 5, I discuss the possible roles of EngA in ribosome biogenesis and the role of the GTPase cycle of EngA in the regulation of its function.

2   CHAPTER TWO - A COOPERATIVE ROLE FOR BOTH G-DOMAINS OF ENGA IN ITS GTPASE ACTIVITY AND RIBOSOMAL FUNCTION.

2.1   Preface

This Chapter was adapted from a publication in

Bharat, A., Jiang, M., Sullivan, S. M., Maddock, J. R., & Brown, E. D. (2006). Cooperative and critical roles for both G domains in the GTPase activity and cellular function of ribosome-associated *Escherichia coli* EngA. *J Bacteriol, 188*(22), 7992-7996.

I performed all of the experiments in this Chapter with the exception of the ribosome cofractionation in Figure 2-3, which was conducted by Mengxi Jiang[1], Susan M. Sullivan[1] and Janine R. Maddock[1]. I wrote the manuscript and edits were contributed by Eric D. Brown.

[1]Department of Molecular, Cellular and Developmental Biology, University of Michigan, 830 North University, Ann Arbor, MI 48109-1048, USA

Permission has been granted by the publisher to reproduce all of the material in this chapter.

2.2   Summary

EngA (YfgK, Der) is an essential, widely distributed bacterial GTPase of unknown function, with a tandem repeat of GTP-binding domains (G-domains). To probe the cellular phenotype and biochemical function associated with the G-domains of *Escherichia coli* EngA, mutations were created to target the phosphate-binding loop in each. The ability of these variants to support life was tested by complementation of the lethal phenotype of an *engA* conditionally-complemented mutant. Neither S16A nor S217A mutations of G-domain 1 and G-domain 2, respectively, were able to support growth, revealing that both G-domains were critical for an essential cellular function. Polysome profiles of EngA-depleted cells showed significantly increased levels of 30S and 50S ribosomal subunits at the expense of 70S ribosomes, showing for the first time, a direct role for EngA in ribosome biogenesis or stability. Furthermore, EngA was found to cofractionate predominantly with the 50S subunit of the ribosome. The abnormal polysome profile associated with EngA depletion could be complemented by a plasmid carrying wild-type *engA,* but not by the S16A or S217A variants. *E. coli* EngA hydrolyzed GTP with k_{cat} of 70 h^{-1} and K_m of 143 µM, however, variants of either G-domain 1 or G-domain 2 demonstrated an approximately 50 to 100-fold reduction in the specificity constant k_{cat} / K_m. Together, these observations suggest that the tandem G-domains of EngA have a cooperative function in ribosome biogenesis or stability.

2.3   Introduction

GTP-binding proteins constitute a superfamily that regulates a diverse range of cellular processes such as signaling, translation and cell cycle control (Caldon*, et al.*, 2001). These proteins typically utilize conformational changes associated with the GTP/GDP cycling of the protein, whereby binding of GTP leads to a productive interaction with an effector and subsequent hydrolysis ends the interaction (Bourne*, et al.*, 1990, 1991).   In prokaryotes, there are 11 universally conserved GTPases (Hwang*, et al.*, 2001) which can be roughly divided into four major subfamilies: FtsY (FtsY and Ffh),

Obg (Obg, YchF and HflX), Era (Era, EngA, ThdF/TrmE and YihA) and the well-characterized translation factors EF-Tu, EF-G and IF2 (Leipe, *et al.*, 2002).

In recent years, there has been an accumulation of evidence to suggest that many prokaryotic GTPases of unknown function are associated with ribosome function, particularly ribosome biogenesis (Brown, 2005). Ribosome biogenesis is a complex process that involves the folding, modification and assembly of 3 rRNA species and over 50 proteins through the formation of pre-ribosomal intermediates. Reconstitution can be accomplished *in vitro* but some steps require unusually high temperature, high ionic strength and long incubation times; thus, these processes are likely facilitated by assembly factors in the cell (Nierhaus, 1991). Indeed, more than 200 *trans*-acting factors have been identified in ribosome biogenesis in yeast (Kressler *et al.*, 1999), but few such factors are known in bacteria.

Studies of Era, YjeQ and Obg (CgtA) have revealed links to the ribosome, ribosomal proteins or rRNA (Brown, 2005). Polysome profiles of mutants of Era, YjeQ, *E. coli* ObgE/CgtA$_E$ and *Caulobacter crescentus* CgtA$_C$ have all shown an accumulation of the 30S and 50S subunits at the expense of 70S ribosomes(Campbell *et al.*, 2005a, 2005b, 2005c; Inoue, *et al.*, 2003; Jiang, 2006; Lin *et al.*, 2004; Sato, *et al.*, 2005). Direct associations with the ribosome or its subunits have been shown for these four proteins as well as for *Vibriyo harveyi* CgtA$_V$ (Jiang, 2006; Lin, *et al.*, 2004; Sikora *et al.*, 2006; Wout, *et al.*, 2004). Thus, there is a growing body of evidence that uncharacterized GTPases are involved in ribosome stability or biogenesis. Conversely, when these bacterial GTPases are mutated or deleted, defects in a diversity of cellular processes such as chromosome segregation, sporulation and cellular differentiation are often observed *in vivo* (Brown, 2005). This apparent pleiotropy is consistent with the idea that a defect in ribosome assembly is likely to have impact on a wide array of bacterial physiology.

In addition to the above-mentioned proteins there is also emerging evidence for a role for EngA in ribosome function (Altschul *et al.*, 1990; Robinson, *et al.*, 2002). The EngA protein is a broadly conserved bacterial GTPase that lacks a human orthologue and has been shown to be indispensable to a variety of Gram-positive and Gram-negative

organisms (Forsyth*, et al.*, 2002; Hwang*, et al.*, 2001; Mehr*, et al.*, 2000; Morimoto*, et al.*, 2002); its physiological role in the cell, however, is currently unresolved. Evidence for a link to the ribosome include the results of a large scale study to map the *E. coli* protein interaction network wherein EngA copurified with five ribosomal proteins: RpsB, RpsC, RplB, RplD and RplN (Butland*, et al.*, 2005). Furthermore, in a mutant of *rrmJ / ftsJ*, an *Escherichia coli* heat-shock methyltransferase, which showed decreased methylation at position U2552 on 23S rRNA as well as a significant decrease in the level of 70S ribosome (Tan*, et al.*, 2002b), the defective polysome profile was rescued by overexpression of two GTPases, EngA and CgtA$_E$ / Obg*,* but methylation was not restored. The only phenotype that has been shown for EngA-depleted cells is cell filamentation in *E. coli* and *B. subtilis* (Hwang*, et al.*, 2001).

The GTP-binding superfamily is very diverse and widely distributed. Interestingly, EngA and its orthologues are the only members of the superfamily that are known to contain two GTP-binding domains.   A 1.9 Å x-ray structure of *T. maritima* EngA shows the two domains are folded on either side of a C-terminal KH-like domain (Robinson*, et al.*, 2002). The tandem repeat may be the result of a gene duplication, although G-domains 1 and 2 share 53% sequence similarity, which is not strikingly higher than the 47% similarity shared with a related GTPase, Era (Altschul*, et al.*, 1990). The results of a study of *T. maritima* EngA suggested that G-domain 2 does not make a contribution to the overall GTPase activity of the protein *in vitro* since an Asn to Asp mutation in the G4 motif of this domain did not alter the observed activity.   In the same study, a truncation variant suggested that G-domain 2 possessed half of the activity of the full length protein (Robinson*, et al.*, 2002). This apparent paradox and a paucity of *in vivo* data regarding the significance of the two G-domains, in particular to ribosome function, prompted the work described here.

Herein, we report the creation of a precise deletion in *E. coli engA* complemented with an ectopic copy at the *araBAD* locus under arabinose control. We found that variants either G-domain 1 or 2 (S16A and S217A, respectively) were not able to support life in the *engA* null, suggesting that the GTPase activity of both domains is indispensable

to the critical cellular function of EngA. Polysome profiles of EngA-depleted cells revealed a decrease in the level of 70S ribosomes and an accumulation of ribosomal subunits compared to fully complemented or wild type cells. That EngA cofractionated with the 50S subunit further suggests a link to ribosome function. S16A and S217A variants were unable to restore wild-type levels of 70S ribosomes in the null strain suggesting that both G-domains are important for both viability and function. Furthermore, steady state kinetic studies of pure recombinant protein revealed that mutations targeting either G-domain had a significant and cooperative impact on the GTPase activity of the protein as a whole.

2.4   Materials and Methods

General methods. Sequences of primers used are listed in Table 1-1. All strains and plasmids are listed in Table 1-2. All strains were grown in rich Luria-Bertani (LB) media at 37°C. Antibiotics were used at the following concentrations: ampicillin (Amp) at 100 μg/ml, kanamycin (Kan) at 50 μg/ml and chloramphenicol (Cm) at 20 μg/ml. L-arabinose (ara) was used at a final concentration of 2% *w/v* on LB-agar and 1% *w/v* in LB. Cloning was carried out in *E. coli* Novablue by standard cloning methods except where indicated. All centrifugations were performed at 4°C. Reagents were purchased from the following companies: antibiotics, Mg(OAc)$_2$, NH$_4$Cl and β-mercaptoethanol (Sigma, Oakville, Ontario), Tris (BioShop, Burlington, Ontario), RNase-free DNase 1 (Roche, Laval, Quebec), and EDTA (EM Science, Gibbstown, New Jersey).

Creation of *E. coli engA* conditionally-complemented null. Strain EB1208 (*araBAD::engA-kan^R*) was created by insertion of a second copy of *engA* at *araBAD*. The gene was amplified from MG1655 chromosomal DNA with primers KI-F and KI-R using Vent polymerase (New England Biolabs, Beverley, MA) and blunt ligated into pBluescriptΔ*araBAD-kan* (Campbell *et al.*, 2002). This plasmid was used as template to amplify *araBAD* upstream and downstream homologous regions as well as *engA* and *kan^R*. Gel purified (Qiagen) PCR product was transformed into MG1655 and a strain containing an insertion of *engA* at *araBAD* was verified by PCR. EB1209 was created by

replacing *engA* with a chloramphenicol resistance cassette (Datsenko *et al.*, 2000). This cassette was amplified from plasmid p34S with primers KO-F and KO-R.

Table 2-1. Primers used in this study

Primer [a]	Sequence	Site [b]
KI-F [c]	GGGGG<u>GTTTAAAC</u>AATAAGGAGGAAAAAAAA**GTGCGTTGTCTGATGATTTAT**	*Pme1*
KI-R [c]	GGGG<u>GTTTAAAC</u>**TTATTTATTTTTCTTGATGTGCTT**	*Pme1*
KO-F [d]	**TTGAAAACGGCTCCTGGACAGGGGCCGTTTTCCTGTTTTTAACAACGACGCGAATATAGC**TTACGCCCCGCCCTGCCACTCATC	
KO-R [e]	**GGTAGCCATTCCCTCTACATTCATAGAGGGAATGGCAGATAAAATACTTACGGATAA**CGACTCTAGAGGATCCCCGGG	
WT-F [c]	GGGG<u>ACAAGTTTGTACAAAAAAGCAGGC</u>TTC*GAAGGAGAT*AGAACCATC**ATGGTACCTGTGGTCGCGCTTG**	*attB1*
WT-R [c]	GGGG<u>ACCACTTTGTACAAGAAAGCTGGG</u>TCTTCA**TTATTTATTTTTCTTGATGTGCTTCATCAG**	*attB2*
K15A-F	GCGCTTGTCGGGCGCCCTAACGTAGGA<u>GCA</u>TCCACGTTATTTAACCGTCT	K15A
K15A-R	GCGAGTTAGACGGTTAAATAACGTGGA<u>TGC</u>TCCTACGTTAGGGCGCCCGACAAGCGC	K15A

Primer [a]	Sequence	Site [b]
S16A-F	GGGCGCCCTAACGTAGGAAAAGCCACGTTA TTTAACCGTCTAACTC	S16A
S16A-R	GAGTTAGACGGTTAAATAACGTGGCTTTTCC TACGTTAGGGCGCCC	S16A
K216A-F	GCGATTGTGGGTCGTCCGAACGTAGGTGCGT CTACACTCACTAACCGTATTCTTGGTG	K216A
K216A-R	CACCAAGAATACGGTTAGTGAGTGTAGACG CACCTACGTTCGGACGACCCACAATCGC	K216A
S217A-F	GGTCGTCCGAACGTAGGTAAGGCTACACTCA CTAACCGTATTC	S217A
S217A-R	GAATACGGTTAGTGAGTGTAGCCTTACCTAC GTTCGGACGACC	S217A
F5033-F	ATATCATATGCGTTGTCTGATGATTTAT	
F5033-R	ATTCCTCGAGGCAATGGCAGATAAAATA	

[a] F and R denote forward and reverse primers, respectively
[b] Underlined sequence indicates restriction site, recombination site or mutation
[c] Boldface indicates complementarity to *engA*
[d, e] Boldface indicates complementarity to *engA* upstream and downstream homologous regions respectively.

Table 2-2. Strains and plasmids used in this study

Strains	Genotype	Source
BL21-AI	F⁻*ompT hsdS*$_B$(r$_B$⁻m$_B$⁻) *gal dcm araB*::*T7RNAP-tetA*	Invitrogen
BL21(DE3)	F⁻*ompT hsdS*$_B$(r$_B$⁻m$_B$⁻) *gal dcm* (DE3)	Novagen
EB1208	*araBAD*::*engA-kan*^{R}	This study
EB1209	*araBAD*::*engA-kan*^{R}*; engA*::*Cm*^{R}	This study
EB1262	EB1209 harboring plasmid K15A-pDEST14	This study
EB1263	EB1209 harboring plasmid S16A-pDEST14	This study
EB1486	EB1209 harboring plasmid K216A-pDEST14	This study
EB1456	EB1209 harboring plasmid S217A-pDEST14	This study
EB1487	EB1209 harboring plasmid *engA*-pDEST14	This study
Plasmids		
pDEST14	Gateway T7 expression vector	Invitrogen
pJM1407	(His$_6$)*engA*-pET28a	This study

Polysome profiling of EB1209. Cells were subjected to one cycle of depletion by growth in the absence of arabinose. These cultures were used to inoculate LB-Cm or LB-Amp to an OD_{600} of 0.01, which were then grown to an OD_{600} of 0.2-0.22. Cultures were cooled for 15 min at 4^oC, centrifuged at 8,000 x g for 12 min and the pellet was suspended in 5 ml of RNase-free buffer A (20 mM Tris, 10.5 mM $Mg(OAc)_2$, 300 mM NH_4Cl, 0.5 mM EDTA, and 3 mM β-mercaptoethanol 10 μg/ml RNase-free DNase 1). This was followed by lysis in a French Pressure cell at 10,000 psi and centrifugation at 30, 000 x g for 45 min. Three millilitres of the clarified lysate was layered onto an equal volume of buffer A + 35% *w/v* sucrose and spun at 100, 000 x g for 15 h. The ribosomal pellet was suspended in 750 μl of buffer A and the distribution of 30S, 50S and 70S in the sample was analyzed by sedimentation velocity on a Beckman Coulter Model XL-I analytical ultracentrifuge. The rotor cells were loaded with 380 μl of sample and 400 μl of buffer A as the reference and centrifuged at 30,000 rpm. Interference *vs* radius from the centre of rotation was measured every 2 sec, generating 300 data points. The method of sedimentation time derivative (Stafford, 1992) was employed, using Microcal Optima v. 6.0 analysis software, to convert this data to the Gaussian distribution of molecules, g(S*), at each sedimentation coefficient, S*. Note that S* is a variation of the Svedberg coefficient (S) which is specified at 20^oC in water. The effects of temperature and buffer composition on the sedimentation rate were adjusted with the program Sednterp v. 1.01 (Philo, Hayes and Laue). Integration of the areas under the 3 peaks gives the proportion of each species in the sample.

Polysome fractionation and EngA localization. For this experiment, gene *engA* was amplified from *E. coli* W3110 using Advantage c-DNA polymerase (Clontech) and primers 5033-F and 5033-R. The gene was then cloned into pET28a (Novagen) in frame with an N-terminal 6xhistidine tag. *E. coli* BL21(DE3) harboring $(His_6)engA$-pET28a was grown to OD_{600} of 0.4 before induction with 50 μM IPTG for 30 min at room temperature. Cultures were incubated with 200 μg/ml chloramphenicol for 30 sec to trap polyribosomes on mRNA. Cells were harvested by centrifugation at 10, 000 x g for 10 min. For every 100 ml of initial culture, the cell pellet was suspended in 1 ml lysis buffer

(10 mM Tris-Cl, pH 7.5, 10 mM $MgCl_2$, 30 mM NH_4Cl, 100 µg/ml chloramphenicol) and vortexed with an equal volume of glass beads (300 µm, Sigma) for 5 min at 4°C. Thirteen OD_{260} units of cleared lysate were layered onto a 10 ml gradient of 7-47% sucrose in buffer I (10 mM Tris-Cl, pH 7.5, 10 mM $MgCl_2$, 100 mM NH_4Cl) poured with a Hoeffer SG15 gradient maker. Sedimentation of the ribosomes and fractionation of the gradients was carried out as previously described (Wout, *et al.*, 2004). Immunoblot analyses of the fractions were carried out as before (Lin *et al.*, 1999) using anti-His antibody (Sigma) at a dilution of 1:2,000.

Creation of *engA*-pDEST14. Gene *engA* (SwissProt annotation) was cloned into pDEST14™ using the phage λ recombination system of the Gateway® Cloning Kit (Invitrogen Canada, Burlington, ON) with primers WT-F and WT-R according to the manufacturer's instructions. Variants K15A, S16A and S217A were created using QuickChange Site Directed Mutagenesis Kit (Stratagene, La Jolla, CA) and plasmid *engA*-pDEST14 as template according to the manufacturer's instructions. Variant K216A was constructed by amplifying *engA* in two segments using internal primers that contain the desired mutation, followed by overlap extension PCR to amplify the entire gene, which was cloned into pDEST14. The mutations were confirmed by sequencing (MOBIX, McMaster University).

Purification of wild-type *E. coli* EngA and its variants. Cultures of *E. coli* BL21-AI (Invitrogen) transformed with pDEST14-*engA* were grown at 37°C in LB/Amp to an OD_{600} of 0.5 before inducing for 4 h with 0.2% (*w/v*) L-arabinose. Cells were harvested by centrifugation at 8,000 *g* for 10 min and washed with 0.85% NaCl. The cells were then suspended in 20 ml of buffer A (50 mM Tris, 30 mM NaCl, 10% glycerol, pH 7.5) plus 100 µg/ml DNase I, 100 µg/ml RNase A and Calbiochem Protease Inhibitor Cocktail, and lysed by three passes through a French pressure cell at 20,000 psi.   The lysate was centrifuged at 40,000 *g* for 60 min and loaded onto a Q-Sepharose Fast Flow anion exchange column (Amersham Biosciences, Baie d'Urfe, PQ). Elution was carried out by a linear gradient of 30 – 500 mM NaCl. Fractions were analyzed by SDS-polyacrylamide (12 % acrylamide) gel electrophoresis and the purest fractions were

pooled and concentrated to 5 mg/ml using Amicon 8200 stirred cell concentrators. The protein was stored in buffer A at -80°C.

GTPase assay. Various concentrations of GTP were incubated with 0.5 μM wild-type EngA and 1 μCi α–^{32}P-GTP in assay buffer (50 mM Tris, 5 mM MgCl$_2$ and 400 mM KCl, pH 8.0) for 10 – 120 min at 22°C. The variants were assayed using 10 μM enzyme. Reactions were terminated with 5.3 M urea and injected onto a 4.5 mm × 50 mm WPQUAT strong ion-exchange column (JT Baker, Phillipsburg, NJ) using a Waters 600 HPCL (Milford, MA). GDP and GTP were resolved with a linear gradient of 25 mM to 0.65 M triethylamine bicarbonate. The peaks for GTP and GDP were integrated using Millenium32 software (Waters). The kinetic constants k$_{cat}$ and K$_m$ were determined from a plot of V$_i$ *vs* [GTP] using SigmaPlot 2000 software to fit the data to a single rectangular 2-parameter hyperbolic function.

2.5   Results

### 2.5.1   Construction of a strain suitable for depletion of EngA.

In order to probe the cellular function of *engA*, a strain was created wherein the gene deletion was complemented from a distant locus on the chromosome under control of the tightly regulated P$_{BAD}$ promoter. The diploid strain (EB1208) contained *engA* at its native locus as well as at the *araBAD* locus, whereas the conditional null (EB1209) contained a replacement of native *engA* by an antibiotic resistance cassette. Growth of EB1208 and EB1209 was characterized on solid rich media in the presence or absence of L-arabinose. The *engA* diploid strain displayed a similar level of growth regardless of the presence of arabinose; the conditional null, however, was dependent on arabinose to form single colonies (Figure 2-1A). In the absence of inducer, growth was only observed for this strain in the area of heavy inoculum and was likely due to a low level of leaky expression from P$_{BAD}$.

2.5.2   Both GTP-binding domains of EngA are essential for cellular function.

To dissect the importance of each G-domain, single residue mutations were made in the phosphate-binding loop of each and tested for *in vivo* complementation of the lethal phenotype of the *engA* null. The 1.9 Å resolution crystal structure of EngA from *T. maritima* shows Lys14 and Ser15 of the G1 motif of G-domain 1 positioned to form hydrogen bonds to 2 free phosphates in the active site (Robinson*, et al.*, 2002). Furthermore, the equivalent lysine in Ras, a small eukaryotic GTPase, is important for binding phosphate while the equivalent serine has a critical role in coordinating a catalytic Mg^{2+} ion (Bourne*, et al.*, 1991). Thus, these two residues, Lys15 and Ser16 in G-domain 1 and Lys 216 and Ser217 in G-domain 2 of *E. coli* EngA were selected for mutation to alanine.

Plasmid pDEST14 encoding wildtype EngA or one of its variants, K15A, S16A, K216A or S217A was placed in the *engA* conditional deletion, EB1209. The ability of these sequences to complement the lethal phenotype of the deletion was checked on solid rich media in the presence or absence of arabinose. The deletion mutant was in a genetic background that does not produce T7 RNA polymerase but its lethal phenotype could be complemented by the leaky expression from the T7 promoter of pDEST14 encoding wild-type *engA*, presumably from nonspecific recognition of promoter elements by *E. coli* RNA polymerase.   K15A was the only variant that supported growth in the absence of arabinose (Figure 2-1B). The inability of either S16A or S217A to complement the deletion provides the first *in vivo* evidence that both of the GTP-binding domains are critical to the cellular function of EngA. Western blot analysis demonstrated that wild-type EngA and all four variants were expressed from pDEST14 to similar levels (Figure 2-1C).
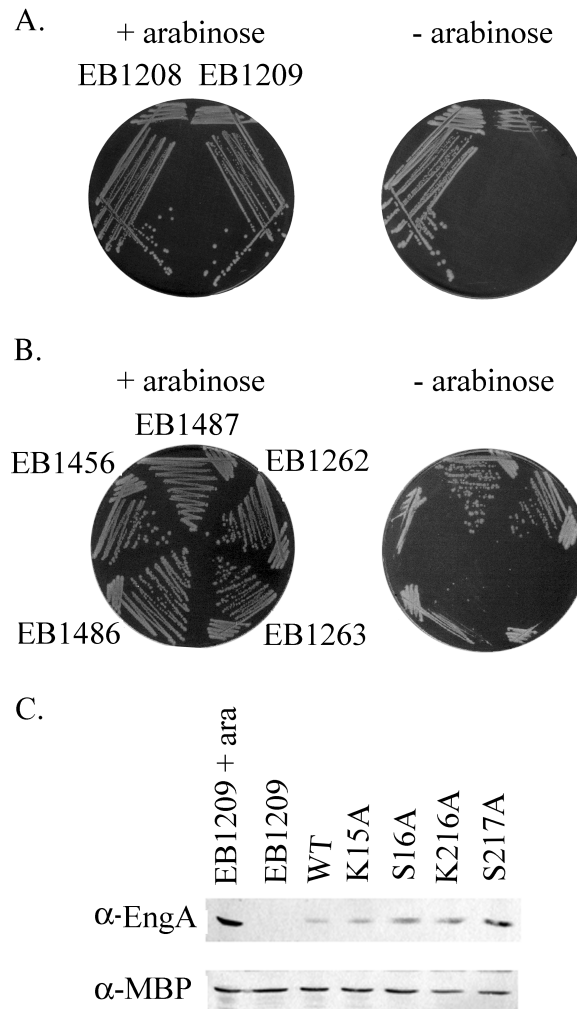
Figure 2-1. Complementation of the lethal phenotype of EB1209 by G-domain mutants.

(A) The *engA* diploid strain (EB1208) and the arabinose-inducible null (EB1209) grown on LB/agar/Kan in the presence (left) or absence (right) of arabinose. (B) Strains were grown on LB/agar/Amp in the presence (left) or absence (right) of 2% L-ara (*w/v*). Shown on each plate is EB1209 harboring pDEST14 encoding wild-type *engA* (EB1487), K15A (EB1262), S16A (EB1263), K216A (EB1486) or S217A (EB1456). (C) Analysis of the expression levels of EngA and its variants from pDEST14 by western blot. Lysates obtained from cultures that were grown to OD_{600} of 0.8 were subjected to western blot analysis using α-EngA (Cocalico Biologicals, Reamstown, PA) or α-Maltose binding protein (New England Biolabs, Beverley, MA) rabbit polyclonal 1° antibody and donkey α-rabbit HRP-conjugated 2° antibody. Lanes 1 and 2 contain EB1209 grown in the presence or absence of 1% L-ara, respectively. The remaining lanes contain EB1209 harboring pDEST14 encoding wild-type *engA* (lane 3), K15A (lane 4), S16A (lane 5), K216A (lane 6) or S217A (lane 7).

2.5.3   EngA-depleted cells have an altered polysome profile.

Sedimentation velocity analytical ultracentrifugation was used to examine the distribution of 30S, 50S and 70S ribosomes and proved to be a robust and reproducible method of polysome profiling. The interference optics of this instrument provides a signal that can be integrated to quantify the distribution of ribosomal subunits. EB1209 grown in the presence of arabinose had a similar profile as wild-type *E. coli* MG1655, with the 70S ribosomes composing at least 60% of total ribosome (Figure 2-2A, 2-2B; Table 2-3). Upon depletion of EngA a shoulder was observed on the middle peak, which may indicate the presence of two species of the large subunit, which sediment at slightly different rates (Figure 2-2C). This shoulder was not seen in the profiles of wildtype or complemented cells (Figure 2-2A, 2-2B). Furthermore, compared to wild-type *E. coli*, an approximately 2-fold increase was observed for the null in the level of the 30S subunit (14.4% to 26.4%) and also the 50S subunit (23.8% to 45.4%). This was accompanied by a 2-fold decrease in the level of 70S (61.7% to 28.1%) (Table 2-3)
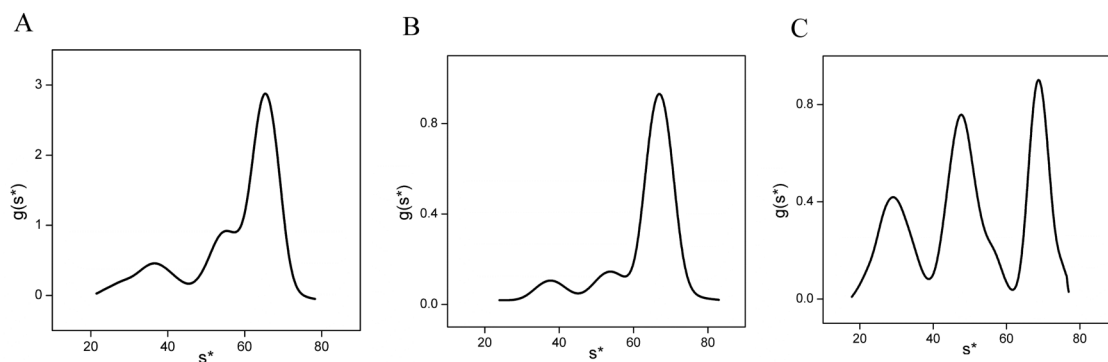
Figure 2-2. Ribosome profiles of EB1209 with or without complementation.
The profiles of (A) *E. coli* MG1655 (B) EB1209 + 1% L-ara and (C) EB1209 are shown. Ribosomes were obtained from clarified lysates by centrifugation over a 35% sucrose cushion. The ribosomal pellet was analyzed by sedimentation velocity on a Beckman Coulter Model XL-I analytical ultracentrifuge. The method of sedimentation time derivative (Stafford, 1992) was employed, using Microcal Optima v. 6.0 analysis software, to find the Gaussian distribution of molecules, g(S*), at each sedimentation coefficient, S*.

Table 2-3. The distribution of 30S, 50S and 70S ribosomes in EB1209 containing *engA* or one of the variants.

	30S (%)[a]			50S (%)[a]			70S (%)[a]		
WT MG1655	14.4	+/-	2.8	23.8	+/-	4.5	61.7	+/-	3.5
EB1209 + 1% ara	13.7	+/-	1.8	20.3	+/-	1.3	66.0	+/-	2.4
EB1209	26.4	+/-	1.7	45.4	+/-	1.8	28.1	+/-	1.3
engA-pDEST14	12.5	+/-	1.4	21.9	+/-	1.9	65.6	+/-	2.3
K15A	20.1	+/-	1.0	35.5	+/-	1.8	44.4	+/-	0.9
S16A	29.9	+/-	5.9	41.2	+/-	1.1	28.9	+/-	4.9
K216A	27.6	+/-	6.9	47.0	+/-	3.1	25.4	+/-	4.1
S217A	23.2	+/-	0.9	39.5	+/-	5.7	37.3	+/-	4.7

[a] Values shown are the average of triplicates.

2.5.4   EngA cofractionated with the large ribosomal subunit.

To further investigate the link between EngA and the ribosome, cells overexpressing His$_6$-EngA were fractionated using a sucrose gradient and probed with anti-His antibody. A$_{254}$ was monitored to produce a polyribosome trace and the fractions were subject to immunoblotting with anti-His antibody (Figure 2-3). EngA was detected in the peak of the polyribosome trace corresponding to the 50S subunit. The fraction of EngA that was not associated with ribosomes was found in the early fractions corresponding to soluble (unbound) protein.

2.5.5   Both G-domains of EngA can be linked to the polysome defect.

The distribution of ribosomes was examined in EB1209 harboring pDEST14 encoding either wild-type EngA or one of the variants thereof, K15A, S16A, K216A or S217A. Sedimentation velocity analysis showed that *engA*-pDEST14 was able to restore a wild-type polysome profile (approximately 12%, 22% and 65% of 30S, 50S and 70S,

respectively); S16A, K216A and S217A mutations, however, resulted in profiles that are similar to the uncomplemented *engA* null (approximately 25%, 45% and 30% of 30S, 50S and 70S, respectively) (Table 2-3). This suggests that inactivation of either domain interferes with the role of EngA in the formation or stability of 70S ribosomes. K15A provided partial complementation of the defective polysome profile (Table 2-3), consistent with the observation that this mutation complements growth (Figure 2-1B). K216A did not display any such complementation, indicating that this lysine may be more important in G-domain 2.
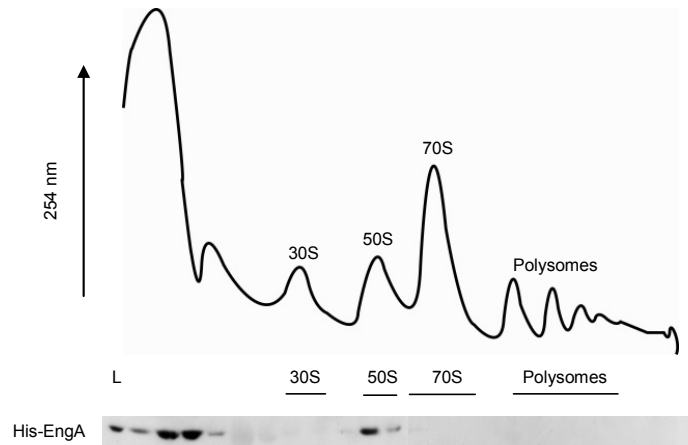
Figure 2-3. His$_6$-EngA cofractionated predominantly with the large ribosomal subunit.
Mid-exponential phase *E. coli* BL21(DE3) harboring (His$_6$)*engA*-pET28a were induced with 50 µM IPTG for 30 min at 22°C. The culture was incubated with chloramphenicol before harvesting to trap polysomes. Ribosomal species were separated on a 7-47% sucrose gradient. Shown is the profile of absorbance at 254 nm resulting from fractionation. The positions of the 30S and 50S subunits, 70S monosomes and the polysomes are indicated. Below the polyribosome trace is an α -His immunoblot of TCA-precipitated fractions showing the amount of His$_6$-EngA detected. L, 1/100th of the total sample loaded onto the gradient.

2.5.6   Active site substitutions in either G-domain impair GTPase activity.

Untagged EngA was purified and subjected to liquid chromatography mass spectrometry, which revealed a molecular mass of 55033 Da +/- 10 Da (expected mass = 55036 Da), confirming the identity of the protein. At steady state, a k_{cat} of 70 h^{-1} and K_m of 143 µM was observed for *E. coli* EngA (Table 2-4), which is comparable to the k_{cat} of 50 h^{-1} and K_m of 110 µM reported for the *T. maritima* enzyme (Robinson*, et al.*, 2002).

Mutations targeting G-domains 1 or 2 demonstrated significant increases in K_m along with decreases in turnover (k_{cat}). Purified recombinant variant enzymes S16A, K216A and S217A had K_m constants of approximately 5 mM, compared to 143 µM for wild-type EngA, and turnovers of approximately 25 h^{-1}, compared to 70 h^{-1} for wildtype (Table 2-4). Since the major impact was on K_m, this indicates that the primary effect of the mutations was a reduction in the productive binding of EngA to GTP. The specificity constant k_{cat}/K_m, which describes the coming together of enzyme and substrate to form a productive complex, is the apparent rate constant at low substrate concentration (Northrop, 1998). This is a particularly useful parameter for describing the variants since the estimated cellular concentration of GTP, < 1 mM (Bochner *et al.*, 1982), is much lower than the K_m of the variants. The k_{cat}/K_m constants were approximately 118-, 104- and 109-fold lower in S16A, K216A and S217A, respectively (Table 2-4), less than 1% that of wild-type EngA. Thus, inactivation of one G-domain had a negatively cooperative impact on the other domain. Interestingly, the K15A variant was the least impacted (45-fold reduction in k_{cat}/K_m) and it is the only variant that provided partial complementation (Figure 2-1B and Table 2-3).

Table 2-4. Kinetic characterization of wild-type EngA and P-loop mutants.

	k_{cat} [a] (h^{-1})	K_m [a] (mM)	Decrease in k_{cat}/K_m [b]
Wild-type	70	143	1
K15A	7.5	695	45
S16A	20	4900	118
K216A	31	6655	104
S217A	21	4770	109

[a] Values shown are the average of duplicates.
[b] Fold decrease relative to wildtype.

2.6   Discussion

The EngA protein is an unusual GTPase with an indispensable role in bacterial physiology that is uncharacterized to date. The tandem repeat of the GTP-binding domain seen in this enzyme is unprecedented among bacterial GTPases and presents a special challenge to understanding the function and mechanism of action of the EngA protein.   Previous *in vitro* characterization of the GTPase activity of *T. maritima* EngA suggested that G-domain 2 makes little or no contribution toward the overall activity of the protein (Robinson*, et al.*, 2002). In that study, the residue chosen for mutation was Asn of the G4 motif NKXD, which provides specificity for GTP by binding the guanine ring (Bourne*, et al.*, 1991). The observation that mutation of this residue in G-domain 2 results in similar activity to the wild-type enzyme may be due to the possibility that this Asn in G-domain 2, like the Lys of G-domain 1 seen here, does not make a significant enough contribution to binding to abolish GTPase activity upon mutation. We found that in the first G-domain, the K15A mutation had a much smaller impact on growth and ribosome function than the S16A mutation.

The data presented here are consistent with unique but cooperative roles for the two G-domains in the function of EngA since each was shown to be important for cell

viability and for normal polysome profiles. There are several structural differences between the N and C-terminal G-domains which suggest that they have unique character (Robinson, et al., 2002). The most striking is the positioning of the GTP-binding sites in relation to the uncharacterized C-terminal KH-like domain. In G-domain 1, the conserved motifs of nucleotide binding are right at the interface, while in G-domain 2, these motifs are distal to the interface. It has been proposed that conformational changes caused by GTP hydrolysis may be transmitted to this KH-like domain to modulate interaction with a binding partner (Robinson, et al., 2002). If this is the case, then the structure suggests that the two G-domains communicate differently with the KH-like domain.

Since inactivation of either domain has the same impact on 70S levels as deletion of the entire gene, the G-domains clearly have a cooperative and critical role in the maintenance or assembly of ribosomes. We have also observed that the GTPase activity of a single G-domain cannot be isolated, suggesting that each is strongly influenced by the activity of the other. This is consistent with strong positive cooperativity between the two G-domains, whereby binding or hydrolysis in one domain considerably stimulates the other.

The finding that EngA is essential for the production of wild-type levels of ribosome suggests that the protein may be a novel ribosome assembly factor. Furthermore, cofractionation experiments showed that the EngA protein was substantially associated with the 50S subunit. Interestingly, the polysome profile of cells depleted of EngA showed a shoulder in the peak corresponding to the large subunit, which may represent a mixture of immature and mature 50S subunits. Taken together, these findings place EngA in a growing group of small bacterial GTPases such as CgtA / Obg, YjeQ and Era, which have been implicated in ribosome function. The remarkable level of cooperativity observed in this enzyme is suggestive of intramolecular regulation between its G-domains, whereby the two activities are exquisitely coordinated to achieve function. More study will be required to investigate this phenomenon and the hypothesis that EngA has a role in ribosomal assembly.

3   CHAPTER THREE – ENGA MAY AID IN MATURATION OF THE 50S SUBUNIT BY ACTING NEAR THE A-SITE

Preface to Chapter 3

The experiments described in this Chapter were carried out myself.

3.1   Summary

The EngA protein is an indispensable bacterial GTPase, which appears to be important for ribosome assembly. Depletion of EngA was also reported to cause defects in cell division and chromosome segregation, which suggests that EngA is involved in cell cycle control. Here, we probe phenotypes associated with loss of EngA in *Escherichia coli* to better understand its role in the cell. Depletion of EngA caused cold sensitivity, a common phenotype of mutation of ribosome-related genes. A reporter of the ribosomal rRNA promoter, P_{rrnH}, was stimulated in response to depletion of EngA. EngA displayed direct nucleotide-dependent binding to ribosomes with a modest preference for the 50S subunit. Various classes of antibiotics that bind near the active site of the ribosome were used to probe the action of EngA on ribosomes. Cells depleted of EngA were sensitized to aminoglycosides but not to macrolides or tetracycline derivatives. Aminoglycosides bind near the amino acyl-tRNA site (A-site) at the subunit interface. Thus, EngA bound ribosomal subunits in a nucleotide-dependent manner and its function appears to be related to the A-site of ribosomes. The data support a ribosomal role for EngA and we suggest that observations of non-ribosomal phenotypes may be downstream effects of a global reduction in protein synthesis.

3.2   Introduction

Ribosome biogenesis involves the coordinated production, folding and assembly of 54 proteins and 3 rRNA species into two subunits, the 30S and 50S subunits. In bacteria, this is a cooperative process that requires several classes of factors, including RNases, helicases, modification enzymes, folding chaperones and GTPases (Brown, 2005). There has been a trend among bacterial GTPases where most of the evidence points to a function in ribosome biogenesis but other evidence suggest roles in diverse non-ribosomal processes. Deletion of the GTPases *yjeQ / rsgA*, *era* or *cgtA$_E$*, led to accumulation of 30S and 50S subunits as well as accumulation of unprocessed 16S and 23S rRNA (Brown, 2005). These GTPases also associate directly with the ribosome or

its subunits (Verstraeten, *et al.*, 2011). For each GTPase, however, phenotypes such as cell cycle progression, DNA replication and metabolism have also been reported (Verstraeten, *et al.*, 2011). This has led to uncertainty about the essential function of these proteins in cells.

EngA is an essential bacterial GTPase with tandem GTP-binding domains and a C-terminal KH-like domain. Polysome profiles of EngA-depleted cells revealed a decrease in the level of 70S ribosomes and an accumulation of 30S and 50S ribosomal subunits in *E. coli* and *Bacillus subtilis* (Bharat *et al.*, 2006). Depletion of EngA also led to accumulation of precursors to the 16S and 23S rRNA (Hwang *et al.*, 2006). When the ribosomal species in cell lysates were resolved on sucrose gradients, EngA cofractionated with the 50S subunit (Bharat, *et al.*, 2006; Hwang *et al.*, 2008; Tomar *et al.*, 2009). Non-ribosomal phenotypes of depletion of EngA have also been reported. Cells that were depleted of *engA* and stained with 4`, 6-diamino-2-phenyl indole (DAPI) showed cell filamentation and abnormal chromosome segregation in *E. coli* (Hwang, *et al.*, 2001) and nucleoid condensation in *B. subtilis* (Morimoto, *et al.*, 2002). In both of these studies, EngA was suggested to act in cell cycle regulation.

One common phenotype of mutation of ribosomal structural proteins or ribosome biogenesis factors is sensitivity to growth at lower temperatures. Cold sensitivity has been reported for mutants of ribosomal structural genes, (e.g., *rpsE* and *rpsO*) as well as ribosome biogenesis factors such as helicases (e.g., *srmB* and *deaD*), modification enzymes (e.g., *ksgA* and *rluC*), and RNA binding proteins (e.g. *rbfA* and *rimP*) (Bubunenko *et al.*, 2006; Charollais, *et al.*, 2003; Connolly, *et al.*, 2008; Dammel *et al.*, 1995; Guthrie *et al.*, 1969; Jiang *et al.*, 2007a; Jones *et al.*, 1996; Nord *et al.*, 2009; Shajani, *et al.*, 2011). Ribosomal RNA undergoes secondary and tertiary folding during ribosome biogenesis to form intermediates, which undergo refolding and fine-tuning in their way to the final structure. A decrease in temperature reduces the energy that is available for normal rRNA fluctuations and may stabilize immature structures. This reduced efficiency of biogenesis at low temperature may be exacerbated by deletion of a gene involved in ribosome biogenesis.

In *E. coli*, there are seven operons (*rrnA, rrnB, rrnC, rrnD, rrnE, rrnG* and *rrnH*) interspersed on the chromosome, which encode the cotranscript of 16S, 23S and 5S rRNA. Each operon is controlled by two promoters, called *rrn* P1 and *rrn* P2. The P1 promoter contains sequences that enable strong activation, including three to five binding sites for the Fis regulatory protein and a UP element. Transcription of rRNA is thought to be the rate-limiting step of ribosome biogenesis and is subject to multiple mechanisms of regulation to ensure that the level of ribosomes matches the requirement of the cell (Paul*, et al.*, 2004b). One of these mechanisms is a negative feedback loop where incorporation of rRNA into translating ribosomes inhibits the transcriptional activity of rRNA promoters (Cole *et al.*, 1987; Jinks-Robertson *et al.*, 1983; Yamagishi *et al.*, 1987). This feedback appears to be regulated by the molecules ppGpp and NTP and the protein DksA (Paul *et al.*, 2004a; Schneider *et al.*, 2003). Disruption of translation by depletion of the initiation factor IF-2 or addition of antibiotics led to an increase in rRNA expression (Cole*, et al.*, 1987; Schneider *et al.*, 2002). Disruption of ribosome biogenesis by overexpression of the r-protein repressor S4, led to increases in expression of rRNA (Cole*, et al.*, 1987; Takebe *et al.*, 1985). We hypothesized that depletion of EngA would lead to lower level of 70S which would cause a higher level of transcription in a reporter of the rRNA promoter, P*rrnH*. A model of feedback inhibition is illustrated in Figure 3-1.
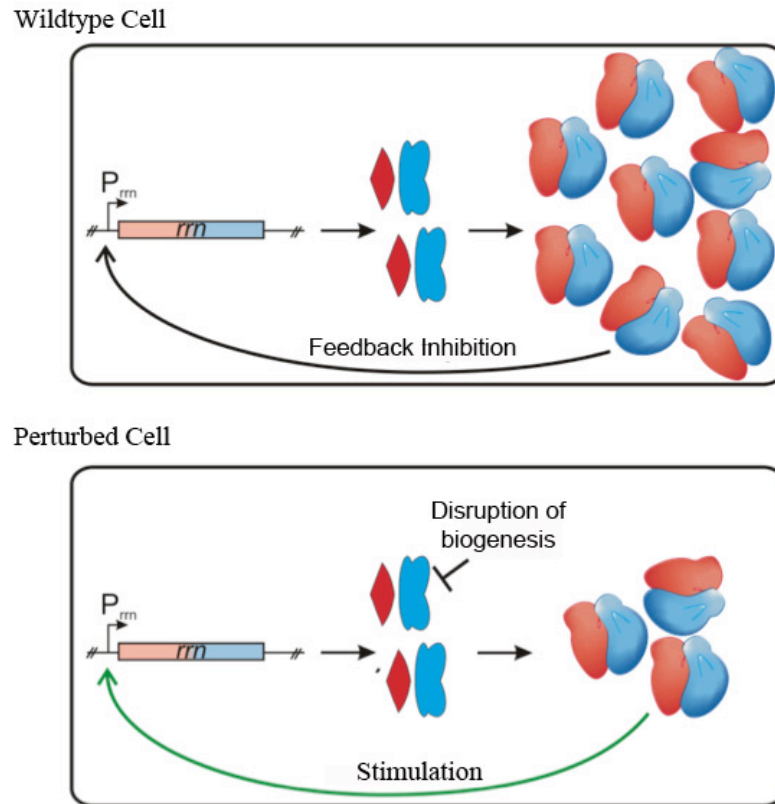
Figure 3-1. Model of ribosomal feedback regulation.
Top, wildtype cell: ribosome biogenesis begins with transcription of the ribosomal rRNA from one of seven *rrn* operons on the *E. coli* chromosome. Ribosome biogenesis proceeds through several intermediates before subunits achieve maturity and undergo initiation of translation. The level of translating 70S ribosomes influences the level of transcription of rRNA. Bottom, perturbed cell: disruption of ribosome biogenesis, which leads to lower levels of mature ribosomes, results in an increase in transcription of rRNA.

In a genetic screen for suppressors of a mutation of G-domain 2 of EngA, DerN321D, it was found that overexpression of RelA suppressed both the slow growth and the ribosome profile defect of this mutant (Hwang*, et al.*, 2008). The ability of RelA to synthesize ppGpp was essential for suppression. During the stringent response to amino acid starvation, RelA transfers a pyrophosphate from ATP onto the 3' position of

either GDP or GTP to form ppGpp or pppGpp, respectively (Magnusson *et al.*, 2005). The global alarmone ppGpp causes global changes in transcription, including a swift downregulation of the synthesis of ribosomal RNA (Magnusson*, et al.*, 2005). The mechanism by which high-level expression of *relA* suppressed the partial loss of the function of EngA is not known. Due to the suppression by RelA and the structural similarity of ppGpp to GTP and GDP, it is possible that EngA binds ppGpp in cells.

Chemical genetic interactions can shed light on the function of a gene. If a chemical worsens the slow growth phenotype of a genetic deletion, this may indicate that they act on the same pathway. The ribosome is the target of many antibiotics, which fall into three categories: aminoglycosides, tetracycline derivative and macrolides. In most cases, aminoglycosides and tetracyclines bind at the A-site while macrolides bind at the P-site. Our laboratory has shown that cells depleted of the *B. subtilis* homologue of the GTPase YjeQ (YloQ) become sensitized to translation inhibitors, as evidenced by a lowered minimum inhibitory concentration (Campbell*, et al.*, 2005c)

To explore the role of EngA in ribosome function, we searched for phenotypes associated with depletion of the protein. Modulatable depletion of *engA* was achieved in strain EB2354 where the deletion was complemented by a copy of *engA* that is under the control of the arabinose-inducible P_{BAD} promoter. Depletion of EngA led to cold sensitive growth and stimulation of a GFP reporter of an rRNA promoter, P_{rrnH}. EngA bound directly to ribosomal subunits in a nucleotide-dependent manner with a preference for the 50S subunit. Different classes of antibiotics that bind the ribosome were used to probe the action of EngA on ribosomes. Depletion of EngA caused sensitization to aminoglycoside antibiotics, which bind at the A-site near the interface side of the 30S subunit. These results support a role for EngA in ribosome biogenesis and imply that EngA may act on the 50S subunit at the interface near the A-site.

3.3   Materials And Methods

Strains. Depletion of EngA was carried out in a conditionally complemented null, which contains a deletion of *engA* at its native locus and a complementing copy of the gene under the control of an arabinose-inducible promoter at the *araBAD* locus in *E. coli* MG1655. Two versions of this strains, carrying different antibiotic resistance markers, were used: EB1209 (*araBAD*::*engA-kan*^{R}, *engA*::*Cm*^{R}) or EB2354 (*araBAD*::*engA-tet*^{R}, *engA*::*Cm*^{R}). EB68 is wildtype *E. coli* MG1655.

Cold Sensitivity of Growth. To achieve partial depletion of EngA, EB2354 and wildtype *E. coli* MG1655 were grown overnight in the absence of arabinose. Cultures were diluted into LB and grown in triplicate at either 15°C or 37°C with shaking at 250 rpm until wildtype reached an OD$_{600}$ of ~ 0.6.

Stimulation of the rRNA promoter, P$_{rrnH}$. Low copy pUA66 reporter plasmids were obtained from a library of known and predicted *E. coli* promoters fused to the GFP fast-folding variant GFPmut2 (Zaslaver *et al.*, 2006). The P$_{rrnH}$ and P$_{lexA}$ reporters were transformed into the EB2354 or EB68. Cultures harboring reporter plasmids were grown overnight in LB-Kan and subcultured twice to deplete EngA. To continuously monitor optical density and fluorescence intensity, cultures were grown at 37°C with shaking in a Synergy Multimode microplate reader. The fluorescence excitation and emission wavelengths used were 485 nm and 520 nm, respectively.

Binding of EngA to nucleotides. All nucleotide-binding assays were carried out using GDP labeled at the 2` or 3` position in ribose ring with 4,4-difluoro-4-bora-3a,4a-diaza-*s*-indacene (BODIPY FL) in black, low-volume, 96-well plates (Costar). Measurements were taken on an Envision multilabel platereader using fluorescence excitation and emission wavelengths of 485 nm and 520 nm, respectively. The direct binding of BODIPY FL-GDP to EngA was measured by the decrease in fluorescence polarization upon binding. The concentration of BODIPY-GDP was kept constant at 0.1 μM and the concentration of enzyme was varied in order to reduce the noise associated with differing concentrations of fluorophore. The dissociation constant, K$_d$, for direct binding of BODIPY FL-GDP to EngA was determined using SigmaPlot software.

The displacement of 0.1 μM BODIPY-GDP from 1 μM EngA by various concentrations of unlabeled GMP, GDP, ppGpp or the nonhydrolyzable GTP analogs, GMPPCP and GMPPCP were tested. The competitive displacement curves were fitted with SigmaPlot software to a four parameter logistic model using Equation 1, where FP is fluorescence polarization, min and max are the fitted minimum and maximum polarization, Hillslope is the slope of the curve at its midpoint and EC_{50} is the concentration of competitive ligand producing 50% displacement.

$$FP = min + \frac{(max - min)}{1 + \frac{[competitor]}{EC_{50}}^{-Hillslope}} \qquad \text{(Eq. 1)}$$

The EC_{50} of the competitive ligand was related to the inhibition constant, K_i, using Equation 2, where L is the concentration of labeled ligand and K_d is the dissociation constant of the labeled ligand, which was previously determined.

$$K_i = \frac{EC_{50}}{1 + \frac{L}{K_d}} \qquad \text{(Eq. 2)}$$

Purification of ribosomal subunits. 30S, 50S and 70S ribosomes were prepared as previously described (Spedding, 1990) with some modification. *E. coli* MG1655 was grown in LB broth to an OD_{600} of 0.6, and slowly cooled to 15°C to produce runoff ribosomes, free of mRNA (Spedding, 1990). Cells were harvested by centrifugation at 8, 500 x g for 15 min, suspended, and washed with buffer R (20 mM Tris-HCl [pH 7.5 at 4°C], 10 mM magnesium acetate, 100 mM NH_4Cl, 100 mM KCl and 3 mM 2-mercaptoethanol). All subsequent steps were performed at 4°C. The cell suspension was lysed by three consecutive passes through a French pressure cell at 10,000 lb/in^2 followed by the addition of 500 U of RNase-free DNase I (Roche, Laval, QC). An S30 fraction was generated by centrifugation of the extract at 30, 000 x g for 1 h. The top three-fourths of the S30 supernatant was overlaid onto an equal volume of 1.1 M sucrose cushions made up in buffer A. Samples were centrifuged at 100, 000 x g for 15 h. The clear

ribosomal pellet was gently washed with buffer R, and then suspended by gentle agitation for 2 hr.

To resolve 30S, 50S and 70S ribosomes, the ribosomal pellet was suspended in buffer R and centrifugation on 10 - 30% (*wt/vol*) linear sucrose gradients at 48, 000 x g for 15 h. The gradients were fractionated by upward displacement using 60% (*vol/vol*) glycerol and 0.5 mL fractions were collected. The centre fractions of each subunit peak were pooled. The pooled fractions were centrifuged at 56, 000 x g for 16 h to pellet the subunits. Ribosomes were quantified by measuring absorbance at 260 nm, where 1 A_{260} unit is equivalent to approximately 69, 34.5 or 23 pmol of 30, 50S or 70S ribosomes, respectively. Aliquots were stored at -80°C in Buffer R.

Binding of EngA to ribosomes. EngA (50 pmol) was incubated with purified 30S, 50S or 70S (150 pmol) in Buffer R (20 mM Tris-HCl [pH 7.5 at 4°C], 10 mM magnesium acetate, 100 mM NH_4Cl, 100 mM KCl and 3 mM 2-mercaptoethanol) with no nucleotide, 1 mM GDP or 1 mM ppGpp for 30 minutes at ambient temperature. Controls lacking ribosomes were also included. The reaction (100 μL) was overlayed onto a 20% (*wt/vol*) sucrose cushion (100 μL) and centrifuged in a TLA-120.1 rotor at 70, 000 x g for 2 hours at 4°C. The pellets, which contained ribosomes and any bound EngA, were resuspended in 200 μL buffer R. All pellet and supernatant fractions were analyzed by western blot using an α-EngA antibody as described in Chapter 2.

Antibiotic enhancement of slow growth of EngA-depleted cells. Minimum inhibitory concentrations were obtained for ribosomal antibiotics in EngA-depleted and EngA-replete conditions. EB1209 was diluted to an OD_{600} of 0.001 and added to 96-well plates. Antibiotic was added in duplicate to the first column and twelve 2-fold serial dilutions were carried out. Cultures were grown at 37°C for 16 hrs without shaking and OD_{600} was read on a SpectraMax spectrophotometer.

3.4   Results

3.4.1   Depletion of EngA caused cold sensitive growth

Sensitivity to growth at low temperature is a common phenotype of mutation of ribosome biogenesis factors and ribosomal structural proteins. Depletion of EngA in EB2354 was achieved by growth in the absence of the inducer, arabinose. Depletion of EngA resulted in a 2-fold reduction in growth at 37°C and a 10-fold reduction in growth at 15°C (Figure 3-2). This represents a cold sensitivity factor of 5-fold.   This is the first demonstration of cold sensitivity due to loss of EngA.
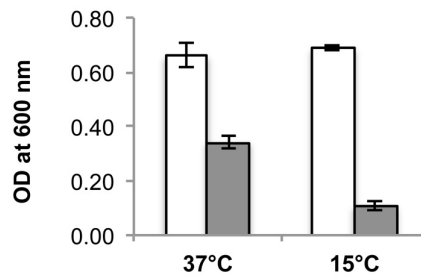
Figure 3-2. Cold sensitivity due to depletion of EngA.
EB68 and EB2354 were grown overnight in LB to partially deplete EngA. Cultures were diluted into LB and grown at the indicated temperatures until wildtype achieved an optical density of 0.7 at 600 nm.   The optical density of wildtype (white bars) and EngA-depleted cultures (gray bars) are shown at 37°C and 15°C. The data represent the average of triplicates.

3.4.2   Stimulation of the rRNA promoter, P_{rrnH} in cells depleted of EngA

Ribosomal feedback regulation refers to the observation that the level of functional 70S ribosomes in the cell influences the rate of transcription of new rRNA. To test the hypothesis that EngA is important for the production of normal levels of 70S ribosomes, the transcriptional activity of an rRNA promoter, P_{rrnH}, was tested. We used a pUA66 reporter plasmid containing the fast-folding GFP variant, GFPmut2 (Zaslaver, *et al.*, 2006). The promoter for *lexA*, a gene that is involved in DNA repair, was used as a

negative control. After two rounds of growth in the absence of inducer, EB2354 harboring P_{rrnH}-pUA66 or P_{lexA}-pUA66 showed profound slow growth compared to wildtype (Figure 3-3, top panels). In EB2354, P_{rrnH}-pUA66 produced an almost wildtype level of fluorescence while P_{lexA}-pUA66 produced a low level of fluorescence that was proportional to the low level of growth of this strain (Figure 3-3, middle panel). Thus, the cell-density normalized fluorescence was 5-fold higher in EngA-depleted cells, compared to wildtype cells (Figure 3-3, bottom panel, left). The cell-density normalized fluorescence of P_{lexA} was nearly identical in wildtype and EngA-depleted cells (Figure 3-3, bottom panel, right).
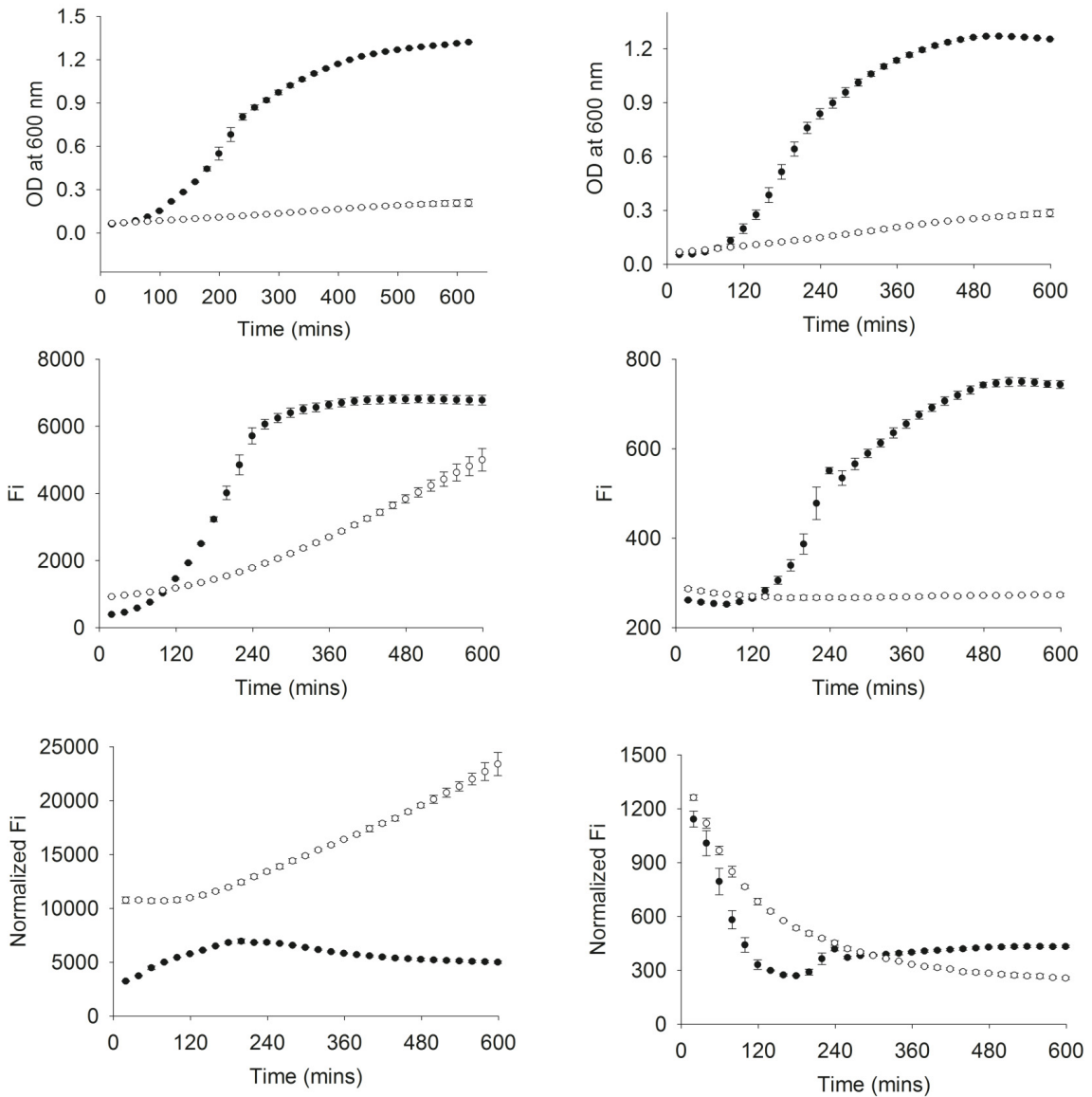
Figure 3-3. Stimulation of an rRNA promoter in EngA-depleted cells using a GFP reporter.

EB68 and EB2354 were grown overnight and subcultured twice in the absence of arabinose to deplete EngA. Cultures were incubated at 37°C with rotation in a Synergy Multimode microplate reader while continuously monitoring optical density at 600 nm and fluorescence intensity (λ_{Ex} 485 nm and λ_{Em} 520 nm). The expression of the ribosomal promoter in a GFP reporter plasmid, P_{rrnH}-pUA66 (left) and a negative control reporter, P_{lexA}-pUA66 (right) in EngA-depleted cells (open circles) or wildtype *E. coli* MG1655 (closed circles) are shown. From top to bottom are cell density, fluorescence intensity (Fi) and cell density-normalized fluorescence of each reporter plasmid.

3.4.3   Affinity of EngA for nucleotides.

The function of GTPase is normally closely tied to its GTPase cycle, whereby nucleotide binding dictates the interaction with an effector molecule. The affinity of EngA for guanine nucleotides was tested to better understand how EngA is regulated in cells. The displacement of fluorescently labeled GDP from EngA by unlabeled nucleotides was measured by fluorescence polarization. When a free fluorophore is excited by plane polarized light, the light is emitted in many planes due to the rapid tumbling of the fluorophore, leading to low polarization (Lakowicz, 1999). If the fluorophore is bound to a large molecule such as a protein, its rotation is slower and more of the emitted light is in the same plane as the excitation light, resulting in higher polarization (Lakowicz, 1999). In this assay, we used GDP labeled at the 2' or 3' hydroxyl of the ribose ring with a 4,4-difluoro-4-bora-3a-4a-diaza-*s*-indacene (BODIPY) fluorescent moiety. This fluorophore produced a stronger signal and less noise than the 2′/3′-O-N-methylanthraniloyl (MANT) label, which is likely due to the higher fluorescence intensity and longer lifetime of BODIPY (Invitrogen, 2005).

BODIPY-GDP bound EngA with a dissociation constant (K_d) of 2 μM. Displacement of BODIPY-GDP from EngA by GMP, GDP and ppGpp were tested. We were interested in the affinity of EngA for ppGpp due to a previous report that overexpression of the ppGpp synthase *relA* suppressed both the slow growth phenotype and the defective ribosome profile of an EngA mutant, DerN321D (Hwang*, et al.*, 2008). EngA bound ppGpp as tightly as GDP, with both displaying inhibition constants of 2 μM (Figure 3-4A). No binding was observed for the mononucleotide GMP. Two nonhydrolyzable GTP analogs GMPPNP and GMPPCP were tested. In GMPPNP, the bridging oxygen between the β and γ phosphates is replaced by a nitrogen atom and in GMPCP, the β phosphate is replaced by a methylene group. Neither molecule demonstrated any binding to EngA up to a concentration of 1 mM (data not shown).

3.4.4   Preferential binding of EngA to the 50S subunit

When cell lysate was resolved on a sucrose gradient, EngA cofractionated with the 50S ribosomal subunit (Bharat*, et al.*, 2006; Hwang*, et al.*, 2006). Here, the interaction was tested with purified components to check for direct binding to ribosomes. Untagged EngA was incubated with a 3-fold excess of *E. coli* 30S, 50S or 70S ribosomes with 1 mM GDP, no nucleotide or 1 mM ppGpp. The reactions were centrifuged over a sucrose cushion to pellet ribosomes and the pellet and supernatant fractions were subjected to Western blot analysis of bound EngA in the ribosomal pellet and unbound EngA in the supernatant.

A.
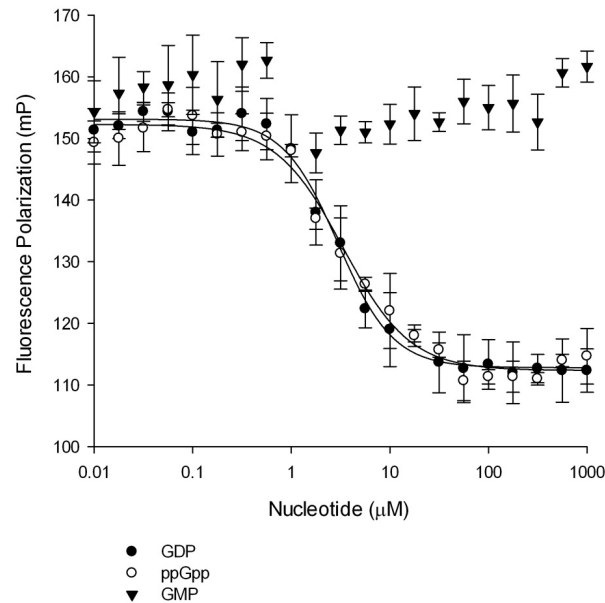
B.
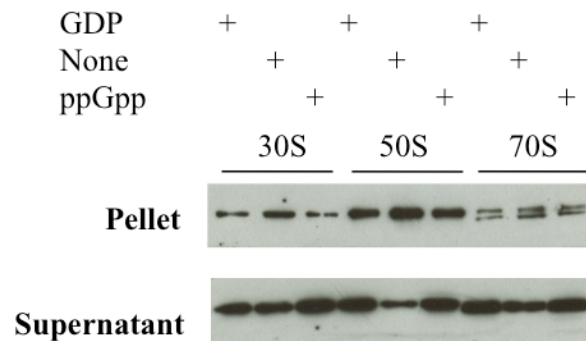
Figure 3-4. Nucleotide dependence of binding of EngA to ribosomal subunits.
(A) The affinity of EngA for GMP, GDP or ppGpp was tested by measuring the displacement of
0.1 μM fluorescent BODIPY FL-GDP from 1 μM EngA by various concentrations of unlabeled
nucleotide. Fluorescence polarization was monitored on an Envision platereader (λ_{Ex} 485 nm and
λ_{Em} 520 nm). The data were fitted to a four parameter logistic equation using SigmaPlot
software. (B) Purified untagged EngA (50 pmole) was incubated with a 3-fold excess of *E. coli*
30S, 50S and 70S ribosomes in the presence of 1 mM GDP, no nucleotide or 1 mM ppGpp. The
reactions were centrifuged at over a sucrose cushion at 70, 000 x g for 2 hours to pellet
ribosomes. Western blot analysis was performed to detect bound EngA in the ribosomal pellet
and unbound EngA in the supernatant.

EngA bound the large 50S subunit with higher affinity than the small 30S subunit or to 70S ribosomes (Figure 3-4B). GDP and ppGpp further inhibited binding. In the timescale of the incubation and centrifugation steps of this assay, bound GTP would be hydrolyzed to GDP so GTP was not tested. Thus, EngA demonstrated sub-stoichiometric but nucleotide-dependent and direct binding to ribosomes.

3.4.5 Depletion of EngA causes sensitization to aminoglycoside antibiotics.

Ribosomal antibiotics whose mechanisms of action and binding sites of the ribosomes are known were used to probe the role of EngA on the ribosome. We looked for sensitization of EngA-depleted cells to antibiotics from the following classes: tetracycline derivatives, aminoglycosides and macrolides. Although the ribosome is very large, most of the translation inhibitors bind near the active site to disrupt either decoding (A-site), peptidyltransferase reaction (P-site) or threading of the nascent polypeptide through the exit tunnel. The MIC of each antibiotic was determined in EngA-depleted and EngA-replete conditions. A cut-off of > 2-fold decrease in MIC upon depletion of EngA was used to determine sensitization.
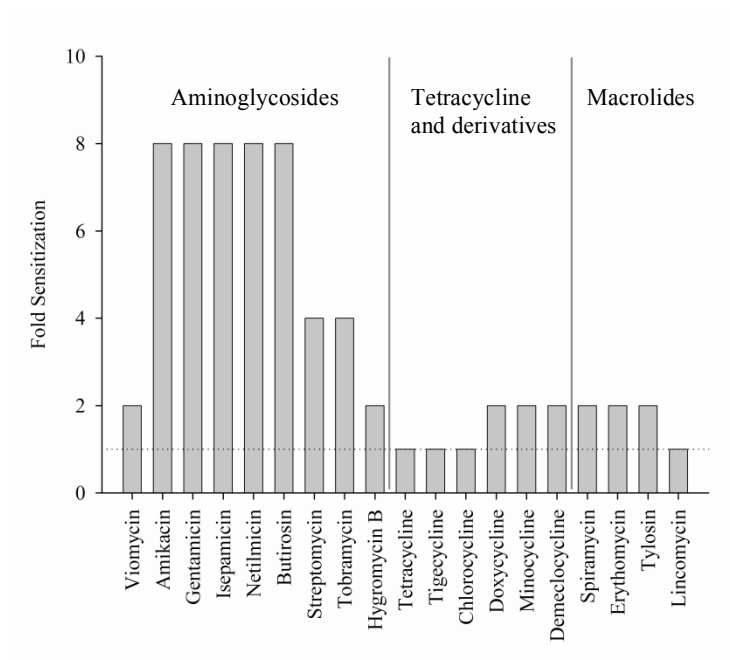
Figure 3-5. Sensitization of EngA-depleted cells to different classes of ribosomal antibiotics.
EB2354 was partially depleted of EngA by growth in the absence of arabinose until stationary phase. Cultures were diluted into LB with or without 1% arabinose in 96-well plates and grown at 37°C without shaking. The minimum inhibitory concentration of each antibiotic was determined. Fold sensitization refers to the decrease in the MIC of the antibiotic in EngA-depleted cells compared to complemented cells. The data represent the average of duplicates. The cut-off for sensitization was set at 2-fold (dashed line).

Of the ribosomal antibiotics, the aminoglycosides were the only class that showed chemical genetic interactions with EngA (Figure 3-5). Depletion of EngA caused 4-fold to 8-fold sensitization to 7 of the 9 aminoglycosides that were tested. Like aminoglycosides, tetracycline derivatives are also A-site inhibitors but these did not cause the same sensitization. Tetracyclines bind to helices 31 and 34 and prevent tRNA binding while the aminoglycosides bind to helix 44 and cause miscoding (Puglisi *et al.*, 2000). Thus, depletion of EngA specifically sensitized cells to the subset of antibiotics that bind helix 44 and interfere with decoding.

3.5   <u>Discussion</u>

Most of the conserved small GTPases in *E. coli* appear to have important roles in ribosome biogenesis, but diverse non-ribosomal phenotypes are also associated with these genes. Here, several phenotypes of depletion of EngA were elucidated, including cold sensitivity, stimulation of an rRNA promoter and sensitivity to aminoglycoside antibiotics. EngA bound ribosomes in a nucleotide-dependent manner. These results are consistent with a ribosomal function for EngA.

Slow growth upon depletion of EngA was enhanced at low temperature. Cold sensitivity is not a definitive phenotype of ribosome function since other processes are also affected by cold temperature but this phenotype is common among mutants of ribosomal genes. Normally, several rounds of growth in the absence of inducer are necessary to achieve adequate depletion of EngA. The exacerbation of slow growth at low temperature is a useful phenotype for future assays because it produces a profound growth phenotype faster than at 37°C.

Depletion of EngA caused a 5-fold increase in expression from the promoter of the rRNA operon, *rrnH*. This observation is consistent with the model of feedback regulation whereby a decrease in the translational activity of the cell leads to higher transcription of rRNA. When ribosome biogenesis was disrupted by overexpression of the repressor r-protein, S4, the synthesis of rRNA was increased by 50% (Takebe*, et al.*, 1985). Among the ribosomal promoters, the rRNA promoters are more suitable than the ribosomal protein promoters for use in a GFP reporter assay because rRNA is regulated at the level of transcription, whereas r-proteins are mainly regulated at the level of translation (Dennis*, et al.*, 2004). The stimulation of P$_{rrnH}$ was observed in rich LB media, which contains a large excess of nutrients, so the results should not be confounded by changes in rRNA expression that are due to nutrient fluctuations. The stimulation of an rRNA promoter in response to depletion of EngA is consistent with a role for EngA in ribosome biogenesis but does not rule out a function in protein translation.

EngA bound the nucleotide GDP with an affinity of 2 µM. This is consistent with the reported binding of GDP to *Salmonella thyphimurium* EngA, where the binding was

fitted to a two-site model, yielding a K_d of 3 µM in a lower affinity site and 0.6 µM in a higher affinity site were found (Lamb *et al.*, 2007). EngA bound ppGpp as strongly as GDP. Binding of EngA to ppGpp is interesting because a mutant of EngA could be rescued by overexpression of RelA, the enzyme that synthesizes ppGpp (Hwang*, et al.*, 2008). The ability of RelA to synthesize ppGpp was essential for suppression. The mechanism of suppression by RelA is not known but our results suggest that this mechanism may involve binding of ppGpp to EngA.

Direct, nucleotide-dependent association was observed between EngA and the 30S, 50S and 70S ribosomes with a preference for 50S subunits. The interactions were strongest in the absence of nucleotide. In Chapter 2, overexpressed EngA was reported to cofractionate exclusively with the 50S subunit. Through a series of mutations, Tomar *et al* have concluded that when both G-domains of EngA are bound to GTP, EngA binds 50S specifically but when G-domain 1 is bound to GDP and G-domain 2 is bound to GTP, it binds 30S, 50S and 70S (Tomar*, et al.*, 2009). In all cases, the interactions were sub-stoichiometric which may be reflective of the transient nature of biological interactions (Droit *et al.*, 2005). The nucleotide-dependence observed here for binding of *E. coli* EngA to ribosomes is the same dependence that was observed for the *B. subtilis* orthologue of EngA (YphC) binding to 70S ribosomes (Schaefer*, et al.*, 2006). The interaction of the related GTPase, Era, with ribosomes was also strongest in the absence of nucleotides (Sayed *et al.*, 1999).

Finally, when EngA-depleted cells were tested for sensitization to ribosomal antibiotics with diverse mechanisms of action, loss of EngA resulted in sensitization to aminoglycosides. Aminoglycosides bind helix 44 in the 30S subunit at the amino-acyl tRNA binding site (A-site) and cause miscoding (Carter *et al.*, 2000). Aminoglycosides protect nucleotides A1408, A1492, A1493, and G1494. This stabilizes a conformation of the ribosome that is normally achieved only after correct codon-anticodon recognition, thereby allowing near-cognate codons to bind, which causes miscoding (Yonath, 2005). Although aminoglycosides bind residues on the 30S subunit, the A-site is formed by both

the 30S and 50S subunit. The loss of EngA may cause conformational changes in the A-site that make it easier for aminoglycosides to bind.

Overexpression of EngA suppressed a deletion of *rrmJ*, which transfers a methyl group from S-adenosyl methionine to U2552 of 23S rRNA (Tan*, et al.*, 2002b). The mechanism of suppression is not known but EngA was able to restore wildtype levels of 70S without restoring the methylation at U2552. This residue is on a loop of 23S rRNA that makes a direct contact with the aminoacyl (A)-site tRNA. Perhaps EngA binds near the A-site and stabilizes a conformation that allows maturation to continue without the methylation of U2552. This is consistent with the sensitization to A-site binding aminoglycosides.

The phenotypes of depletion of EngA as well as direct, nucleotide-dependent binding of EngA to ribosomes suggest a ribosome-related function for this essential GTPase. Depletion of EngA resulted in cold sensitivity, stimulation of an rRNA promoter and sensitization to aminoglycosides. EngA bound the nucleotides GDP and ppGpp with similar affinity and binding to nucleotides reduced its affinity for ribosomes. EngA was sensitized to aminoglycosides, which bind at the A-site and was previously reported to suppress RrmJ, which methylates a residue near the A-site. Thus, these observations point to the A-site of the 50S subunit as the site of action of EngA.

4   CHAPTER FOUR – IN SEARCH OF AN INHIBITOR OF BACTERIAL RIBOSOME BIOGENESIS: A HIGH-THROUGHPUT SCREEN OF THE GTPASE ACTIVITY OF *ESCHERICHIA COLI* ENGA.

Preface to Chapter 4

All of the experiments described in this Chapter were carried out myself. Jenny Wang and Jan Blanchard from the McMaster High-throughput screening laboratory provided assistance with the primary screen and data analysis.

4.1 Summary

Ribosome biogenesis is an essential process that is aided by *trans*-acting factors, such as the GTPase EngA, a promising antibacterial target that is essential in bacteria and absent in humans. To search for an inhibitor of *Escherichia coli* EngA, a high-throughput screen of 31, 800 molecules was carried out against its GTPase activity. The malachite green assay for phosphate detection was optimized for a robust screen at 384-well density. Of the 44 active molecules identified in the screen, compounds that were prone to aggregation or reactivity or those that interfered with the malachite green assay were eliminated. The 4 remaining inhibitors displayed half maximal inhibition constants (IC_{50}) of 5 μM – 15 μM and had antibacterial activity against *Bacillus subtilis*. The inhibition by these 4 compounds was, however, not competitive with substrate and displayed equivocal signs of aggregate-based inhibition such as time dependence and reversal of inhibition in the presence of higher concentrations of Triton X-100 or BSA. More definitive evidence of non-specificity was provided by a test for inhibition of the unrelated enzyme, dihydrofolate reductase. A specific inhibitor has not yet been identified, however, this robust high throughput assay can be used to screen larger collections of small molecule libraries.

4.2 Introduction

In *Escherichia coli*, ribosomes constitute up to a third of the dry mass of the cell and, correspondingly, the synthesis of ribosomes consumes a significant portion of the cell's energy. An inhibitor of ribosome biogenesis could potentially be developed into an antibacterial with a novel mechanism of action. Experiments aimed at elucidating the role of *engA*, which is an essential gene, require protein depletion in a strain where the deletion is complemented by an inducible copy of the gene. The length of time that is necessary to achieve protein depletion increases the chances of secondary effects and suppressor mutations. An inhibitor of EngA would provide quick, reversible inhibition and would thus be a useful tool for studying the function EngA.   This molecule may also

shed light on the biogenesis of the 50S subunit by producing immature subunits on a short time scale.

In prokaryotes, the 70S ribosome is composed of a 30S small subunit and a 50S large subunit. Bacterial ribosome biogenesis involves the processing, folding and assembly of 54 proteins and 3 rRNAs in an extremely complex process that is both sequential and cooperative (Culver *et al.*, 1999a). Ribosomal subunit assembly has been reconstituted *in vitro* with purified components, however, the reaction requires long incubations, high ionic concentrations and elevated temperature (Christiansen *et al.*, 1976; Traub *et al.*, 1968). During fast growth in *E. coli*, the synthesis of a ribosome takes only about two minutes because several classes of *trans*-acting factors aid the process. The classes of ribosome biogenesis factors (RBFs) in prokaryotes include RNases, helicases, methyltransferases, pseudouridylases, folding chaperones and GTPases (Brown, 2005). Unlike the other classes, many of the GTPases, such as EngA, CgtA, YihA and Era are essential for bacterial survival. The essential GTPases may represent good targets for development of new antibacterial agents that inhibit ribosome biogenesis. These proteins have been shown to bind ribosomal subunits and protein depletion causes accumulation of 30S and 50S subunits as well as accumulation of unprocessed rRNA (Brown, 2005; Verstraeten*, et al.*, 2011).

EngA is a broadly conserved bacterial GTPase that lacks a human orthologue and has been shown to be indispensable to a variety of Gram-positive and Gram-negative organisms (Forsyth*, et al.*, 2002; Hwang*, et al.*, 2001; Mehr*, et al.*, 2000; Morimoto*, et al.*, 2002). This essentiality and absence in humans makes EngA a promising target for the development of a new antibacterial. EngA appears to be important for maturation of the 50S subunit. Polysome profiles of EngA-depleted cells revealed a decrease in the level of 70S ribosomes and an accumulation of 30S and 50S ribosomal subunits compared to fully complemented or wild type cells (Bharat*, et al.*, 2006). EngA cofractionated with the 50S subunit on sucrose gradients (Bharat*, et al.*, 2006; Hwang*, et al.*, 2006). In *B. subtilis*, the 50S subunit from cells that were depleted of YphC (the EngA orthologue) migrated slower on a sucrose cushion compared to wildtype 50S

subunits. These slower-migrating subunits had reduced levels of the r-proteins L16, L27 and L36. Depletion of EngA also led to accumulation of the unprocessed rRNA precursors pre-23S and pre-16S (Hwang*, et al.*, 2006). EngA was a high copy suppressor of the 23S rRNA methyltransferase *rrmJ / ftsJ* (Tan *et al.*, 2002a) and it copurified with the ribosomal proteins RpsB, RpsC, RplB, RplD and RplN.

The GTPase activity of EngA is essential to its ribosomal function. GTPases function as molecular switches, whereby binding of GTP leads to a productive interaction with an effector and subsequent hydrolysis ends the interaction (Bourne*, et al.*, 1990, 1991). EngA is unique in that it contains a tandem duplication of its GTP-binding domain (G-domain). Steady state kinetic studies revealed that mutations targeting either G-domain had a significant and cooperative impact on the GTPase activity of the protein as a whole (Bharat*, et al.*, 2006). Thus, an inhibitor of either G-domain is likely to inactivate the entire protein. The catalytic rate of EngA is about 5-fold higher than other GTPases in its class (Verstraeten*, et al.*, 2011). This makes EngA more suitable for a high throughput screen of its GTPase activity.

Here, an assay based on detection of phosphate by malachite green was optimized for a high-throughput screen in 384-well plates. We screened 31, 800 compounds from a collection containing synthetic molecules and natural products. Four inhibitors of EngA were identified but further tests revealed that these molecules might be nonspecific aggregate-based inhibitors. Identification of aggregate-based inhibitors can be challenging because each symptom of this type of inhibition may also be displayed in a special case of a specific inhibitor. The screen developed here can be used to screen other compound collections to continue the search for a ribosome biogenesis inhibitor.

4.3   **Materials and Methods**

Materials. The Canadian Chemical Collection includes the Custom Library of 16, 000 compounds (Maybridge), the DIVERSet of 9, 989 compounds (ChemBridge), the Prestwick Chemical Library of 1, 120 compounds (Prestwick), the Natural Products Library of 361 compounds (BioMol), the Lopac[1280] (International Version) of 885

compounds (Sigma) and the Spectrum Collection of 1, 214 compounds (MicroSource). The targeted Kinase Library of 1000 compounds is from Chemical Diversity Labs. Guanosine triphosphate sodium salt (GTP), TrisHCl, $MgCl_2$, KCl, malachite green oxalate and ammonium molybdate tetrahydrate were from obtained from Sigma (Oakville, Ontario). High purity OmniSolv dimethylsulfoxide (DMSO), 98% sulfuric acid, potassium phosphate dibasic and potassium phosphate monobasic were from EMD Biosciences (Gibbstown, New Jersey).

GTPase Assay. All enzymatic assays were carried out with recombinant untagged EngA that was expressed from pDEST14 in BL21-AI cells and purified by Q-Sepharose Fast Flow anion exchange (Amersham Biosciences, Baie D'Urfe, Quebec). One micromolar EngA was incubated with 300 μM GTP in assay buffer (100 mM TrisHCl, 20 mM $MgCl_2$ and 400 mM KCl, pH 7.5) containing 5% *vol/vol* DMSO in a final reaction volume of 50 μL. Reactions were allowed to proceed for 25 minutes at ambient temperature before addition of 20 μL malachite reagent containing 1.65 M sulfuric acid, 0.99% *wt/vol* ammonium molybdate tetrahydrate, 0.066% *wt/vol* malachite green oxalate and 0.1% Tween-20 (method adapted from (Baykov *et al.*, 1988)). This quenched assay was incubated for 25 minutes at ambient temperature for color development. Optical density at 600 nm was read in an EnVision™ multilabel plate reader (Perkin Elmer Life Sciences, Waltham, Massachusetts). The OD_{600} was related to the amount of phosphate produced using the equation of the line of a standard curve.

Primary Screen. EngA was screened against the Canadian Chemical Collection and the Kinase Library, using the GTPase assay described above. We tested 31, 800 compounds in duplicate in 384-well plates. Reactions were set up on an automated SAGIAN™ core system (Beckman Coulter Inc., Fullerton, CA). Compounds dissolved in DMSO were added to a final compound concentration of 20 μM and a final DMSO concentration of 2% *vol/vol*. The same concentration of DMSO was added to high controls (with enzyme) and low controls (without enzyme). Each 384-well plate contained 64 controls in the first two and last two columns; high and low controls alternated from top to bottom.

Z` is a statistical parameter that reflects the quality of a high-throughput screen (Zhang *et al.*, 1999). Z` was calculated for the high and low controls using Equation 1, where σ represents the standard deviation, μ represents the mean and H and L represent high and low controls, respectively.

$$Z` = 1 - \left(\frac{(3\sigma_H + 3\sigma_L)}{|\mu_H - \mu_L|} \right) \qquad \text{(Eq. 1)}$$

The percent activity of each well was calculated from the absorbance data using Equation 2, where C represents the compound value and H and L represent the averages of the high and low controls, respectively, on the same plate.

$$\% \text{ Residual Activity} = \left(\frac{C-L}{H-L} \right) \times 100 \qquad \text{(Eq. 2)}$$

A hit was defined as a compound with a residual activity of less than three standard deviations from the average of the compound data of either replicate, which yielded 44 molecules.

Secondary Screen. The 44 compounds that were selected from the primary screen were retested at 50 μM, using the GTPase assay described above, in the presence or absence of 0.01% Triton X-100 or 2 mM DTT. Susceptibility to Triton X-100 or DTT was defined as restoration of the GTPase activity of EngA to > 70% of the uninhibited activity. The compounds that were not sensitive to Triton X-100 or DTT were tested for interference with the malachite green assay by looking at the signal produced by 30 μM phosphate (KH_2PO_4) in the presence or absence of 50 μM compound. Phosphate and compound were incubated for 25 minutes and A_{600} was read. Compounds that reduced the signal of the phosphate standard by > 70% were eliminated.

HPLC analysis of GTPase activity. The effect of the four candidate inhibitors on the enzymatic conversion of $^{32}_{\alpha}$P-GTP to $^{32}_{\alpha}$P-GDP was monitored by paired ion chromatography (PIC) on a Waters 600 HPLC (Milford, MA). Reactions were quenched

with two volumes of 8M urea and loaded onto an Inertsil ODS-3 column (4 mm x 150 mm, 5 μm) (GL Sciences Inc, Torrance, California). Resolution and elution of GTP and GDP was achieved with a two minute linear gradient from Pic A (15 mM dibasic potassium phosphate and 10 mM tetrabutylammonium hydrogen sulfate, pH 7.0) to Pic B (Pic A containing 30% *vol/vol* acetonitrile), followed by five minutes of Pic B. Analytes were visualized by in-line scintillation counting and quantified by integration of GTP and GDP peaks using the Waters Millenium® software.

      Assay of dose-response and mechanism of inhibition. Various concentrations of the four active molecules were tested in the GTPase assay with 0.5 μM EngA and 100 μM or 1 mM GTP. To obtain dose-response curves, SigmaPlot software was used to fit the data to the four parameter logistic Equation 3, where min and max are the fitted minimum and maximum activities, Hillslope is the slope of the curve at its midpoint and IC_{50} is the concentration of compound producing 50% inhibition.

$$\% \text{ GTPase Activity} = \min + \left(\frac{(\max - \min)}{1 + \frac{[\text{inhibitor}]}{IC_{50}}^{-\text{Hillslope}}} \right) \qquad \text{(Eq. 3)}$$

To calculate the expected change in IC_{50} at low and high substrate concentrations, Equation 4 was used, where K_i is the inhibition constant of a competitive inhibitor, S is substrate concentration and K_M is the Michaelis-Menten constant.

$$K_i = \frac{IC_{50}}{1 + \frac{S}{K_M}} \qquad \text{(Eq. 4)}$$

The K_i of a competitive inhibitor is constant and does not depend on the substrate concentration:

$$(K_i)_{low} = (K_i)_{high}$$

Substituting substrate concentrations of 100 µM or 1000 µM GTP and a K_M of 20 µM into the right side of Equation 4 yields

$$\frac{(IC_{50})_{low}}{\left(1 + \frac{100 \ \mu M}{20 \ \mu M}\right)} = \frac{(IC_{50})_{high}}{\left(1 + \frac{1000 \ \mu M}{20 \ \mu M}\right)}$$

$$8.5 * (IC_{50})_{low} = (IC_{50})_{high}$$

To test the mechanism of inhibition of MAC-0080023, a matrix of concentrations of substrate and inhibitors was tested in the GTPase assay against 0.15 µM EngA. SigmaPlot software was used to fit the data to competitive, uncompetitive or mixed models of inhibition using the sum of the least squares method of regression.

4.4   Results

4.4.1   Optimization of an assay of the GTPase activity of EngA for a High-throughput screen.

EngA catalyzes the hydrolysis of GTP to GDP and phosphate (Pi).   In the presence of strong acid, free phosphate forms a complex with ammonium molybdate and the dye malachite green, resulting in strong absorbance at 600 – 650 nm. Several variations of the malachite green assay and commercial kits were tested. The protocol published by Baykov *et al* produced the biggest signal window between high and low controls (Baykov*, et al.*, 1988). Detection was linear from 5 µM to 80 µM which is appropriate for the amount of phosphate produced in the screen i.e. 10 µM Pi in the low controls and approximately 45 µM Pi in the high controls (Figure 4-1A).   A reaction time of 25 minutes and a concentration of EngA of 1 µM EngA were chosen to ensure that the reaction was linear with time and with enzyme concentration (Figure 4-1B, 4-1C). This linearity indicates that the reaction rate is following first order kinetics, thus increasing the sensitivity to inhibition.
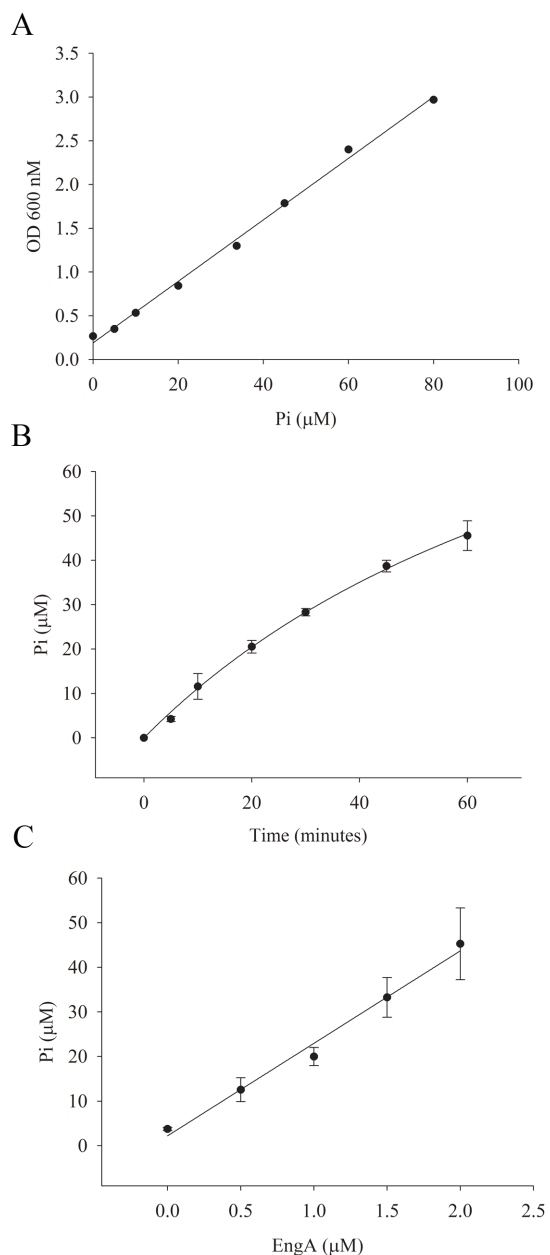
Figure 4-1. Development of an assay of the GTPase activity of EngA for the high-throughput screen.

Standard curve of phosphate using the malachite green assay. Serial dilution of a phosphate standard (KH_2PO_4) was performed with GTPase assay buffer. A solution containing malachite green, ammonium molybdate and Tween-20 was added and color development proceeded for 25 minutes. Optical density at 600 nm was read in an EnVision™ multilabel plate reader. The equation of the line of the standard curve is $y = 0.0352x + 0.1906$ and the R^2 value is 0.996. (B) Reaction progress curve carried out with 1 μM EngA and 300 μM GTP in the presence of 10% *vol/vol* DMSO. The production of phosphate was detected by malachite green and the measured absorbance was related to [Pi] using the equation of the line of the standard curve. (C) Reaction

dependence on enzyme concentration. Various concentrations of EngA were incubated with 300 μM GTP in the presence of 10% *vol/vol* DMSO for 25 minutes. The production of phosphate was detected by malachite green and the measured absorbance was related to [Pi] using the equation of the line of the standard curve.

4.4.2   Primary Screen of the GTPase activity of EngA

EngA was screened against 30, 800 compounds of the Canadian Compound Collection (CCC) and 1000 compounds from the Kinase Library. The CCC is a compilation of synthetic molecules, purified natural products, off-patent and FDA approved drugs and known bioactives while the Kinase Library is a set of molecules that may have a higher likelihood of inhibiting nucleotide-binding enzymes such as EngA. The high controls represent the uninhibited GTPase reaction while the low controls lacked enzyme (Figure 4-2A). The Z` parameter, which takes into account the separation between the high and low controls and the noise of the assay, was 0.68 for this screen. A Z` of 0.5 to 1.0 indicates a primary screen that is sufficiently robust (Zhang, *et al.*, 1999).

Each compound was screened in duplicate at 20 μM. A replica plot of the primary screen showed good reproducibility between the two replicates (Figure 4-2B). A hit was defined as a molecule with residual activity that was more than 3 standard deviations away from the mean of all compounds in either replicate, which corresponded to 63% residual activity. There were 44 hits, representing an overall hit rate of 0.15%. Specifically, compounds sourced from Chembridge, Biomol or Prestwick had hit rates around 0.2% while those sourced from Maybridge had a lower rate (0.03%) and those sourced from Microsource had a higher rate (1%) compared to the overall rate.
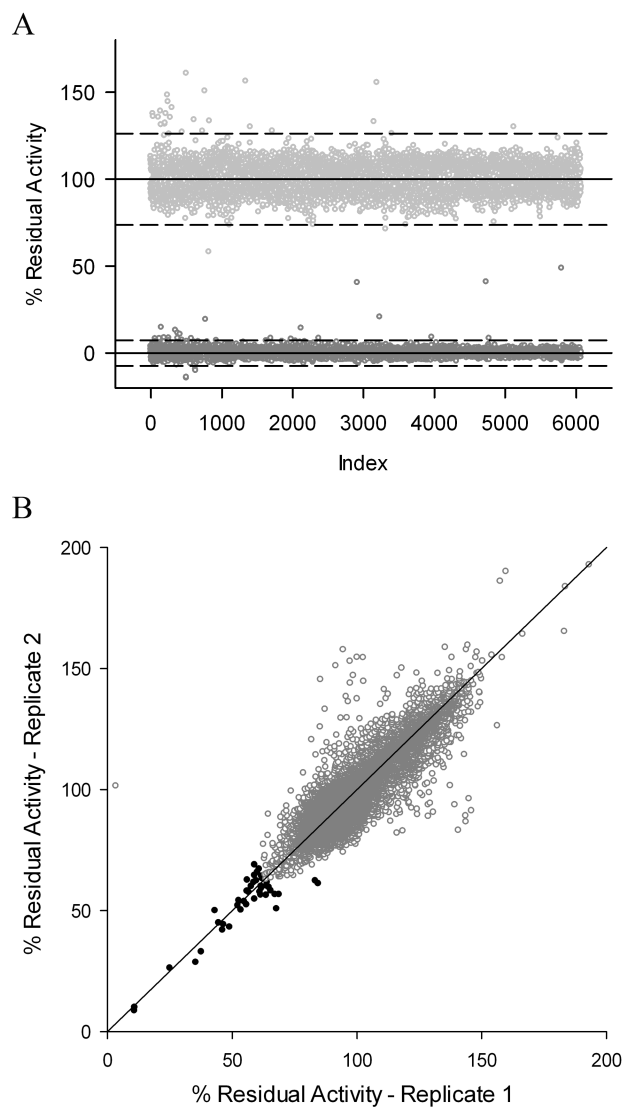
Figure 4-2. Primary screen of the GTPase activity of EngA.

(A) Evaluation of the controls of the screen.   The high controls (light gray circles) represent the GTPase activity of EngA while the low controls (dark gray circles) lack enzyme. Solid lines represent the mean of each sample set while hashed lines represent three standard deviations above and below each mean. Equation 1 was used to calculate a Z` of 0.68, which indicates a good screening window. (B) Replica plot of the primary screen of EngA. The GTPase activity of EngA was screened against 31, 8000 compounds in duplicate. The percent residual activity was calculated using Equation 2 and plotted for each replicate. The diagonal line represents perfect replication. A hit (black circle) was defined as an inhibitor had a percent residual activity that was more than 3 standard deviations away from the mean of the sample set in either replicate.

Figure 4-3 provides an overview of the primary and secondary screen. The structures of the 44 hits from the primary screen can be found in Appendix – Table A1 as well as their potency and reason for elimination.

```
┌──────────────────┐
│ 31, 800 compounds │
└──────────────────┘
         │  Inhibitition in primary
         ↓  screen
     ┌────────┐
     │   44   │
     └────────┘
         │  Inhibition confirmed
         ↓
     ┌────────┐
     │   38   │
     └────────┘
         │  Insensitive to Triton X-100
         ↓
     ┌────────┐
     │   20   │
     └────────┘
         │  Insensitive to Dithiothreitol
         ↓
     ┌────────┐
     │   15   │
     └────────┘
         │  No interference with
         ↓  malachite green assay
     ┌────────┐
     │    4   │
     └────────┘
```
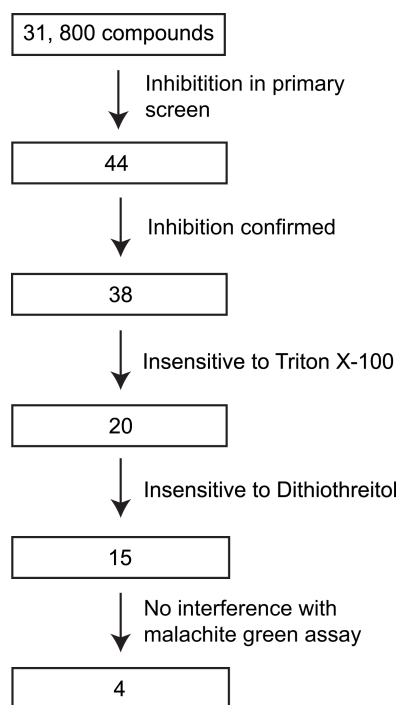
Figure 4-3. An overview of the secondary screen of EngA.
The inhibitors that were identified in the primary screen were tested in four secondary assays in order to select compounds with a higher likelihood of inhibiting EngA specifically. The follow-up tests were (i) confirmation of inhibition, (ii) inhibition in the presence of 0.01% Triton X-100 to check for aggregation, (iii) inhibition in the presence of 2 mM dithiothreitol to check for reactivity and (iv) assay interference by testing the effect of the compound on detection of a phosphate standard.

4.4.3   Confirmation of hits and elimination of aggregating or reactive compounds

Inhibition was confirmed for 38 of the 44 compounds. The majority of hits obtained in any high-throughput screen may due to detergent-sensitive nonspecific inhibition by invisible compound aggregates (Feng *et al.*, 2007; Jadhav *et al.*, 2010). For 18 of the 38 compounds, inhibition was reversed by addition of 0.01% Triton X-100. The structures of the detergent-sensitive molecules were diverse (Appendix 1). Another mechanism of nonspecific inhibition is covalent modification of the enzyme by electrophilic compounds, which can be reversed by a sacrificial nucleophile such as DTT (Blanchard *et al.*, 2004; Dragovich *et al.*, 1998). For 5 of the remaining 20 molecules, inhibition was reversed by addition of 2 mM DTT. In all cases, an arbitrary, but conservative requirement of 30% inhibition was used. To test for interference with phosphate detection by malachite green, each compound was incubated with phosphate alone and the signal from this mixture was measured. In all but four cases, the compound decreased the signal from the phosphate standard by > 30%.

4.4.4   Structure of the four candidate active molecules.

The structures of these four candidates are shown in Figure 4-4. MAC-0174809 and MAC-0080023 are synthetic compounds from the Chembridge library. These two compounds have similar structures i.e. the first and the third rings are identical in the two molecules. The second two molecules are natural products with more complex structures. MAC-0182099 is garcinol, which comes from the Garcinia plant while MAC-0182344 is theaflavin monogallate, which is a polyphenol, found in tea leaves.

MAC0174809   MAC0080023   MAC0182099   MAC0182344
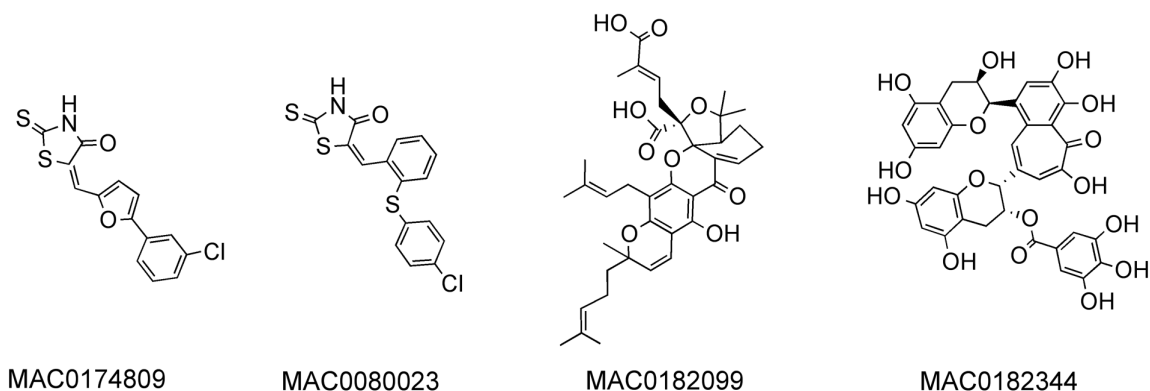
Figure 4-4. Structures of the Inhibitors.

The first two compounds, MAC-0174809 and MAC-0080023, are similar synthetic molecules that both contain rhodanine and chlorobenzene rings. The latter two compounds are natural products. MAC-0182099 is a polyisoprenylated benzophenone compound from the *Garcinia indica* plant, also known as garcinol. MAC-0182344 is theaflavin monogallate, which is a polyphenol found in tea leaves.

4.4.5   Antibacterial Activity of the four inhibitors

A disc diffusion assay was carried out on solid rich media using the antibiotic kanamycin as a positive control and the solvent DMSO as a negative control. The two synthetic compounds (MAC-0174809 and MAC-0080023) and garcinol (MAC-0182099) caused various degrees of growth inhibition in the two Gram-positive organisms *B. subtilis* and *M. luteus* but not the hyperpermeable Gram-negative *E. coli MC1061* (Figure 4-5). The antibacterial activity was strongest in *B. subtilis*. MAC-0182344 only displayed growth inhibition against *B. subtilis*.
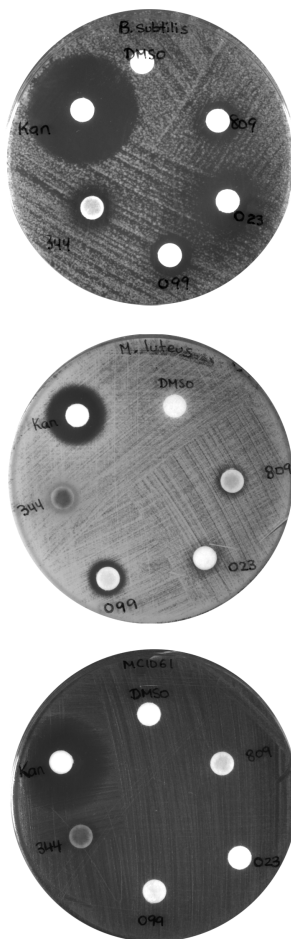
Figure 4-5. Antibacterial activity of the four inhibitors.
Discs were spotted with 10 μL of 5 mM compound, kanamycin or DMSO on LB-agar
plates that were inoculated with *B. subtilis* (top), *M. luteus* (middle) or *E. coli MC1061*
(bottom). Plates were incubated at 37°C for 24 hours. The plates are all in the same
orientation and the positions of the compounds (MAC-0174809, MAC-0080023, MAC-
0182099 and MAC-0182344) are indicated by the last three numbers of the compound
IDs.

4.4.6 *In vitro* **potency of the four inhibitors**

The inhibitor concentrations yielding 50% inhibition (IC_{50}) were 13.3 μM for MAC-0174809, 12.5 μM for MAC-0080023, 14.3 μM for MAC -0182099 and 4.6 μM for MAC-0182344. Reversible inhibitors usually reduce the activity of an enzyme from 90% to 10% over an 81-fold change in inhibitor concentration (Wu, 2010). This yields a slope in the dose response curve that is assigned a Hill slope value of -1. Inhibitors that display aggregate based inhibition tend to reduce the activity of the enzyme over a short range of inhibitor concentration, which causes steeper slopes and higher Hill values (Feng, *et al.*, 2007). However, a higher Hill slope may also result from cooperative binding of the inhibitor to both GTPase domains of EngA (Shoichet, 2006). All four compounds produced steep slopes in the dose-response curves with Hill slopes close to 4 (Figure 4-6A).
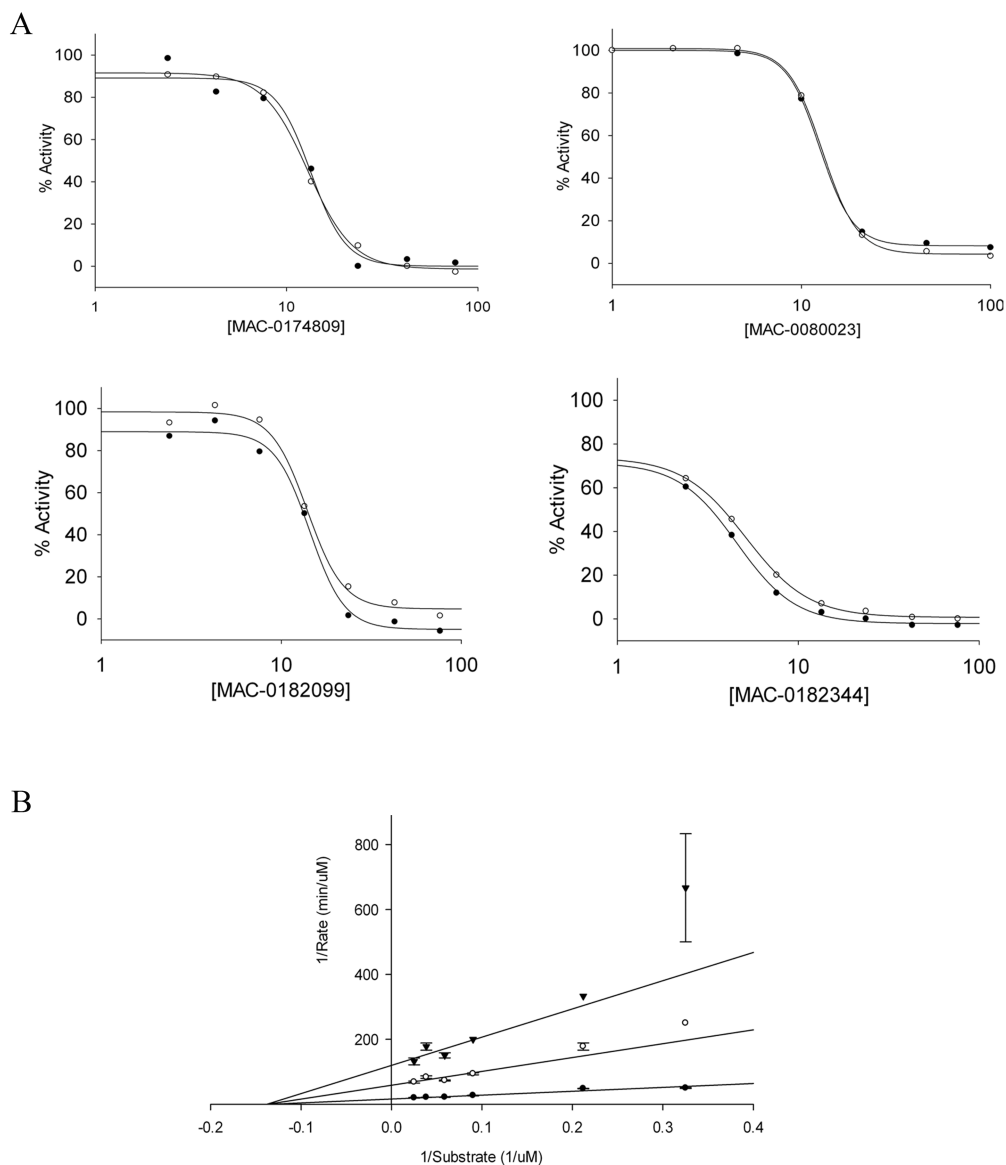
Figure 4-6. Inhibition of EngA by the four active compounds.
(A) Dose-response curves of the inhibitors at two substrate concentrations. The effect of various concentrations of inhibitor on the GTPase activity of 1 μM EngA was tested at 100 μM GTP (open circles) and 1 mM GTP (closed circles). GDP and GTP were resolved and quantified by paired ion chromatography HPLC. SigmaPlot software was used to fit the data to a four parameter logistic model using Equation 3. (B) Mechanism of inhibition of MAC-0080023. The inhibition of 0.075 μM EngA by MAC-0080023 is presented as a double reciprocal plot of 1/rate *versus* 1/[substrate]. The inhibitor was held constant at 0 μM (closed circles), 4.5 μM (open circles) and 5.6 μM (triangles) while GTP was varied from 3 μM – 25 μM. The data was fit to all models of inhibition by nonlinear sum of least squares regression using the Enzyme Kinetics module of Sigma Plot 11.0. A mixed model of inhibition as defined in Eq 5 best described the data.

4.4.7   Mechanism of Inhibition of the four inhibitors

An inhibitor that is competitive with substrate should have a higher IC_{50} in the presence of a higher concentration of GTP. The dose-response curves of the inhibitors were obtained at 100 μM GTP and 1 mM GTP, which should produce an 8.5-fold difference in IC_{50}'s for a competitive inhibitor. The IC_{50}'s of the four inhibitors were almost the same at the high and low concentrations of substrate, indicating that the compounds were probably not competitive inhibitors (Figure 4-6B). A more thorough examination of the mode of inhibition of MAC-0080023 was carried out for with a matrix of concentrations of compound and GTP. The best fit of the data was to the model of mixed inhibition (sometimes referred to as noncompetitive inhibition) with a Hill coefficient of 4. This model is defined in Equation 5, where v_i is initial velocity, V_{max} is the maximal velocity, S is substrate concentration, K_M is the substrate concentration producing half maximal velocity, I is inhibitor, h is the Hill coefficient, K_i is the dissociation constant of the enzyme + inhibitor complex and αK_i is the dissociation constant of the enzyme + substrate + inhibitor complex.

$$v_i = \frac{V_{max}[S]}{K_M\left(1+\frac{[I]^h}{K_i}\right)+S\left(1+\frac{[I]^h}{\alpha K_i}\right)} \qquad \text{(Eq. 5)}$$

Competitive inhibitors bind only the free enzyme and uncompetitive inhibitors bind only the enzyme-substrate complex but mixed inhibitors bind both the free enzyme and the enzyme-substrate complex. Thus, competitive and uncompetitive inhibitors show specificity for one form of the enzyme but mixed inhibitors do not and tend to be nuisance compounds.

4.4.8   Tests for potential aggregate-based inhibition.

The high Hill slopes and lack of competition with substrate may indicate aggregate-based inhibition, however, specific inhibitors may also display these traits. We tested for additional symptoms of aggregate-based inhibition such as time-dependence and sensitivity of inhibition to detergent or BSA. Without pre-incubation of enzyme and compound, the inhibition by MAC-0174809 and MAC-0182099 was reduced, indicating

partial time-dependence (Table 4-1). Inhibition was tested with pre-incubation of enzyme and compound in the presence of 0.01% Triton X-100, 0.1% Triton X-100, 0.1 mg/mL bovine serum albumin (BSA) or 1 mg/mL BSA. Except for MAC-0174809, inhibition was only reversed at high concentrations of Triton X-100 or BSA (Table 4-1). These tests did not make it clear if these compounds were indeed aggregate-based inhibitors.

Table 4-1. Effect of detergent, BSA and pre-incubation on the inhibition of EngA by four compounds.

	% Activity in GTPase Assay			
Inhibitor	MAC-0174809	MAC-0080023	MAC-0182099	MAC-0182344
Reference [a]	16 ± 0	5.8 ± 0.9	11 ± 4.8	6.3 ± 4.8
No pre-incubation	41 ± 2.0	10 ± 3.5	50 ± 1.7	12 ± 3.3
0.01% Triton X-100	54 ± 6.0	6.1 ± 0.5	5.5 ± 0.9	19 ± 4.2
0.1% Triton X-100	84 ± 8.6	97 ± 3.8	33 ± 2.2	76 ± 7.9
0.1 mg/mL BSA	79 ± 9.5	7.9 ± 4.5	11 ± 5.6	14 ± 4.3
1 mg/mL BSA	91 ± 0.9	89 ± 2.3	83 ± 2.8	25 ± 4.1

[a] 0.5 μM EngA and 50 μM compound were pre-incubated for 30 mins before initiation of the GTPase assay.

4.4.9   Specificity of Inhibition.

A more definitive assay of nonspecific inhibition was testing the compounds against an unrelated enzyme. We used dihydrofolate reductase (DHFR), which reduces dihydrofolate to tetrahydrofolate using NADPH as an electron acceptor. Each of the four compounds was tested at 100 μM against DHFR using a spectrophotometric assay whereby the consumption of NADPH was measured by a decrease in absorbance at 340 nm. At this concentration all of the compounds reduced the activity of DHFR to 20% - 40% of uninhibited controls (Figure 4-7).
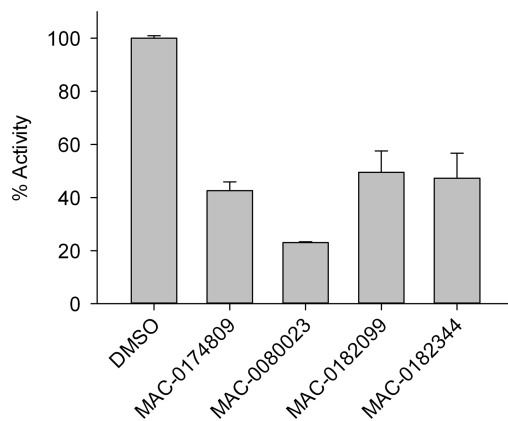
Figure 4-7. Effect of the four inhibitors on an unrelated enzyme, DHFR.
The activity of human DHFR, which reduces dihydrofolate to tetrahydrofolate, was measured by the decrease in absorbance at 340 nm caused by the consumption of NADPH. Reactions contained 50 mM Tris, 1 mM β –mercaptoethanol, 30 μM dihydrofolate, 150 μM NADPH, Triplicate samples were monitored continuously in a spectrophotometer. The decrease in the rate of the DHFR reaction in the presence of 100 μM compound or an equivalent volume of DMSO is shown.

4.5   Discussion

An inhibitor of ribosome biogenesis would be a useful probe for studying this poorly understood but important process and could be developed into an antibacterial with a novel mechanism of action. EngA is a particularly attractive target because it is essential in bacteria and absent in humans. Although a specific inhibitor was not identified in this library of 31, 000 compounds, the screen can be extended to other compound libraries. In this screen, assay conditions were chosen where the formation of product was linear with time and enzyme concentration in order to increase sensitivity to inhibition. The assay was also optimized for low noise and good separation between the high controls and low controls to maximize the screening window. The screen was robust with a Z`-score of 0.68 and good reproducibility between the replicates. The four inhibitors that remained after the secondary screen were determined to be nonspecific

inhibitors. In future screens, it would be useful to prioritize the follow-up test for interference with the malachite green assay and the counter screen against an unrelated enzyme.

Of the compounds that were tested for interference with the malachite green assay, a large percentage showed interference. Two possible reasons for this interference are complexation of phosphate by compound or a change in the redox state of the transition metal molybdenum in the presence of the compound. The formation of the phosphomolybdate complex is sensitive to the redox state of the molybdenum (Katano *et al.*, 2011). As is typical in biochemical screens, many of the inhibitors were non drug-like molecules that inhibited nonspecifically. Two mechanisms of nonspecific inhibition that have been proposed are (i) covalent modification and (ii) formation of large compound aggregates that sequester proteins. These compounds are normally removed by testing for reversal of inhibition by the nucleophile DTT or the detergent Triton X-100.

Of the four most promising inhibitors, the synthetic molecules contained a rhodanine ring, which is a potentially problematic substructure, and the natural products are associated with inhibition of several other enzymes. MAC-0174809 and MAC-0080023, both contained a rhodanine ring. An analysis by Baell *et al* to identify nuisance compounds, which they termed PAINS (Pan Assay Interference compounds), revealed that 40% of compounds containing the rhodanine substructure were inhibitors in at least 2 of the 6 screens analyzed (Baell *et al.*, 2010). MAC-0182099 (garcinolic acid) and MAC-0182099 (theaflavin 3`-gallate) were reported to have a range of effects on enzymes and cells (Arif *et al.*, 2009; Balasubramanyam *et al.*, 2004; Chen *et al.*, 2005; Jankun *et al.*, 2011).

While most non-specific inhibitors could be eliminated with confidence, the specificity of some inhibitors was more equivocal. A compound that inhibits specifically in one assay system may form aggregates in another assay system. Three of the four inhibitors identified in this screen were only sensitive to high concentrations of detergent or BSA and only two inhibitors were somewhat time-dependent, which led to uncertainty

about whether they were *bona fide* inhibitors. All four compounds were about 10-fold more potent against EngA than DHFR. It is possible that significant aggregation happened at 100 μM (the concentration tested for DHFR) but not at 10 μM (near the IC_{50} for EngA), however, due to the lack of competition with substrate or specificity over DHFR, we have concluded that all four molecules are likely inhibiting by aggregation. An *in silico* screen of the X-ray crystal structure of the *Thermotoga maritima* orthologue of EngA yielded three molecules that inhibited EngA and other GTPases (Hwang *et al.*, 2012). The specificity or mechanism of inhibition of these molecules have not been reported.

EngA was previously shown to have a Michaelis-Menten constant (K_M) of 143 μM and a catalytic constant (k_{cat}) of 70 h^{-1} (Bharat*, et al.*, 2006). Although the effect of DMSO on the activity of EngA was minimal at the GTP concentration that was used for the screen, we later discovered that DMSO stimulates EngA at low GTP concentrations, thus lowering the K_M to 20 μM (Appendix - Figure A2). To increase the chance of identifying an inhibitor that is competitive with substrate, future screens should avoid compound libraries that are dissolved in DMSO. The assay developed here allowed a robust high-throughput screen of the GTPase activity of EngA. Although no specific inhibitors were discovered in the Canadian Compound Collection, this high throughput assay can be used with the modifications discussed to continue the search for an inhibitor of ribosome biogenesis.

5   CHAPTER 5 - CONCLUSIONS AND FUTURE DIRECTIONS

5.1 Three possible roles for EngA in ribosome biogenesis

While the role of EngA in ribosome biogenesis has not been resolved, I will discuss three possibilities of how it may aid in subunit maturation. EngA may function in (i) binding the 50S subunit to facilitate a late step of its maturation, (ii) binding free r-proteins to chaperone them to the ribosome, or (iii) sensing the status of guanine nucleotides to regulate rRNA synthesis. The mechanism of action of EngA most likely involves its GTPase cycle, which appears to act as a switch to turn the protein on and off.

5.1.1 Hypothesis 1: EngA binds the 50S subunit and facilitates a late step in maturation

EngA may bind 50S subunits near the end of maturation and facilitate a late step in assembly. EngA was shown here to bind the 50S subunit when overexpressed in *E. coli* cells and to bind 50S preferentially when tested with purified components *in vitro*. Binding to the 50S subunit in cells has been confirmed in other studies (Hwang*, et al.*, 2006; Hwang *et al.*, 2010b). The 50S subunit from EngA-depleted cells migrates at a similar rate or slightly slower than mature 50S on a sucrose gradient, which implies that this species is near maturity (Schaefer*, et al.*, 2006). Subunit maturation involves progressive binding of r-proteins, rearrangement of rRNA and enzymatic modifications. EngA may bind the ribosome at a late stage and facilitate one of these steps. Others have shown that 50S subunits from cells depleted of EngA are missing certain ribosomal proteins in *E. coli* (L2 / RplB, L6 / RplF, L9 / RplI and L18 / RplR) and in *B. subtilis* (L16 / RplP, L27 / RpmA and L36 / RpmJ) (Hwang*, et al.*, 2006; Schaefer*, et al.*, 2006). Addition of putative ribosome biogenesis factors increased the rate of incorporation of specific r-proteins. RimP caused S9 and S19 to bind faster while RimM caused S5 and S12 to bind faster (Bunner*, et al.*, 2010). Similar experiments with EngA could help to clarify if it plays a similar role.

5.1.2   Hypothesis 2: EngA binds free ribosomal proteins and chaperones them to the ribosome

It is possible that EngA chaperones proteins to the ribosome since it was found to interact with the ribosomal proteins RpsB / S2, RpsC / S3, RplB / L2, RplD / L4 and RplN / L14 (Butland, *et al.*, 2005). Except for protein S2, which has a pI of 6.7, the other putative interactors are highly basic with pI of 9.7 – 10.9. The linker between the two GTPase domains of EngA is acidic, with a pI of 2.9. While these ionic interactions may contribute to the binding of EngA to these 4 r-proteins, there are many other basic r-proteins in the cell so the interaction is probably not solely ionic. One of the interaction partners, RplB, was also reduced in the 50S subunit of EngA-depleted cells in *E. coli* (Hwang, *et al.*, 2006). This protein is required for subunit joining to form 70S (Diedrich *et al.*, 2000).

5.1.3   Hypothesis 3: EngA is a sensor of GTP or ppGpp to regulate 70S production

EngA may help to coordinate the translational capacity of the cell with the level of ribosomes by sensing either the balance of GDP:GTP or the level of ppGpp. EngA converts GTP to GDP. GTP is used in translation by several translation factors, such as EF-Tu, EF-G and IF-2, where the binding and hydrolysis of GTP regulates activities of these GTPases. In conditions of low GTP, EngA and other ribosome biogenesis GTPases may catalyze less ribosome synthesis and thus the level of ribosomes would more closely match the translational capacity. EngA was also shown here to bind ppGpp, which attenuates synthesis of rRNA. High levels of ppGpp may bind EngA and inhibit its ribosome synthesis activity.

5.2   EngA binds the 50S subunit

EngA was shown to bind the 50S subunit in cells and *in vitro*. The action of EngA might be at the site of 50S subunit that helps to form the A-site of ribosomes since depletion of EngA leads to sensitization to aminoglycosides. Depletion of another ribosome biogenesis GTPase, YjeQ / RsgA, lead to sensitization to macrolides, which are P-site antibiotics (Campbell, *et al.*, 2005c). This indicates that sensitization to

aminoglycosides is not a general response to perturbation of ribosome biogenesis and may be a clue to the specific function of EngA on the ribosome. Further studies are necessary in order to understand the reason for this sensitization. This might include a costructure of EngA with the 50S subunit to see if it binds near the A-site. The structure of the 50S subunit from cells depleted of EngA may reveal differences in this area.

Some ribosome biogenesis factors are suggested to prevent immature ribosomal subunits from entering translation by occupying the same binding sites as initiation factors, initiation f-met-tRNA or mRNA (Demirci *et al.*, 2010; Jomaa*, et al.*, 2011b; Tu *et al.*, 2011). Thus, Era, YjeQ and KsgA were proposed to provide a quality control check that gives the signal to continue biogenesis. So far the only evidence for a similar function for EngA is the sensitization to aminoglycosides, which may suggest that EngA binds at the intersubunit interface near the active site.

The C-terminal KH-like domain may contain the site of interaction with ribosomes or ribosomal proteins. This is the interaction domain of the related GTPase, Era, however, Era contains a canonic RNA-binding sequence while EngA does not contain any known RNA-binding motifs (Sharma*, et al.*, 2005). Random mutations in the KH-like domain of EngA were created by PCR and tested for complementation of the slow growth of an *rrmJ* null (Hwang*, et al.*, 2010b). Four mutations were identified that reduced the binding of EngA to the 50S subunit, suggesting that the KH domain is important for interaction with 50S.

5.3   The two GTPase domains act cooperatively to achieve function

The data presented here are consistent with unique but cooperative roles for the two G-domains in the function of EngA since each was shown to be important for cell viability and for normal polysome profiles. There are several structural differences between the N and C-terminal G-domains which suggest that they have unique character (Robinson*, et al.*, 2002). The most striking is the positioning of the GTP-binding sites in relation to the uncharacterized C-terminal KH-like domain (Robinson*, et al.*, 2002). In G-domain 1, the conserved motifs of nucleotide binding are right at the interface, while in

G-domain 2, these motifs are distal to the interface. It has recently been shown that G-domain 1 undergoes a rearrangement upon GDP binding which exposes a positively charged face on the KH-like domain (Muench *et al.*, 2006). The structure suggests that the two G-domains communicate differently with the KH-like domain. The remarkable level of cooperativity observed in this enzyme is also suggestive of intramolecular regulation whereby the two activities are exquisitely coordinated to achieve function.

5.4   The GTPase cycle of EngA appears to regulate its function

Canonical TRAFAC GTPases are regulators, which take advantage of a molecular switch mechanism where binding and hydrolysis of GTP turns the protein "on" and "off", respectively. In its "on" state, the GTPase is able bind its interaction partner. Hydrolysis of GTP ends the interaction and the GTPase dissociates. For some GTPases, GTPase activating proteins (GAPs), which stimulate hydrolysis of GTP, or guanine nucleotide exchange factors (GEFs), which promote exchange of GDP for GTP, have been identified. Here, EngA was shown to catalyze the hydrolysis of GTP with a k_{cat} of 70 h^{-1}, which is about 5 times higher than the maximum estimates of activity for other small bacterial GTPases such as Era, YjeQ, Obg and YchF (Verstraeten*, et al.*, 2011). GAPs normally increase hydrolysis by several orders of magnitude. Other than the non-essential protein YihI, which stimulated the activity of EngA about 2-fold, no other GAPs or GEFs have been identified for EngA (Hwang *et al.*, 2010a). Neither the ribosome nor the putative interaction partners of EngA stimulated EngA under the conditions tested (data not shown), however, there may be unknown factors missing from these assays.

The structure of EngA resembles a cloverleaf where the two GTPase domains fold on either side of the central KH domain (Robinson*, et al.*, 2002). In this study, EngA interacted with ribosomes in a nucleotide-dependent manner i.e. binding was inhibited in the presence of excess GDP. This suggests that the GDP-bound form of EngA is in a conformation that is unfavorable for binding ribosomes. This is consistent with the evidence from comparison of two crystal structures of EngA, where GTP binding appears to cause a large shift in the first G-domain that exposes a positively charged face on the

KH domain (Muench, *et al.*, 2006).   This positively charged face may be involved in binding rRNA, which contains negatively charged phosphates and comprises two-thirds of the ribosome. The structure of *T. maritima* EngA contained two phosphates in the active site of G-domain 1 that occupied the positions of the β and γ phosphates of GTP while G-domain 2 contained GDP (this configuration is referred to hereafter as pseudo GTP; GDP). The structure from *B. subtilis* contained GDP in the active sites of both G-domain 1 and 2 (referred to as GDP; GDP). Compared to the GDP-form, when G-domain 1 was bound to pseudo GTP, there was a large shift of up to 60 Å such that the opposite face of this G-domain was presented to the C-terminal KH. This resulted in a positively charged face of the KH domain being exposed to solvent. Like other TRAFAC GTPases, this transition between "on" and "off" states likely dictates the association and dissociation of EngA from the ribosome.

5.5   Concluding Remarks

The synthesis of ribosomes is a major metabolic expense of the cell that requires coordinated synthesis, folding and binding of 54 r-proteins and 3 large rRNAs. Several classes of *trans*-acting factors, including GTPases, likely aid ribosome biogenesis. Two previous observations suggested a role for EngA on the ribosome: genetic suppression of a 23S rRNA methyltransferase and copurification with ribosomal proteins. Depletion of EngA was also associated with non-ribosomal phenotypes such as cell filamentation and nucleoid condensation. Here we show that biochemical and *in vivo* experiments point to a role for EngA in ribosome biogenesis, specifically at a late step in maturation of the 50S subunit. Sensitization to aminoglycosides suggests that depletion of EngA caused profound changes on the ribosome and that the function of EngA may be linked to the A-site. The two GTPase domains of EngA appear to act cooperatively in carrying out the ribosomal function of EngA. A high throughput screen for inhibitors of the GTPase activity was developed to screen compound libraries for an inhibitor, which would be a valuable probe of ribosome biogenesis.

6   <u>REFERENCES</u>

Altschul, S. F., Gish, W., Miller, W., Myers, E. W., & Lipman, D. J. (1990). Basic local alignment search tool. *J Mol Biol, 215*(3), 403-410.

Arif, M., Pradhan, S. K., Thanuja, G. R., Vedamurthy, B. M., Agrawal, S., Dasgupta, D., & Kundu, T. K. (2009). Mechanism of p300 specific histone acetyltransferase inhibition by small molecules. *J. Med. Chem., 52*(2), 267-277.

Baell, J. B., & Holloway, G. A. (2010). New Substructure Filters for Removal of Pan Assay Interference Compounds (PAINS) from Screening Libraries and for Their Exclusion in Bioassays. *J. Med. Chem., 53*(7), 2719-2740.

Balasubramanyam, K., Altaf, M., Varier, R. A., Swaminathan, V., Ravindran, A., Sadhale, P. P., & Kundu, T. K. (2004). Polyisoprenylated benzophenone, garcinol, a natural histone acetyltransferase inhibitor, represses chromatin transcription and alters global gene expression. *J. Biol. Chem., 279*(32), 33716-33726.

Baykov, A. A., Evtushenko, O. A., & Avaeva, S. M. (1988). A malachite green procedure for orthophosphate determination and its use in alkaline phosphatase-based enzyme immunoassay. *Anal Biochem, 171*(2), 266-270.

Bharat, A., Jiang, M., Sullivan, S. M., Maddock, J. R., & Brown, E. D. (2006). Cooperative and critical roles for both G domains in the GTPase activity and cellular function of ribosome-associated *Escherichia coli* EngA. *J Bacteriol, 188*(22), 7992-7996.

Blanchard, J. E., Elowe, N. H., Huitema, C., Fortin, P. D., Cechetto, J. D., Eltis, L. D., & Brown, E. D. (2004). High-throughput screening identifies inhibitors of the SARS coronavirus main proteinase. *Chem Biol, 11*(10), 1445-1453.

Bochner, B. R., & Ames, B. N. (1982). Complete analysis of cellular nucleotides by two-dimensional thin layer chromatography. *J Biol Chem, 257*(16), 9759-9769.

Boucher, H. W., Talbot, G. H., Bradley, J. S., Edwards, J. E., Gilbert, D., Rice, L. B., . . . Bartlett, J. (2009). Bad bugs, no drugs: no ESKAPE! An update from the Infectious Diseases Society of America. *Clin Infect Dis, 48*(1), 1-12.

Bourne, H. R., Sanders, D. A., & McCormick, F. (1990). The GTPase superfamily: a conserved switch for diverse cell functions. *Nature, 348*(6297), 125-132.

Bourne, H. R., Sanders, D. A., & McCormick, F. (1991). The GTPase superfamily: conserved structure and molecular mechanism. *Nature, 349*(6305), 117-127.

Britton, R. A. (2009). Role of GTPases in bacterial ribosome assembly. *Annu Rev Microbiol, 63*, 155-176.

Brown, E. D. (2005). Conserved P-loop GTPases of unknown function in bacteria: an emerging and vital ensemble in bacterial physiology. *Biochem Cell Biol, 83*(6), 738-746.

Bubunenko, M., Korepanov, A., Court, D. L., Jagannathan, I., Dickinson, D., Chaudhuri, B. R., . . . Culver, G. M. (2006). 30S ribosomal subunits can be assembled in vivo without primary binding ribosomal protein S15. *RNA, 12*(7), 1229-1239.

Bunner, A. E., Nord, S., Wikström, P. M., & Williamson, J. R. (2010). The effect of ribosome assembly cofactors on *in vitro* 30S subunit reconstitution. *J Mol Biol , 398*(1), 1-7.

Bush, K., Courvalin, P., Dantas, G., Davies, J., Eisenstein, B., Huovinen, P., . . . Zgurskaya, H. I. (2011). Tackling antibiotic resistance. *Nature Reviews Microbiology, 9*(12), 894-896.

Butland, G., Peregrín-Alvarez, J. M., Li, J., Yang, W., Yang, X., Canadien, V., . . . Emili, A. (2005). Interaction network containing conserved and essential protein complexes in *Escherichia coli. Nature, 433*(7025), 531-537.

Caldas, T., Binet, E., Bouloc, P., Costa, A., Desgres, J., & Richarme, G. (2000). The FtsJ/RrmJ heat shock protein of *Escherichia coli* is a 23 S ribosomal RNA methyltransferase. *J Biol Chem, 275*(22), 16414-16419.

Caldon, C. E., & March, P. E. (2003). Function of the universally conserved bacterial GTPases. *Curr Opin Microbiol, 6*(2), 135-139.

Caldon, C. E., Yoong, P., & March, P. E. (2001). Evolution of a molecular switch: universal bacterial GTPases regulate ribosome function. *Mol Microbiol, 41*(2), 289-297.

Campbell, T. L., & Brown, E. D. (2002). Characterization of the depletion of 2-C-methyl-D-erythritol-2,4-cyclodiphosphate synthase in *Escherichia coli* and *Bacillus subtilis*. *J Bacteriol, 184*(20), 5609-5618.

Campbell, T. L., Daigle, D. M., & Brown, E. D. (2005c). Characterization of the *Bacillus subtilis* GTPase YloQ and its role in ribosome function. *Biochem J, 389*(3), 843-852.

Carter, A. P., Clemons, W. M., Brodersen, D. E., Morgan-Warren, R. J., Wimberly, B. T., & Ramakrishnan, V. (2000). Functional insights from the structure of the 30S ribosomal subunit and its interactions with antibiotics. *Nature, 407*(6802), 340-348.

Charollais, J., Pflieger, D., Vinh, J., Dreyfus, M., & Iost, I. (2003). The DEAD-box RNA helicase SrmB is involved in the assembly of 50S ribosomal subunits in *Escherichia coli*. *Mol. Microbiol., 48*(5), 1253-1265.

Chen, C. N., Lin, C. P., Huang, K. K., Chen, W. C., Hsieh, H. P., Liang, P. H., & Hsu, J. T. (2005). Inhibition of SARS-CoV 3C-like Protease Activity by Theaflavin-3,3'-digallate (TF3). *Evidence-based complementary and alternative medicine : eCAM, 2*(2), 209-215.

Chow, C. S., Lamichhane, T. N., & Mahto, S. K. (2007). Expanding the nucleotide repertoire of the ribosome with post-transcriptional modifications. *ACS chemical biology, 2*(9), 610-619.

Christiansen, L., & Neirhaus, K. H. (1976). Ribosomal proteins of *Escherichia coli* that stimulate stringent-factor-mediated pyrophosphoryl transfer *in vitro*. *Proc Natl Acad Sci U S A, 73*(6), 1839-1843.

Cohen, M. L. (1998). Candidate bacterial conditions. *Bull. W.H.O., 76* (Suppl 2), 61.

Cole, J. R., Olsson, C. L., Hershey, J. W., Grunberg-Manago, M., & Nomura, M. (1987). Feedback regulation of rRNA synthesis in *Escherichia coli*. Requirement for initiation factor IF2. *J. Mol. Biol., 198*(3), 383-392.

Connolly, K., Rife, J. P., & Culver, G. (2008). Mechanistic insight into the ribosome biogenesis functions of the ancient protein KsgA. *Mol. Microbiol., 70*(5), 1062-1075.

Cooper, E. L., Garcia-Lara, J., & Foster, S. J. (2009). YsxC, an essential protein in *Staphylococcus aureus* crucial for ribosome assembly/stability. *BMC Microbiol., 9*, 266.

Culver, G. M., & Noller, H. F. (1999a). Efficient reconstitution of functional *Escherichia coli* 30S ribosomal subunits from a complete set of recombinant small subunit ribosomal proteins. *RNA, 5*(6), 832-843.

Daigle, D. M., & Brown, E. D. (2004). Studies of the interaction of *Escherichia coli* YjeQ with the ribosome *in vitro*. *J. Bacteriol., 186*(5), 1381-1387.

Dammel, C. S., & Noller, H. F. (1995). Suppression of a cold-sensitive mutation in 16S rRNA by overexpression of a novel ribosome-binding factor, RbfA. *Genes Dev, 9*(5), 626-637.

Datsenko, K. A., & Wanner, B. L. (2000). One-step inactivation of chromosomal genes in *Escherichia coli* K-12 using PCR products. *Proc Natl Acad Sci U S A, 97*(12), 6640-6645.

Datta, K., Skidmore, J. M., Pu, K., & Maddock, J. R. (2004). The *Caulobacter crescentus* GTPase CgtAC is required for progression through the cell cycle and for maintaining 50S ribosomal subunit levels. *Mol. Microbiol., 54*(5), 1379-1392.

Datta, P. P., Wilson, D. N., Kawazoe, M., Swami, N. K., Kaminishi, T., Sharma, M. R., . . . Agrawal, R. K. (2007). Structural aspects of RbfA action during small ribosomal subunit assembly. *Mol. Cell, 28*(3), 434-445.

Demirci, H., Murphy, F., Belardinelli, R., Kelley, A. C., Ramakrishnan, V., Gregory, S. T., . . . Jogl, G. (2010). Modification of 16S ribosomal RNA by the KsgA methyltransferase restructures the 30S subunit to optimize ribosome function. *RNA, 16*(12), 2319-2324.

Dennis, P. P., Ehrenberg, M., & Bremer, H. (2004). Control of rRNA synthesis in *Escherichia coli:* a systems biology approach. *MMBR, 68*(4), 639-668.

Diedrich, G., Spahn, C. M., Stelzl, U., Schafer, M. A., Wooten, T., Bochkariov, D. E., . . . Nierhaus, K. H. (2000). Ribosomal protein L2 is involved in the association of the ribosomal subunits, tRNA binding to A and P sites and peptidyl transfer. *EMBO J., 19*(19), 5241-5250.

Dragovich, P. S., Webber, S. E., Babine, R. E., Fuhrman, S. A., Patick, A. K., Matthews, D. A., . . . Worland, S. T. (1998). Structure-based design, synthesis, and biological evaluation of irreversible human rhinovirus 3C protease inhibitors. 1. Michael acceptor structure-activity studies. *J. Med. Chem., 41*(15), 2806-2818.

Droit, A., Poirier, G. G., & Hunter, J. M. (2005). Experimental and bioinformatic approaches for interrogating protein-protein interactions to determine protein function. *J Mol Endocrinol, 34*(2), 263-280.

Drummond, A., Kearse, M., Heled, J., Moir, R., Thierer, T., & Ashton, B. (2006). Geneious v5.5.7, from http://www.geneious.com

Duggan, S. T. (2011). Fidaxomicin: In Clostridium difficile Infection. *Drugs, 71*(18), 2445-2456.

Feng, B. Y., Simeonov, A., Jadhav, A., Babaoglu, K., Inglese, J., Shoichet, B. K., & Austin, C. P. (2007). A high-throughput screen for aggregation-based inhibition in a large compound library. *J. Med. Chem., 50*(10), 2385-2390.

Food and Drug Administration. (2009). Antimicrobials sold or distributed for use in food-producing animals.

Forsyth, R. A., Haselbeck, R. J., Ohlsen, K. L., Yamamoto, R. T., Xu, H., Trawick, J. D., . . . Zyskind, J. W. (2002). A genome-wide strategy for the identification of essential genes in *Staphylococcus aureus*. *Mol Microbiol, 43*(6), 1387-1400.

Goto, S., Kato, S., Kimura, T., Muto, A., & Himeno, H. (2011). RsgA releases RbfA from 30S ribosome during a late stage of ribosome biosynthesis. *EMBO J, 30*(1), 104-114.

Guillier, M., Allemand, F., Dardel, F., Royer, C. A., Springer, M., & Chiaruttini, C. (2005). Double molecular mimicry in *Escherichia coli:* binding of ribosomal protein L20 to its two sites in mRNA is similar to its binding to 23S rRNA. *Mol. Microbiol., 56*(6), 1441-1456.

Guthrie, C., Nashimoto, H., & Nomura, M. (1969). Structure and function of *Escherichia coli* ribosomes. 8. Cold-sensitive mutants defective in ribosome assembly. *Proc Natl Acad Sci U S A, 63*(2), 384-391.

Hwang, J., & Inouye, M. (2001). An essential GTPase, *der*, containing double GTP-binding domains from *Escherichia coli* and *Thermotoga maritima*. *J Biol Chem, 276*(33), 31415-31421.

Hwang, J., & Inouye, M. (2006). The tandem GTPase, Der, is essential for the biogenesis of 50S ribosomal subunits in *Escherichia coli. Mol. Microbiol., 61*(6), 1660-1672.

Hwang, J., & Inouye, M. (2008). RelA functionally suppresses the growth defect caused by a mutation in the G domain of the essential Der protein. *J. Bacteriol., 190*(9), 3236-3243.

Hwang, J., & Inouye, M. (2010a). A bacterial GAP-like protein, YihI, regulating the GTPase of Der, an essential GTP-binding protein in *Escherichia coli. J. Mol. Biol., 399*(5), 759-772.

Hwang, J., & Inouye, M. (2010b). Interaction of an essential *Escherichia coli* GTPase, Der, with the 50S ribosome via the KH-like domain. *J. Bacteriol., 192*(8), 2277-2283.

Hwang, J., Tseitin, V., Ramnarayan, K., Shenderovich, M. D., & Inouye, M. (2012). Structure-based design and screening of inhibitors for an essential bacterial GTPase, Der. *J Antibiot (Tokyo), 65*(5), 237-243.

Infectious Diseases Society of America. (2010). The 10 × '20 Initiative: Pursuing a Global Commitment to Develop 10 New Antibacterial Drugs by 2020. *Clin. Infect. Dis., 50*(8), 1081-1083.

Inoue, K., Alsina, J., Chen, J., & Inouye, M. (2003). Suppression of defective ribosome assembly in a *rbfA* deletion mutant by overexpression of Era, an essential GTPase in *Escherichia coli. Mol Microbiol, 48*(4), 1005-1016.

Invitrogen. (2005). Note 1.5 - Technical Focus: Fluorescence Polarization (FP)

Jadhav, A., Ferreira, R. S., Klumpp, C., Mott, B. T., Austin, C. P., Inglese, J., . . . Simeonov, A. (2010). Quantitative analyses of aggregation, autofluorescence, and

reactivity artifacts in a screen for inhibitors of a thiol protease. *J. Med. Chem., 53*(1), 37-51.

Jagessar, K. L., & Jain, C. (2010). Functional and molecular analysis of *Escherichia coli* strains lacking multiple DEAD-box helicases. *RNA, 16*(7), 1386-1392.

Jain, N., Dhimole, N., Khan, A. R., De, D., Tomar, S. K., Sajish, M., . . . Prakash, B. (2009). *Escherichia coli* HflX interacts with 50S ribosomal subunits in presence of nucleotides. *Biochem. Biophys. Res. Commun., 379*(2), 201-205.

Jankun, J., Skotnicka, M., Lysiak-Szydlowska, W., Al-Senaidy, A., & Skrzypczak-Jankun, E. (2011). Diverse inhibition of plasminogen activator inhibitor type 1 by theaflavins of black tea. *Int. J. Mol. Med., 27*(4), 525-529.

Jensen, B. C., Wang, Q., Kifer, C. T., & Parsons, M. (2003). The NOG1 GTP-binding protein is required for biogenesis of the 60 S ribosomal subunit. *J Biol Chem, 278*(34), 32204-32211.

Jiang, M., K. Datta, A. Walker, J. Strahler, P. Bagamasbad, P.C. Andrews and J.R. Maddock. . (2006). The *Escherichia coli* GTPase CgtA$_E$ is involved in late steps of large ribosome assembly. *J Bacteriol*.

Jiang, M., Sullivan, S. M., Walker, A. K., Strahler, J. R., Andrews, P. C., & Maddock, J. R. (2007a). Identification of novel *Escherichia coli* ribosome-associated proteins using isobaric tags and multidimensional protein identification techniques. *J Bacteriol, 189*(9), 3434-3444.

Jiang, M., Sullivan, S. M., Wout, P. K., & Maddock, J. R. (2007b). G-protein control of the ribosome-associated stress response protein SpoT. *J. Bacteriol., 189*(17), 6140-6147.

Jinks-Robertson, S., Gourse, R. L., & Nomura, M. (1983). Expression of rRNA and tRNA genes in *Escherichia coli*: evidence for feedback regulation by products of rRNA operons. *Cell, 33*(3), 865-876.

Jomaa, A., Stewart, G., Martín-Benito, J., Zielke, R., Campbell, T. L., Maddock, J. R., . . . Ortega, J. (2011a). Understanding ribosome assembly: the structure of in vivo assembled immature 30S subunits revealed by cryo-electron microscopy. *RNA, 17*(4), 697-709.

Jomaa, A., Stewart, G., Mears, J. A., Kireeva, I., Brown, E. D., & Ortega, J. (2011b). Cryo-electron microscopy structure of the 30S subunit in complex with the YjeQ biogenesis factor. *RNA, 17*(11), 2026-2038.

Jones, P. G., Mitta, M., Kim, Y., Jiang, W., & Inouye, M. (1996). Cold shock induces a major ribosomal-associated protein that unwinds double-stranded RNA in *Escherichia coli*. *Proc Natl Acad Sci U S A, 93*(1), 76-80.

Kaltschmidt, E., & Wittmann, H. G. (1970). Ribosomal proteins. XII. Number of proteins in small and large ribosomal subunits of *Escherichia coli* as determined by two-dimensional gel electrophoresis. *Proc Natl Acad Sci U S A, 67*(3), 1276-1282.

Kaplan, W., & Laing, R. (2004). Priority medicines for Europe and the world.

Katano, H., & Ueda, T. (2011). Spectrophotometric determination of phosphate anion based on the formation of molybdophosphate in ethylene glycol-water mixed solution. *Analytical Sciences, 27*(10), 1043-1047.

Kipper, K., Sild, S., Hetényi, C., Remme, J., & Liiv, A. (2011). Pseudouridylation of 23S rRNA helix 69 promotes peptide release by release factor RF2 but not by release factor RF1. *Biochimie, 93*(5), 834-844.

Kressler, D., Hurt, E., & Bassler, J. (2010). Driving ribosome assembly. *Biochimica et biophysica acta, 1803*(6), 673-683.

Kressler, D., Linder, P., & de La Cruz, J. (1999). Protein trans-acting factors involved in ribosome biogenesis in *Saccharomyces cerevisiae*. *Mol Cell Biol, 19*(12), 7897-7912.

Lakowicz, J. R. (1999). *Principles of fluorescence spectroscopy* (2nd ed.). New York: Kluwer Academic/Plenum.

Lamb, H. K., Thompson, P., Elliott, C., Charles, I. G., Richards, J., Lockyer, M., . . . Hawkins, A. R. (2007). Functional analysis of the GTPases EngA and YhbZ encoded by Salmonella typhimurium. *Protein science, 16*(11), 2391-2402.

Leipe, D. D., Wolf, Y. I., Koonin, E. V., & Aravind, L. (2002). Classification and evolution of P-loop GTPases and related ATPases. *J. Mol. Biol., 317*(1), 41-72.

Li, Z., & Deutscher, M. P. (1995). The tRNA processing enzyme RNase T is essential for maturation of 5S RNA. *Proc Natl Acad Sci U S A, 92*(15), 6883-6886.

Li, Z., Pandit, S., & Deutscher, M. P. (1999a). Maturation of 23S ribosomal RNA requires the exoribonuclease RNase T. *RNA, 5*(1), 139-146.

Li, Z., Pandit, S., & Deutscher, M. P. (1999b). RNase G (CafA protein) and RNase E are both required for the 5' maturation of 16S ribosomal RNA. *EMBO J, 18*(10), 2878-2885.

Lin, B., Covalle, K. L., & Maddock, J. R. (1999). The *Caulobacter crescentus* CgtA protein displays unusual guanine nucleotide binding and exchange properties. *J Bacteriol, 181*(18), 5825-5832.

Lin, B., Thayer, D. A., & Maddock, J. R. (2004). The *Caulobacter crescentus* CgtA$_C$ protein cosediments with the free 50S ribosomal subunit. *J Bacteriol, 186*(2), 481-489.

Lindahl, L. (1975). Intermediates and time kinetics of the in vivo assembly of *Escherichia coli* ribosomes. *J. Mol. Biol., 92*(1), 15-37.

Linder, P., & Jankowsky, E. (2011). From unwinding to clamping - the DEAD box RNA helicase family. *Nature reviews. Molecular cell biology, 12*(8), 505-516.

Lu, Q., & Inouye, M. (1998). The gene for 16S rRNA methyltransferase (*ksgA*) functions as a multicopy suppressor for a cold-sensitive mutant of *era,* an essential RAS-like GTP-binding protein in *Escherichia coli*. *J. Bacteriol., 180*(19), 5243-5246.

Magnusson, L. U., Farewell, A., & Nystrom, T. (2005). ppGpp: a global regulator in *Escherichia coli*. *Trends Microbiol, 13*(5), 236-242.

Marshall, B. M., & Levy, S. B. (2011). Food animals and antimicrobials: impacts on human health. *Clin. Microbiol. Rev., 24*(4), 718-733.

Mehr, I. J., Long, C. D., Serkin, C. D., & Seifert, H. S. (2000). A homologue of the recombination-dependent growth gene, *rdgC*, is involved in gonococcal pilin antigenic variation. *Genetics, 154*(2), 523-532.

Misra, T. K., & Apirion, D. (1979). RNase E, an RNA processing enzyme from *Escherichia coli*. *J Biol Chem, 254*(21), 11154-11159.
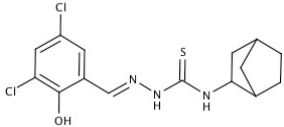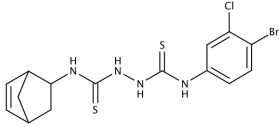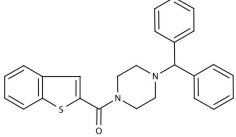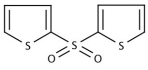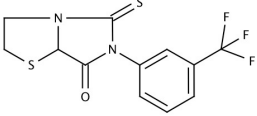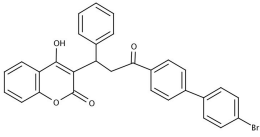
Mizushima, S., & Nomura, M. (1970). Assembly mapping of 30S ribosomal proteins from *Escherichia coli*. *Nature, 226*(5252), 1214.

Morimoto, T., Loh, P. C., Hirai, T., Asai, K., Kobayashi, K., Moriya, S., & Ogasawara, N. (2002). Six GTP-binding proteins of the Era/Obg family are essential for cell growth in *Bacillus subtilis*. *Microbiology, 148*(Pt 11), 3539-3552.

Muench, S. P., Xu, L., Sedelnikova, S. E., & Rice, D. W. (2006). The essential GTPase YphC displays a major domain rearrangement associated with nucleotide binding. *Proc Natl Acad Sci U S A*.

Nguyen, B., Ticu, C., & Wilson, K. S. (2010). Intramolecular movements in EF-G, trapped at different stages in its GTP hydrolytic cycle, probed by FRET. *J. Mol. Biol., 397*(5), 1245-1260.

Nierhaus, K. H. (1991). The assembly of prokaryotic ribosomes. *Biochimie, 73*(6), 739-755.

Nierhaus, K. H., & Dohme, F. (1974). Total reconstitution of functionally active 50S ribosomal subunits from *Escherichia coli*. *Proc Natl Acad Sci U S A, 71*(12), 4713-4717.

Nomura, M., & Erdmann, V. A. (1970). Reconstitution of 50S ribosomal subunits from dissociated molecular components. *Nature, 228*(5273), 744-748.

Nomura, M., & Traub, P. (1968). Structure and function of *Escherichia coli* ribosomes. 3. Stoichiometry and rate of the reconstitution of ribosomes from subribosomal particles and split proteins. *J. Mol. Biol., 34*(3), 609-619.

Nord, S., Bylund, G. O., Lovgren, J. M., & Wikstrom, P. M. (2009). The RimP protein is important for maturation of the 30S ribosomal subunit. *J Mol Biol, 386*(3), 742-753.

Northrop, D. (1998). On the meaning of K_m and V/K in enzyme kinetics. *J Chem Ed, 75*(9), 1154.

Paul, B. J., Barker, M. M., Ross, W., Schneider, D. A., Webb, C., Foster, J. W., & Gourse, R. L. (2004a). DksA: a critical component of the transcription initiation machinery that potentiates the regulation of rRNA promoters by ppGpp and the initiating NTP. *Cell, 118*(3), 311-322.

Paul, B. J., Ross, W., Gaal, T., & Gourse, R. L. (2004b). rRNA transcription in *Escherichia coli*. *Annu. Rev. Genet., 38*, 749-770.

Polkinghorne, A., Ziegler, U., Gonzalez-Hernandez, Y., Pospischil, A., Timms, P., & Vaughan, L. (2008). Chlamydophila pneumoniae HflX belongs to an uncharacterized family of conserved GTPases and associates with the *Escherichia coli* 50S large ribosomal subunit. *Microbiology, 154*(11), 3537-3546.

Puglisi, J. D., Blanchard, S. C., & Green, R. (2000). Approaching translation at atomic resolution. *Nat Struct Biol, 7*(10), 855-861.

Ramakrishnan, V. (2002). Ribosome structure and the mechanism of translation. *Cell, 108*(4), 557-572.

Rice, L. (2008). Federal Funding for the Study of Antimicrobial Resistance in Nosocomial Pathogens: No ESKAPE. *J. Infect. Dis.* 197(8): 1079-1081.
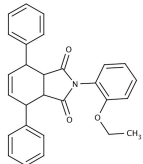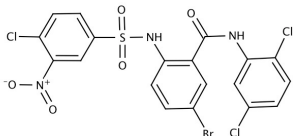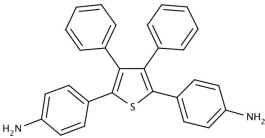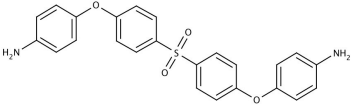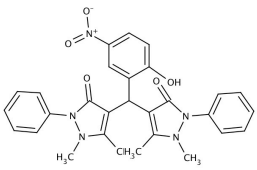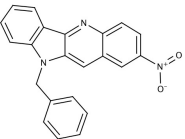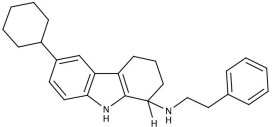
Robinson, V. L., Hwang, J., Fox, E., Inouye, M., & Stock, A. M. (2002). Domain arrangement of Der, a switch protein containing two GTPase domains. *Structure, 10*(12), 1649-1658.

Rohl, R., & Nierhaus, K. H. (1982). Assembly map of the large subunit (50S) of *Escherichia coli* ribosomes. *Proc Natl Acad Sci U S A, 79*(3), 729-733.

Sato, A., Kobayashi, G., Hayashi, H., Yoshida, H., Wada, A., Maeda, M., . . . Wada, C. (2005). The GTP binding protein Obg homolog ObgE is involved in ribosome maturation. *Genes Cells, 10*(5), 393-408.

Sayed, A., Matsuyama, S., & Inouye, M. (1999). Era, an essential *Escherichia coli* small G-protein, binds to the 30S ribosomal subunit. *Biochem. Biophys. Res. Commun., 264*(1), 51-54.

Schaefer, L., Uicker, W. C., Wicker-Planquart, C., Foucher, A.-E., Jault, J.-M., & Britton, R. A. (2006). Multiple GTPases participate in the assembly of the large ribosomal subunit in *Bacillus subtilis. J. Bacteriol., 188*(23), 8252-8258.

Schneider, D. A., Gaal, T., & Gourse, R. L. (2002). NTP-sensing by rRNA promoters in *Escherichia coli* is direct. *Proc Natl Acad Sci U S A, 99*(13), 8602-8607.

Schneider, D. A., & Gourse, R. L. (2003). Changes in *Escherichia coli* rRNA promoter activity correlate with changes in initiating nucleoside triphosphate and guanosine 5' diphosphate 3'-diphosphate concentrations after induction of feedback control of ribosome synthesis. *J. Bacteriol., 185*(20), 6185-6191.

Selmer, M., Dunham, C. M., Murphy, F. V., Weixlbaumer, A., Petry, S., Kelley, A. C., . . . Ramakrishnan, V. (2006). Structure of the 70S ribosome complexed with mRNA and tRNA. *Science, 313*(5795), 1935-1942.

Shajani, Z., Sykes, M. T., & Williamson, J. R. (2011). Assembly of bacterial ribosomes. *Annu. Rev. Biochem., 80*, 501-526.

Sharma, M. R., Barat, C., Wilson, D. N., Booth, T. M., Kawazoe, M., Hori-Takemoto, C., . . . Agrawal, R. K. (2005). Interaction of Era with the 30S ribosomal subunit implications for 30S subunit assembly. *Mol. Cell, 18*(3), 319-329.

Shoichet, B. K. (2006). Interpreting steep dose-response curves in early inhibitor discovery. *J. Med. Chem., 49*(25), 7274-7277.

Siibak, T., & Remme, J. (2010). Subribosomal particle analysis reveals the stages of bacterial ribosome assembly at which rRNA nucleotides are modified. *RNA, 16*(10), 2023-2032.

Sikora, A. E., Zielke, R., Datta, K., & Maddock, J. R. (2006). The *Vibrio harveyi* GTPase CgtA$_V$ is essential and is associated with the 50S ribosomal subunit. *J Bacteriol, 188*(3), 1205-1210.

Silver, L. L. (2011). Challenges of antibacterial discovery. *Clin. Microbiol. Rev., 24*(1), 71-109.

Spedding, G. (1990). *Ribosomes and protein synthesis : a practical approach*. Oxford England ; New York: IRL Press at Oxford University Press.

Srivastava, A. K., & Schlessinger, D. (1990). Mechanism and regulation of bacterial ribosomal RNA processing. *Annu. Rev. Microbiol., 44*, 105-129.
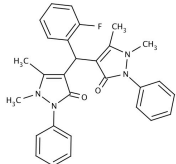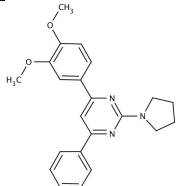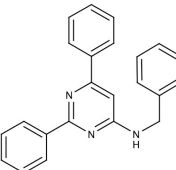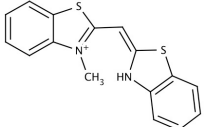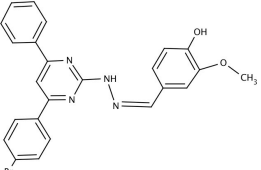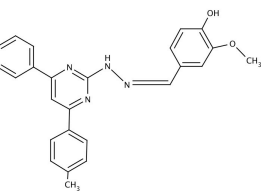
Stafford, W. F., 3rd. (1992). Boundary analysis in sedimentation transport experiments: a procedure for obtaining sedimentation coefficient distributions using the time derivative of the concentration profile. *Anal Biochem, 203*(2), 295-301.

Stamm, W., Grayson, M., Nicolle, L., & Powell, M. (2001). WHO Global Strategy for Containment of Antimicrobial Resistance (Document no: WHO/CDS/CSR/DRS/2001.2). *Geneva, World Health Organization*.

Sykes, M. T., Shajani, Z., Sperling, E., Beck, A. H., & Williamson, J. R. (2010). Quantitative proteomic analysis of ribosome assembly and turnover *in vivo*. *J. Mol. Biol., 403*(3), 331-345.

Takebe, Y., Miura, A., Bedwell, D. M., Tam, M., & Nomura, M. (1985). Increased expression of ribosomal genes during inhibition of ribosome assembly in *Escherichia coli*. *J. Mol. Biol., 184*(1), 23-30.

Tan, J., Jakob, U., & Bardwell, J. C. (2002a). Overexpression of two different GTPases rescues a null mutation in a heat-induced rRNA methyltransferase. *J Bacteriol, 184*(10), 2692-2698.

Tan, J., Jakob, U., & Bardwell, J. C. A. (2002b). Overexpression of two different GTPases rescues a null mutation in a heat-induced rRNA methyltransferase. *J. Bacteriol., 184*(10), 2692-2698.

Tatusov, R. L., Fedorova, N. D., Jackson, J. D., Jacobs, A. R., Kiryutin, B., Koonin, E. V., . . . Natale, D. A. (2003). The COG database: an updated version includes eukaryotes. *BMC Bioinformatics, 4*, 41.

Tomar, S. K., Dhimole, N., Chatterjee, M., & Prakash, B. (2009). Distinct GDP/GTP bound states of the tandem G-domains of EngA regulate ribosome binding. *Nucleic Acids Res., 37*(7), 2359-2370.

Traub, P., & Nomura, M. (1968). Structure and function of *Escherichia coli* ribosomes. V. Reconstitution of functionally active 30S ribosomal particles from RNA and proteins. *Proc Natl Acad Sci U S A, 59*(3), 777-784.

Traub, P., & Nomura, M. (1969). Structure and function of *Escherichia coli* ribosomes. VI. Mechanism of assembly of 30S ribosomes studied *in vitro*. *J. Mol. Biol., 40*(3), 391-413.

Tu, C., Zhou, X., Tarasov, S. G., Tropea, J. E., Austin, B. P., Waugh, D. S., . . . Ji, X. (2011). The Era GTPase recognizes the GAUCACCUCC sequence and binds helix 45 near the 3' end of 16S rRNA. *Proc Natl Acad Sci U S A, 108*(25), 10156-10161.

Tu, C., Zhou, X., Tropea, J. E., Austin, B. P., Waugh, D. S., Court, D. L., & Ji, X. (2009). Structure of ERA in complex with the 3' end of 16S rRNA: implications for ribosome biogenesis. *Proc Natl Acad Sci U S A, 106*(35), 14843-14848.

Uicker, W. C., Schaefer, L., & Britton, R. A. (2006). The essential GTPase RbgA (YlqF) is required for 50S ribosome assembly in *Bacillus subtilis*. *Mol Microbiol, 59*(2), 528-540.

Uicker, W. C., Schaefer, L., Koenigsknecht, M., & Britton, R. A. (2007). The essential GTPase YqeH is required for proper ribosome assembly in *Bacillus subtilis*. *J. Bacteriol., 189*(7), 2926-2929.
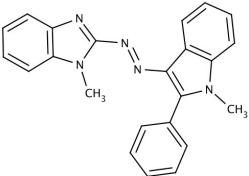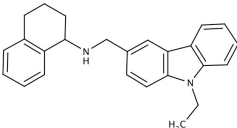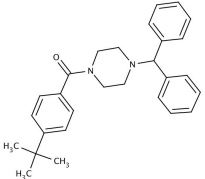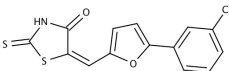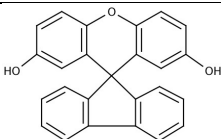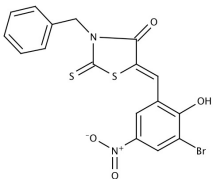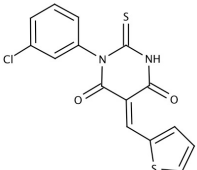
Verstraeten, N., Fauvart, M., Versées, W., & Michiels, J. (2011). The universally conserved prokaryotic GTPases. *MMBR, 75*(3), 507-542.

Wicker-Planquart, C., Foucher, A.-E., Louwagie, M., Britton, R. A., & Jault, J.-M. (2008). Interactions of an essential *Bacillus subtilis* GTPase, YsxC, with ribosomes. *J. Bacteriol., 190*(2), 681-690.

Wilson, D. N., & Nierhaus, K. H. (2005). Ribosomal proteins in the spotlight. *Crit. Rev. Biochem. Mol. Biol., 40*(5), 243-267.

Wilson, D. N., & Nierhaus, K. H. (2007). The weird and wonderful world of bacterial ribosome regulation. *Crit. Rev. Biochem. Mol. Biol., 42*(3), 187-219.

Woodson, S. A. (2008). RNA folding and ribosome assembly. *Curr. Opin. Chem. Biol., 12*(6), 667-673.

Wout, P., Pu, K., Sullivan, S. M., Reese, V., Zhou, S., Lin, B., & Maddock, J. R. (2004). The *Escherichia coli* GTPase CgtA$_E$ cofractionates with the 50S ribosomal subunit and interacts with SpoT, a ppGpp synthetase/hydrolase. *J Bacteriol, 186*(16), 5249-5257.

Wright, G. D. (2010). The antibiotic resistome. *Expert Opinion on Drug Discovery, 5*(8), 779-788.

Wu, G. (2010). *Assay development : fundamentals and practices*. Hoboken, N.J.: Wiley.

Xu, Z., O'Farrell, H. C., Rife, J. P., & Culver, G. M. (2008). A conserved rRNA methyltransferase regulates ribosome biogenesis. *Nat Struct & Mol Biol, 15*(5), 534-536.

Yamagishi, M., de Boer, H. A., & Nomura, M. (1987). Feedback regulation of rRNA synthesis. A mutational alteration in the anti-Shine-Dalgarno region of the 16 S rRNA gene abolishes regulation. *J. Mol. Biol., 198*(3), 547-550.

Yonath, A. (2005). Antibiotics targeting ribosomes: resistance, selectivity, synergism and cellular regulation. *Annu Rev Biochem, 74*, 649-679.

Zaslaver, A., Bren, A., Ronen, M., Itzkovitz, S., Kikoin, I., Shavit, S., . . . Alon, U. (2006). A comprehensive library of fluorescent transcriptional reporters for *Escherichia coli*. *Nat. Methods, 3*(8), 623-628.

Zhang, J. H., Chung, T. D., & Oldenburg, K. R. (1999). A Simple Statistical Parameter for Use in Evaluation and Validation of High Throughput Screening Assays. *J. Biomol. Screen., 4*(2), 67-73.

7   APPENDICES

Table A1. Structures and Activities of the 44 hits from the primary screen of EngA.
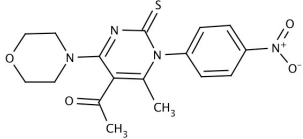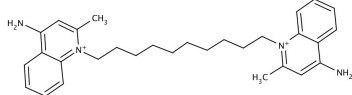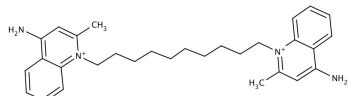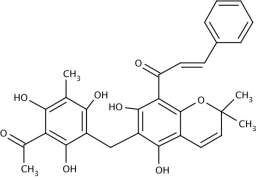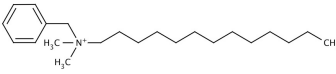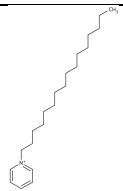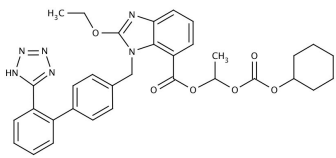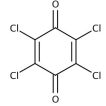
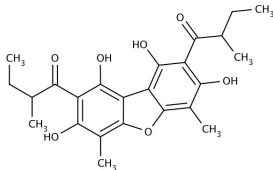| Compound ID	Structure	Activity (%)	Basis for Elimination
MAC-0009753		106.7	Low potency
MAC-0009913		11.9	Triton sensitivy
MAC-0017207		58.7	Triton sensitivity
MAC-0027109		103.8	Low potency
MAC-0028865		71.3	Low potency
MAC-0168220		54.1	Triton sensitivity
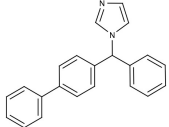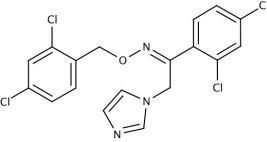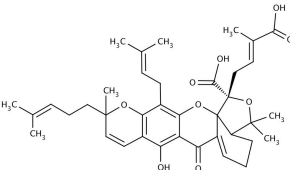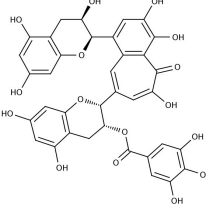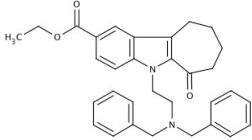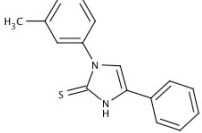
Compound ID	Structure	Activity (%)	Basis for Elimination
MAC-0168812		154.7	Low potency
MAC-0169562		13.5	Triton sensitivity
MAC-0169400		2.5	Assay Interference
MAC-0169474		68.5	Triton sensitivity
MAC-0170098		67.9	DTT sensitivity
MAC-0170219		57.4	Triton sensitivity
MAC-0171475		27.9	Triton sensitivity

Compound ID	Structure	Activity (%)	Basis for Elimination
MAC-0172122		40.9	Assay Interference
MAC-0172276		46.9	Assay Interference
MAC-0172228		39.8	Assay Interference
MAC-0172384		64.5	Triton sensitivity
MAC-0172716		51.9	Triton sensitivity
MAC-0172696		59.0	Triton sensitivity

Compound ID	Structure	Activity (%)	Basis for Elimination
MAC-0174124		34.8	Assay Interference
MAC-0174266		75.5	Low potency
MAC-0174377		43.6	Assay Interference
MAC-0174809		8.1	--
MAC-0174926		48.6	Triton sensitivity
MAC-0176121		24.2	Triton sensitivity
MAC-0176241		22.4	DTT sensitivity

Compound ID	Structure	Activity (%)	Basis for Elimination
MAC-0089304		62.2	DTT sensitivity
MAC-0178504		39.8	Triton sensitivity
MAC-0179041		-22.4	Detergent-like
MAC-0179657		25.6	Triton sensitivity
MAC-0181734		-22.8	Detergent-like
MAC-0182920		-17.7	Detergent-like
MAC-0182434		36.7	Triton sensitivity
MAC-0181419		4.8	DTT sensitivity

Compound ID	Structure	Activity (%)	Basis for Elimination
MAC-0182600		34.6	Assay Interference
MAC-0182598		19.0	Assay Interference
MAC-0182099		12.2	Not eliminated
MAC-0182211		24.8	Triton sensitivity
MAC-0182344		20.5	Not eliminated
MAC-0151070		29.3	Triton sensitivity
MAC-151135		58.5	DTT sensitivity
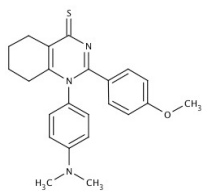
MAC-151196   71.4   Low potency
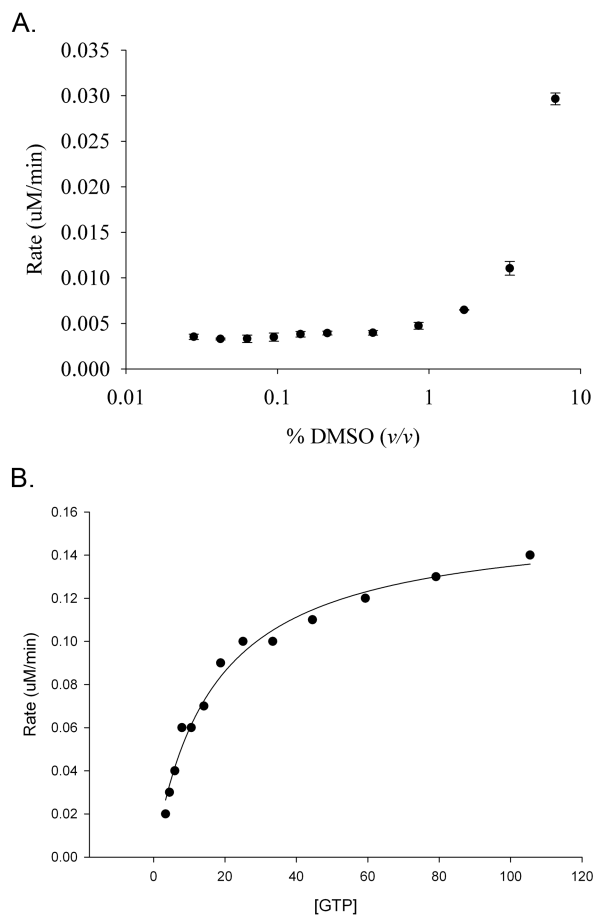
Figure A1. Effect of DMSO on the activity of EngA at low substrate concentration.
(A) The activity of 0.075 μM EngA was tested with 2 μM GTP in the presence of various [DMSO] in the GTPase assay described in Chapter 4. GTP and GDP were resolved and quantified by paired ion chromatography on an HPLC. The correspondence of the rate of the reaction with the percentage of DMSO is plotted. (B) The Michaelis-Menten curve of 0.1 μM EngA and various [GTP] in the presence of 5% DMSO. The data were fit to a hyperbolic function using the equation, $v_i = (v_{max} [S]) / (K_M + [S])$ with SigmaPlot 12.0 software.